

6/22

Dr. 1601-2

## CONTRACTOR REPORT

SAND83-7094  
Unlimited Release  
UC-32

SAND--83-7094

DE83 015023

I-10313

# A New Multigroup Monte Carlo Scattering Algorithm Suitable for Neutral and Charged-Particle Boltzmann and Fokker-Planck Calculations

Daniel Parl Sloan  
The University of New Mexico  
Albuquerque, New Mexico

Prepared by Sandia National Laboratories Albuquerque, New Mexico 87185  
and Livermore, California 94550 for the United States Department of Energy  
under Contract DE-AC04-76DP00789

Printed May 1983

MASTER

## **DISCLAIMER**

This report was prepared as an account of work sponsored by an agency of the United States Government. Neither the United States Government nor any agency thereof, nor any of their employees, makes any warranty, express or implied, or assumes any legal liability or responsibility for the accuracy, completeness, or usefulness of any information, apparatus, product, or process disclosed, or represents that its use would not infringe privately owned rights. Reference herein to any specific commercial product, process, or service by trade name, trademark, manufacturer, or otherwise does not necessarily constitute or imply its endorsement, recommendation, or favoring by the United States Government or any agency thereof. The views and opinions of authors expressed herein do not necessarily state or reflect those of the United States Government or any agency thereof.

## **DISCLAIMER**

**This report was prepared as an account of work sponsored by an agency of the United States Government. Neither the United States Government nor any agency Thereof, nor any of their employees, makes any warranty, express or implied, or assumes any legal liability or responsibility for the accuracy, completeness, or usefulness of any information, apparatus, product, or process disclosed, or represents that its use would not infringe privately owned rights. Reference herein to any specific commercial product, process, or service by trade name, trademark, manufacturer, or otherwise does not necessarily constitute or imply its endorsement, recommendation, or favoring by the United States Government or any agency thereof. The views and opinions of authors expressed herein do not necessarily state or reflect those of the United States Government or any agency thereof.**

## **DISCLAIMER**

**Portions of this document may be illegible in electronic image products. Images are produced from the best available original document.**

Printed May 1983  
Unlimited Release

SAND83-7094  
Category UC-32  
Contract# 61-9208

A NEW MULTIGROUP MONTE CARLO SCATTERING ALGORITHM  
SUITABLE FOR NEUTRAL- AND CHARGED-PARTICLE  
BOLTZMANN AND FOKKER-PLANCK CALCULATIONS

BY

DANIEL PARL SLOAN

B.S., Brigham Young University, 1978

M.S., University of New Mexico, 1981

DISSERTATION

Submitted in Partial Fulfillment of the  
Requirements for the Degree of

Doctor of Philosophy in Engineering

The University of New Mexico  
Albuquerque, New Mexico

April, 1983

Sandia Contracting Representative: Jim E. Morel, 1231

## ACKNOWLEDGEMENTS

This work was made possible by a contract (Document No. 61-9208) between Sandia National Laboratories and the University of New Mexico. The typing and final preparation of the manuscript was performed by the Bureau of Engineering Research (UNM). I would like to thank Sandia National Laboratories for the use of their computer facilities and the many courtesies extended me in the form of office space and technical support. I wish to extend special gratitude to my wife, Amy, for her encouragement and enduring patience, and Dr. J. C. Robertson (UNM) for his continuous and generous support throughout my graduate studies. And finally, I wish to acknowledge my deep indebtedness to Dr. J. E. Morel (SNL) for initiating the contract, supervising the research, and proofreading the final manuscript. I appreciate his invaluable comments, criticisms, and suggestions which have given this work direction and perspective.

A NEW MULTIGROUP MONTE CARLO SCATTERING ALGORITHM  
SUITABLE FOR NEUTRAL- AND CHARGED-PARTICLE BOLTZMANN  
AND FOKKER-PLANCK CALCULATIONS

Daniel Parl Sloan

B.S., Chemical Engineering, Brigham Young University, 1978  
M.S., Nuclear Engineering, University of New Mexico, 1981  
Ph.D., Nuclear Engineering, University of New Mexico, 1983

Morel (1981) has developed multigroup Legendre cross sections suitable for input to standard discrete ordinates transport codes for performing charged-particle Fokker-Planck calculations in one-dimensional slab and spherical geometries. Since the Monte Carlo neutron transport code, MORSE, uses the same multigroup cross section data that discrete ordinates codes use, it was natural to consider whether Fokker-Planck calculations could be performed with MORSE. An investigation showed, however, that the Fokker-Planck cross sections possessed two characteristics which rendered them unacceptable to the Gauss quadrature scattering algorithm used in MORSE: (1) the cross sections modeling the energy operator contain delta functions, and (2) the cross sections modeling the angular operator are nonphysical (i.e., they do not represent a cross section which is fully positive with respect to the angular cosine). Therefore, in order to extend the unique three-dimensional forward or adjoint capability of MORSE to Fokker-Planck calculations, the MORSE code was modified to correctly treat the delta-function scattering of the energy operator, and a new set of physically acceptable cross sections was derived to model the angular operator. These new developments were tested for one-dimensional slab geometries by comparing energy and charge

deposition profiles from MORSE with corresponding solutions from a discrete ordinates code (ONETRAN). The agreement was found to be excellent. Results from forward and adjoint test runs to compute energy deposition in a sphere also showed good agreement.

Morel (1979) has also developed multigroup Legendre cross sections suitable for input to standard discrete ordinates codes for performing electron Boltzmann calculations. These electron cross sections may be treated in MORSE with the same methods developed to treat the Fokker-Planck cross sections. The large magnitude of the elastic scattering cross section, however, severely increases the computation or run time. It is well-known that approximate elastic cross sections are easily obtained by applying the extended transport (or delta function) correction to the Legendre coefficients of the "exact" cross section. The extended transport corrected cross sections are extremely effective in decreasing the run time in discrete ordinates calculations and would be expected to similarly decrease run times in MORSE. However, these corrected cross sections are nonphysical and are therefore rejected by the scattering algorithm in MORSE. In order to correct this problem, a new method for performing the transport correction, utilizing a Radau quadrature technique, was developed and tested. The technique is an exact method for performing the extended transport cross section correction in that it produces cross sections which are physically acceptable. Sample calculations using electron cross sections have demonstrated this new technique to be very effective in decreasing the large magnitude of the cross sections.

## TABLE OF CONTENTS

	<u>Page</u>
LIST OF FIGURES. . . . .	viii
LIST OF TABLES . . . . .	ix
I. INTRODUCTION. . . . .	1
Research Objectives . . . . .	2
Comparison Between Monte Carlo and Discrete-Ordinates Techniques. . . . .	4
Importance Sampling . . . . .	6
Group-to-Group Transfer Cross Sections in MORSE . . . . .	8
II. GENERATION OF DISCRETE SCATTERING ANGLES USING RADAU QUADRATURE. . . . .	14
Legendre Polynomial Expansions of Angular Distributions .	15
Discrete Angle Approximations of Angular Distributions. .	21
Comparison Between Radau Quadrature and the Extended Transport Cross Section Correction. . . . .	31
III. GENERATION OF CHARGED-PARTICLE MULTIGROUP CROSS SECTIONS USING THE FOKKER-PLANCK APPROXIMATION . . . . .	37
Theoretical Basis for the Decoupled Cross Section . . . . .	43
Physical Basis for the Decoupled Cross Section. . . . .	46
Coefficients for $\sigma^a$ . . . . .	52
Coefficients for $\sigma^e$ . . . . .	73
Computational Results and Analysis. . . . .	77
APPENDICES	
Appendix A - Derivation of the Fokker-Planck Equation . . .	101
Appendix B - Generalized Gauss and Radau Quadrature . . . .	125
Appendix C - Implementation of Radau Quadrature into the MORSE Code System. . . . .	166
SELECTED BIBLIOGRAPHY. . . . .	191

LIST OF FIGURES

<u>Figure</u>		<u>Page</u>
2-1	Comparison of water group-to-group elastic scattering cross section with an eighth-order Legendre polynomial approximation . . . . .	20
3-1	Triangular impulse function. . . . .	65
3-2	Energy deposition profile comparison for Problems 1, 2, and 3. . . . .	81
3-3	Energy deposition profile comparison for Problem 1 . .	82
3-4	Energy deposition profile comparison for Problem 2 . .	83
3-5	Energy deposition profile comparison for Problem 3 . .	84
3-6	Charge deposition profile comparison for Problems 1, 2, and 3. . . . .	87
3-7	Charge deposition profile comparison for Problem 1 . .	89
3-8	Charge deposition profile comparison for Problem 2 . .	90
3-9	Charge deposition profile comparison for Problem 3 . .	91
3-10	Reflected current spectrum comparison for Problem 2. .	94
3-11	Transmitted current spectrum comparison with various group structures for Problem 2 . . . . .	94
3-12	Reflected current spectrum comparison for Problem 2. .	95
3-13	Transmitted current spectrum comparison for Problem 2. . . . .	98
A-1	Standard phase-space coordinate system . . . . .	104
A-2a	Direction-space coordinate system. . . . .	106
A-2b	Direction-space coordinate system. . . . .	109
A-2c	Direction-space coordinate system. . . . .	110
C-1	Flowchart of quadrature subroutines in MORSE . . . . .	167

## LIST OF TABLES

## CHAPTER I

### INTRODUCTION

Transport theory is the study of the phenomenon whereby particles are "transported" from one element of phase space (position, solid angle, energy, and time) to a different element of phase space through interactions such as elastic or inelastic scattering, absorption, or radiative collisions. The mathematical equation which describes this radiation propagation is known as the Boltzmann or transport equation (the transport equation and a description of its variables is given in the first part of Appendix A). Although the transport equation is relatively simple to derive, it is unfortunately quite difficult to solve for any but the simplest model problems. The solution to the transport equation is usually obtained through different numerical schemes, such as the discrete-ordinates method, or by direct simulation of the particle behavior as it travels through matter; i.e., the Monte Carlo method.

One code system based on the Monte Carlo technique is called MORSE. It has been used extensively at Sandia National Laboratories and in the general transport community because of some distinct features which make it adaptable to many transport problems. MORSE (Multigroup Oak Ridge Stochastic Experiment) is specifically a multi-purpose neutron and gamma-ray transport Monte Carlo code. It was developed at ORNL and the University of Tennessee in the late 1960s

by Straker et al. (1970). Some of its features include (Emmett, 1975):

- (1) the ability to treat the transport of either neutrons or gamma-rays, or a coupled neutron and secondary gamma-ray problem,
- (2) the use of multigroup cross sections,
- (3) forward or adjoint transport capability,
- (4) modular input-output, including cross section analysis and geometry modules,
- (5) debugging routines,
- (6) time dependence for both shielding and criticality problems,
- (7) albedo option at any material boundary,
- (8) three-dimensional combinatorial geometry package, and
- (9) several types of optional importance sampling.

#### Research Objectives

The primary research objective of this work is to extend the transport capabilities of MORSE. The research consists of two distinct but related parts:

- (1) provide an option in MORSE whereby each group-to-group transfer may be sampled at a forward scattering angle of zero degrees (for treating cross sections having forward-peaked delta function components), and

- (2) develop multigroup Legendre cross sections suitable for input to MORSE for performing charged-particle Fokker-Planck calculations.

The first research topic will be introduced in Chapter II, and the second in Chapter III. The research is sponsored by a contract (Document Number 61-9208) between Sandia National Laboratories and the Department of Chemical and Nuclear Engineering of the University of New Mexico (contractor).

It is not our intent or within the scope of this paper to describe in depth the MORSE code or the Monte Carlo technique. The documentation on MORSE by Emmett (1975) and Dupree and Lighthill (1982) detail thoroughly the capabilities and effective use of the code. For the Monte Carlo technique, the references by Carter and Cashwell (1975), Renken (1980), Selph and Garrett (1973), and Spanier and Gelbard (1969) are just a few examples of the available study material.

In the rest of this chapter, we first briefly discuss some general comparisons between Monte Carlo and discrete-ordinates codes in order to better understand the relative importance of extending the capabilities of MORSE. We will then highlight two topics which particularly concern our research: the Monte Carlo technique of biased sampling and the processing of multigroup cross section sets in MORSE.

### Comparison Between Monte Carlo and Discrete-Ordinates Techniques

Both Monte Carlo (MC) and discrete-ordinates (DO) methods for transport calculations have certain advantages and disadvantages which must be evaluated in selecting the type of code best suited for a particular problem. We will briefly discuss some of these factors below.

The basic difference between MC and DO is that the MC technique is a simulation of particle transport, whereas DO methods attempt to solve the Boltzmann equation via direct discretization of the phase space variables. This results in inherent statistical uncertainty in MC solutions, but deterministic solutions for DO. The accuracy of the DO solution is dependent upon the extent to which the discrete phase space mesh can be refined. The reliability of the MC estimate, however, depends upon the number of particles tracked and the use of various variance reducing techniques. Because standard (analog or continuous) MC calculations are sometimes impractical to perform, certain types of discrete approximations are often employed in the MC algorithm. The multigroup Legendre cross section employed in MORSE is an example of this type of approximation. In such cases, the MC solutions are subject to both statistical and discretization errors.

One advantage of DO is the ease with which adjoint calculations may be performed in comparison with continuous MC. However, adjoint calculations are also quite easy with the MORSE code system, due to its use of multigroup cross sections. Adjoint calculations for

continuous MC are still currently an area of active research in the radiation transport field.

A common disadvantage of DO codes for two and three dimensions is the so-called "ray effect." This effect results from a lack of rotational invariance in the DO equations and manifests itself in the form of non-physical oscillations in the flux solution. The MORSE code also suffers from a type of ray effect, though generally not as severe as the DO ray effect, caused by its discretized representation of the scattering angles. Continuous MC and one-dimensional DO codes do not show these effects. In general, both types of ray effects are diminished for media characterized by comparatively high scattering-to-absorption cross section ratios. In MORSE, the ray effect may also be decreased by inputting higher order Legendre cross section expansions so as to allow for more discrete scattering angles (see Chapter II).

An advantage of MC codes is that they are not geometry limited; i.e., they may be adapted to complex physical geometries in as much detail as necessary. The DO method on the other hand requires that the geometry be expressed in terms of a standard (i.e., cartesian, spherical, cylindrical, etc.) coordinate system.

The running time on the computer is also a factor in choosing between MC and DO. The DO codes are much faster in one-dimensional geometries, but for two or three dimensions with steady-state conditions, the comparative running time becomes problem specific. If the

transport problem is time dependent and uses multidimensional geometries, the MC codes are easily the most efficient.

### Importance Sampling

As mentioned previously, the Monte Carlo method attempts to estimate the solution of a transport problem by analog or direct simulation of the real world. The simulation requires that "samples" or individual particles be tracked through the medium geometry from its source to the point where its case history is terminated through leakage from the medium, absorption, Russian roulette, by time kill, or energy kill. The tracking, or "random walk", is accomplished by choosing alternative events for the particle through random sampling of known cumulative probability distributions. Since the tracking of individual microscopic particles can never be predicted with certainty, the random walk is non-deterministic. However, by applying the law of large numbers, or in the limit as the number of samples increases, the solution obtained from the samples should adequately represent the true solution from the "parent population". The relationship between the Boltzmann equation and Monte Carlo is often viewed as empirical; that is, Monte Carlo simply models in detail the principles from which the transport equation was derived. However, the Monte Carlo technique can also be shown to correspond to each term of the Boltzmann in a more direct manner (see Section 4.10 of Emmett, 1975).

To fully simulate particle transport, one would certainly include particle elimination by absorption. However, if the transport medium is characterized by high absorption cross sections and the solution requires deep penetration of particles, then a Monte Carlo code would typically require many case histories to obtain relatively good statistics on such a calculation. In order to reduce the variance in the result for a given amount of computer time, MORSE does not permit particles to die by absorption. Instead, a quantity known as the "weight" is assigned to the particle as it leaves the source. This weight is used in calculating the particle's contribution to the solution and is changed as the particle proceeds through the system so as to compensate for the lack of absorption. This technique is known as "survival biasing".

There are many ways in which a calculation may be biased. Some examples of biasing, or "importance sampling", are source direction biasing, Russian roulette, path stretching or exponential transform, splitting, and time and energy cutoffs. Biasing essentially involves sampling from fictitious probability density functions. It is a method whereby certain alternative events which are more likely to contribute to the desired result are sampled more frequently, while other events which contribute little to the result are sampled less frequently.

Choosing the best method to bias the particle random-walk process often involves some degree of insight, experience, and trial and

error. It is for this reason that the efficient and proper use of Monte Carlo, although based on scientific principles of probability, has come to be viewed somewhat as an "art". If we are not careful, some methods of importance sampling may actually increase rather than decrease the statistical error. Thus, it would certainly be advantageous to have a theoretical basis for choosing the best bias technique. Such a basis exists and takes the form of a so-called "importance function". The importance function identifies those trajectories which are "important" to the solution of the problem. Coveyou et al. (1967), and Renkin (1970 and 1980) explain that a near-optimal choice for this importance function is the solution to an appropriate adjoint transport equation. The importance function is usually as difficult to calculate as the transport solution itself. However, even a crude approximation to the importance function is often sufficient to significantly reduce the variance of the calculation. One advantage of MORSE is its ability to perform adjoint calculations. Therefore, if for a certain transport problem, the discrete approximations in MORSE cause it to be inadequate, then it would be appropriate to perform an adjoint calculation and then use the resulting importance function to bias an analog Monte Carlo calculation.

#### Group-to-Group Transfer Cross Sections in MORSE

The implementation of multigroup, multitable cross section sets into Monte Carlo codes offers three distinct advantages over continuous or analog Monte Carlo:

- (1) the cross section sets are already generally available since they are used extensively in discrete ordinate applications,
- (2) they permit a relatively easy solution of the adjoint transport equation (coupled neutron-photon or electron-photon adjoint capability for continuous energy Monte Carlo is currently unavailable), and
- (3) they offer a simple technique for the simultaneous treatment of several types of radiation (i.e., neutrons and photons, electrons and photons, etc.).

The primary disadvantage of using multigroup cross sections is that the fine structure detail in the cross section is lost.

Continuous Monte Carlo essentially samples probabilities of interaction, collision parameters, etc., by interpolating from a table of numbers at discrete energies. A coupled neutron-photon code for continuous Monte Carlo called MCNP is currently in use at the Los Alamos Scientific Laboratory (see LASL, 1981). However, at the outset of the development of MORSE, such a code was not available, and the simultaneous transport of neutrons and photons was obtained through separate neutron and photon codes in a kind of bootstrapping operation. Since the physics of the interaction processes for neutrons and photons is so different, a coupled neutron-photon code would have required excessive core storage to handle all of the cross section input and also a large computer access time. The calculations then, were computer capability limited. The combination of

multigroup cross section sets with Monte Carlo offered a very practical solution to the problem for several reasons (Emmett, 1975):

- (1) each energy group contains the cross section for all processes,
- (2) multigroup cross sections have the same format for neutrons and gammas,
- (3) the logic of the random walk process becomes the same for neutrons and gammas,
- (4) for anisotropic scattering, each group-to-group transfer cross section contains an angular distribution which is a weighted average over the various cross sections involved in the energy process; i.e., the neutron cross section is a weighted average of elastic and inelastic probabilities, and the gamma cross section is a weighted average of the photoelectric effect, pair production, and Compton scattering probabilities, and
- (5) the generation of a secondary gamma ray may be considered as just another group-to-group transfer.

In summary, the use of multigroup cross sections reduces the effort required to produce, store, and sample from the cross section libraries.

For input into the MORSE code system, the cross sections must be in the AMPX working library format. The ORNL AMPX package (see Greene et al., 1976) is a modular system for producing (generating

and collapsing) coupled multigroup neutron-gamma ray cross section sets. The basic neutron and gamma cross section data used as input for AMPX are obtained from the ENDF/B libraries. MORSE initially used multigroup cross sections in the ANISN format. One feature of converting to the AMPX format is that none of the zeros in the scattering matrix are stored. This produces a slightly more complex data system for input into MORSE but it also saves considerable computer core. One of the useful AMPX routines is called LAVA (Let ANISN Visit AMPX) which will read ANISN-formatted cross sections and write an AMPX working library cross section set.

The older versions of MORSE (along with many discrete-ordinates codes) were sometimes "cross section limited" because they read in all the cross sections at one time. The current version of MORSE at Sandia National Laboratories is termed MORSE-SGC (Super-Grouped Cross Sections). MORSE-SGC has the capability of loading cross sections into the core, one table at a time. After some processing, the cross sections are stored on a disk and may be recalled into the core a few groups (or one supergroup) at a time for further processing. This reduces the amount of central memory usually allotted to cross sections.

The multigroup cross section processing steps in MORSE-SGC are enumerated below (Emmett, 1975).

First: MORSE-SGC reads AMPX cross sections for media or elements. The types of cross sections which may be processed are neutron only, gamma-ray only, coupled neutron-gamma ray, or gamma ray

from coupled neutron-gamma ray. Fission probabilities may also be included. The fission and total cross section for each energy group are first read for a particular element into a buffer area and then stored. Then each  $P_0$  coefficient from the group-to-group Legendre expansions is read and placed into its particular slot in a downscatter matrix. A downscatter matrix is similarly formed from the  $P_1$  coefficients, the  $P_2$  coefficients, etc. The cross sections are transposed and stored if an adjoint problem is being solved.

Second: after the cross sections for all the elements are read and stored, the cross sections are mixed to obtain the media cross sections.

Third: the nonabsorption probability and the gamma production probabilities are determined for each energy group by dividing the sum of all the probabilities of transfer from that energy group by its total cross section. The fission cross section for each energy group is also divided by its total cross section to obtain corresponding probabilities of fission. The downscatter matrices are converted to probability tables by dividing by the scattering cross sections.

Fourth: the Legendre expansion for each group-to-group transfer is used as a weight function in a generalized Gaussian quadrature technique to obtain discrete angles and probabilities of scattering at those angles; i.e.,

$$\int_{-1}^{+1} f(\mu_0) g(\mu_0) d\mu_0 = \sum_{i=1}^n g(\mu_i) w_i , \quad (1-1)$$

where  $g(\mu_0)$  = any polynomial of order  $2n-1$  or less,

$f(\mu_0)$  = the angular distribution for  $\mu_0$ , the cosine of the scattering angle,

$\mu_i$  = the set of discrete cosines, and

$w_i$  = the associated probability for each scattering cosine.

Chapter II and Appendix B treat this subject in depth.

## CHAPTER II

### GENERATION OF DISCRETE SCATTERING ANGLES USING RADAU QUADRATURE

The first phase of the research intended to extend the capabilities of MORSE is to provide MORSE with the option of calculating a set of discrete scattering angles, one of which is a forward scattering angle at zero degrees. The second phase of the research is introduced in Chapter III.

MORSE currently converts the multigroup Legendre expansions to a set of discrete scattering angles and probabilities of scattering at those angles using a generalized Gauss quadrature technique. The probabilities (or weights) are summed and then normalized to form a cumulative probability distribution. MORSE samples a scattering angle in its random walk process by generating a random number between 0 and 1, locating the probability interval in the cumulative distribution between whose limits the random number lies, and then matching the chosen probability with its appropriate scattering angle. The discrete scattering angles tend to concentrate in those regions of the actual angular distribution which have high probabilities or peaks.

The Gauss quadrature technique generates discrete direction cosines only on the open interval  $(-1, +1)$ . However, it is desirable in certain particle transport applications to have some finite probability in each group-to-group transfer for scattering at zero degrees.

One such application, the extended transport cross section correction, is discussed in a later section. In order to obtain a forward scattering angle for sampling, a generalized Radau quadrature technique has been implemented in MORSE. The rest of this chapter continues to introduce the Gauss and Radau quadrature techniques as methods for obtaining sampling angles in MORSE, Appendix B details the theory of the two quadrature methods, and Appendix C contains a listing of the updated version of MORSE with the Radau quadrature option.

#### Legendre Polynomial Expansions of Angular Distributions

Scattering angular distributions ( $\sigma$ ) are most often expressed through a Legendre expansion of the distribution in terms of the cosine of the scattering angle ( $\mu_0 = \cos \theta_0$ ). Since elastically scattered neutrons are scattered symmetrically about the azimuthal angle ( $\phi_0$ ), the scattering distribution may be represented as

$$\frac{d\sigma}{d\Omega} = \frac{\sigma(E)}{2\pi} f(E, \mu_0) , \quad (2-1a)$$

where  $E$  is the energy of the incident neutron,  $\sigma(E)$  is the total scattering cross section for that energy,  $E$ , and

$$\int_{-1}^{+1} f(E, \mu_0) d\mu_0 = 1 . \quad (2-1b)$$

We may expand  $f(E, \mu_0)$  in terms of Legendre polynomials

$$f(E, \mu_0) = \sum_{\ell=0}^{\infty} \frac{2\ell + 1}{2} f_{\ell}(E) P_{\ell}(\mu_0) . \quad (2-2)$$

(Davis (1966) and Horsley (1966) discuss the techniques involved in evaluating angular distributions and reducing the data into the expansion form convenient for computer calculations). The energy-dependent Legendre coefficients ( $f_{\ell}(E)$ ) of the angular distribution may be obtained by applying the principle of orthogonality of the Legendre polynomials:

$$\begin{aligned} & \int_{-1}^{+1} \frac{d\sigma}{d\Omega} P_k(\mu_0) d\mu_0 \\ &= \frac{\sigma(E)}{2\pi} \sum_{\ell=0}^{\infty} \frac{2\ell + 1}{2} f_{\ell}(E) \int_{-1}^{+1} P_{\ell}(\mu_0) P_k(\mu_0) d\mu_0 . \quad (2-3) \end{aligned}$$

Since

$$\int_{-1}^{+1} P_{\ell}(\mu_0) P_k(\mu_0) d\mu_0 = \begin{cases} 0 & , \quad k \neq \ell \\ \frac{2}{2\ell + 1} & , \quad k = \ell \end{cases} \quad (2-4)$$

then

$$f_{\ell}(E) = \frac{2\pi}{\sigma(E)} \int_{-1}^{+1} \frac{d\sigma}{d\Omega} P_{\ell}(\mu_0) d\mu_0 . \quad (2-5)$$

If  $\ell=0$ , we have  $f_0(E)$  equals 1. Since an infinite number of coefficients ( $f_{\ell}$ ) would require too much memory space, the expansion is truncated at some convenient order ( $n$ )

$$f^*(E, \mu_0) = \sum_{\ell=0}^n \frac{2\ell + 1}{2} f_{\ell}(E) P_{\ell}(\mu_0) . \quad (2-6)$$

These Legendre expansions are often found to be very useful because they offer significant analytical simplifications and compact storage of cross section data in computer codes. However, the primary disadvantage of the Legendre expansions is that its truncated version may contain severe distortions of the actual cross sections, and even regions of negativity between (-1,+1). These truncated expansions may then produce nonphysical fluctuations in the computed angular flux.

The errors resulting from premature truncation of the Legendre expansion tend to increase as the anisotropy of the cross sections increases. Highly anisotropic cross sections are very common in transport calculations, particularly for problems involving (1) radiative or charged particle transport, (2) elastic scattering from light elements, or (3) group-to-group transfer cross sections with fine energy group structure. The MORSE code system uses group-to-group transfer cross sections.

The group  $g$  to group  $k$  transfer cross section (refer to Bell and Glasstone, 1970) can be defined as

$$\sigma_{g \rightarrow k} \equiv \int_{E_{k+1}}^{E_k} dE \int_{E_{g+1}}^{E_g} dE' \psi(\bar{r}, \bar{\Omega}', E') \sigma(\bar{r}, E' + E, \mu_0) / \int_{E_{g+1}}^{E_g} dE' \psi(\bar{r}, \bar{\Omega}', E') , \quad (2-7)$$

where  $\psi$  is the angular flux as a function of position, initial solid angle, and initial energy, and where  $\sigma$  is the differential cross section for scattering from  $E'$  to  $E$  through  $\mu_0$ . If we postulate that within an energy group, the dependence of  $\psi$  on  $E'$  is separable from its dependence on  $\bar{\Omega}'$  and  $\bar{r}$ ; then

$$\psi(\bar{r}, \bar{\Omega}', E') = f_1(\bar{r}, \bar{\Omega}') f_2(E') . \quad (2-8)$$

If we further assume that  $f_2(E')$  is a constant, then Equation (2-7) becomes

$$\sigma_{g \rightarrow k} = \int_k dE \int_g dE' \sigma(\bar{r}, E' \rightarrow E, \mu_0) / \Delta E' . \quad (2-9)$$

Expanding both  $\sigma_{g \rightarrow k}$  and  $\sigma(\bar{r}, E' \rightarrow E, \mu_0)$  in terms of Legendre polynomials,  $P_\ell(\mu_0)$ , we obtain a slightly different equation:

$$\sigma_{\ell, g \rightarrow k} = \int_k dE \int_g dE' \sigma_\ell(\bar{r}, E' \rightarrow E) / \Delta E' . \quad (2-10)$$

Both elastic and inelastic scattering probabilities contribute to the cross section. However, inelastically scattered neutrons are usually assumed to be emitted isotropically in the center of mass system. Also, for heavy scatterers, the laboratory and center of mass systems become almost equivalent, and the inelastic scattering becomes isotropic in the laboratory system as well. Therefore, the inelastic group-to-group transfer may be accounted for by the addition of a constant over the entire range of scattering angles to the

elastic group-to-group cross section (Odom and Shultis, 1976).

Focussing then just on elastic scattering, the differential cross section may be written as

$$\sigma(E' \rightarrow E, \mu_0) = \sigma(E' \rightarrow E) \delta(\mu_0 - \mu_s) , \quad (2-11)$$

where the  $\delta$ -function represents the direct coupling between energy and angle, and  $\mu_s$  is a function of  $(E', E)$ . The Legendre expansion of the differential cross section will have the coefficients

$$\sigma_\ell(E' \rightarrow E) = \int_{-1}^{+1} \sigma(E' \rightarrow E) \delta(\mu_0 - \mu_s) P_\ell(\mu_0) d\mu_0 \quad (2-12a)$$

$$= \sigma(E' \rightarrow E) P_\ell(\mu_s) \quad (2-12b)$$

which may be substituted into Equation (2-10) to calculate  $\sigma_{\ell,g+k}$ .

We will usually refer to the normalized coefficients of  $\sigma_{\ell,g+k}$  for some arbitrary  $g$  and  $k$  simply as  $f_\ell$ . More detailed information on the generation and use of multigroup cross sections may be found in references by Bucholz (1980), Kidman et al. (1972), and Weisbin et al. (1974).

Figure (2-1) shows a comparison between an actual group-to-group transfer cross section and an eighth-order Legendre polynomial approximation. Note that the truncated Legendre expansion predicts two regions of unrealistic negative cross section values. For "direct" sampling of some partially negative function,  $f^*(\mu_0)$ , a scattering angle  $\mu_s$  is sampled from the density function

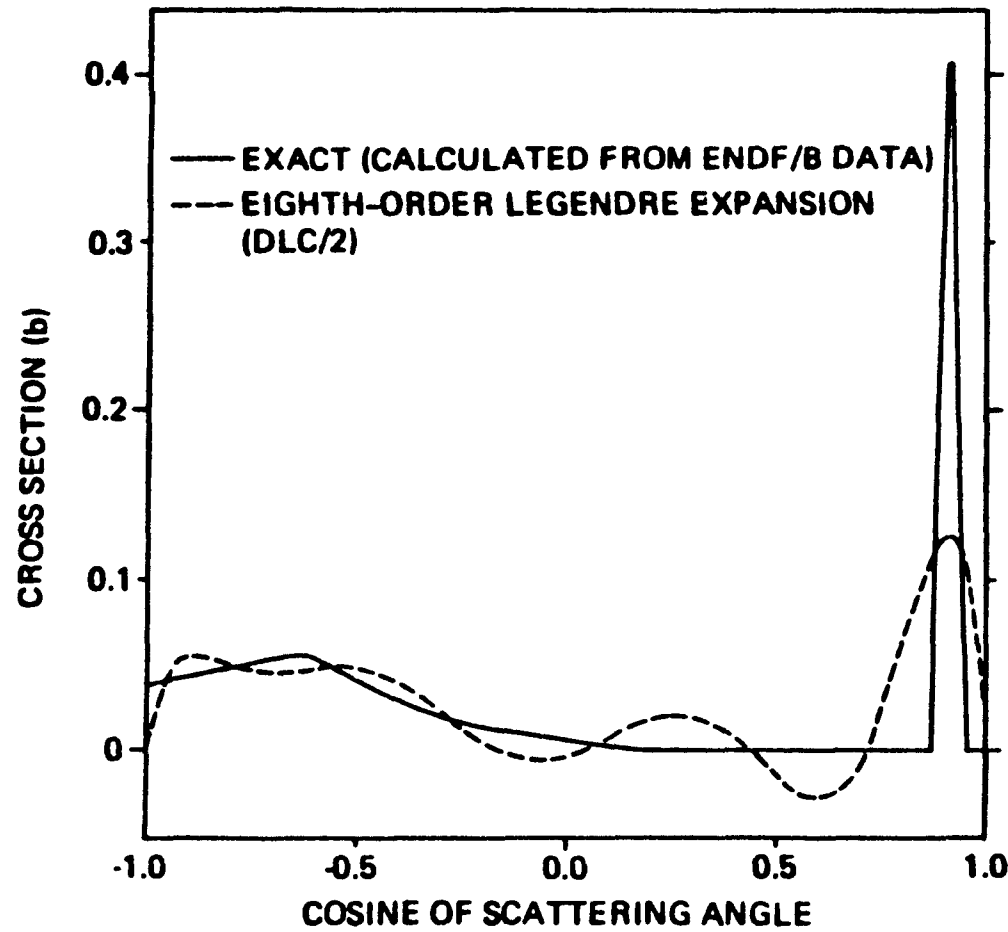


Figure 2-1. Comparison of water group-to-group elastic scattering cross section with an eighth-order Legendre polynomial approximation (Odom and Shultz, 1976). The energy groups (in MeV) are (3.0119-3.3287) to (2.4660-2.7253).

$$f_p(\mu_0) = \left| f^*(\mu_0) \right| / \int_{-1}^{+1} \left| f^*(\mu'_0) \right| d\mu'_0, \quad (2-13)$$

where  $f_p(\mu_0)$  is an everywhere positive, renormalized distribution function, and then the weight of the particle is multiplied by  $f^*(\mu_0)/f_p(\mu_0)$  to account for the use of a "biased" distribution. Whenever  $f^*(\mu_0)$  is negative, the particle weight becomes negative; this is reasonable since the number of particles that scatter into  $d\mu_0$  about  $\mu_0$  is proportional to  $f^*(\mu_0) d\mu_0$ . However, these "negative" particles tend to increase the statistical errors in the Monte Carlo random walk.

#### Discrete Angle Approximations of Angular Distributions

Gauss Quadrature. In order not to sample negative probabilities, we seek to replace  $f^*(\mu_0)$  with a discrete distribution,  $f_d(\mu_0)$ ,

$$f_d(\mu_0) = \sum_{i=1}^n \omega_i \delta(\mu_0 - \mu_i), \quad (2-14)$$

where  $f_d(\mu_0)$  must meet two obvious requirements for sampling:

- (1)  $\omega_i > 0$  for  $i = 1, n$  and
- (2)  $-1 < \mu_i < 1$  for  $i = 1, n$ .

A third requirement is clearly desirable for  $f_d(\mu_0)$ :

- (3) its first  $2n$  moments,  $\{(M_d)_k\}_{k=0}^{2n-1}$ , are identical to those of the truncated expansion of  $f(\mu_0)$ .

The above three requirements are satisfied if the  $\mu_i$  and  $w_i$  of  $f_d(\mu_0)$  are obtained through Gauss quadrature operating on  $f^*(\mu_0)$ . Requirements 1 and 2 are discussed in Appendix B. For the third requirement, let us first review the Gauss quadrature formulae:

Given a non-negative weight function,  $f(x) \geq 0$  (Restriction I), with  $x$  as a dummy variable, we want

$$\int_{-1}^{+1} f(x) g(x) dx = \sum_{i=1}^n w_i g(x_i) \quad (\text{Restriction II}) \quad (2-15)$$

to hold for all  $g(x)$  where  $g(x)$  is a polynomial of degree  $\leq 2n-1$ .

To obtain  $w_i$  and  $x_i$ , we determine a set of polynomials  $Q_i(x)$  orthogonal with respect to  $f(x)$

$$\int_{-1}^{+1} Q_i(x) Q_j(x) f(x) dx = \delta_{ij} N_i, \quad (2-16)$$

where  $\delta_{ij}$  is the Kronecker delta and  $N_i$  is the normalization constant. Then the  $x_i$  are given by the  $n$  roots of  $Q_n(x)$  and

$$w_i = \left\{ \sum_{k=0}^{n-1} Q_k^2(x_i) / N_k \right\}^{-1}. \quad (2-17)$$

Since the functions  $\{x^k\}_{k=0}^{2n-1}$  are independent and form a basis function for the space of polynomials  $g(x)$ , it is equivalent to Restriction II (Equation (2-15)) to require that

$$M_k = \int_{-1}^{+1} x^k f(x) dx = \sum_{i=1}^n w_i x_i^k \quad \text{for } k=0, 2n-1. \quad (2-18)$$

The integral ( $M_k$ ) above is defined as the  $k^{\text{th}}$  moment of  $f(x)$ .

The moment of  $f_d(x)$  is defined as

$$(M_d)_k = \int_{-1}^{+1} x^k f_d(x) dx = \sum_{i=1}^n \omega_i \int_{-1}^{+1} x^k \delta(x - x_i) dx \quad (2-19a)$$

$$= \sum_{i=1}^n \omega_i x_i^k, \quad k=0, 2n-1. \quad (2-19b)$$

Comparing Equations (2-18) and (2-19b), we see that for  $M_k$  and  $(M_d)_k$  to be equivalent, then the  $\omega_i$  and  $x_i$  of  $f_d(x)$  must be obtained through Gauss quadrature operating on  $f(x)$ .

The derivation of the formulas for Gauss quadrature is found in Appendix B. It is also shown in Appendix B that

- (a) Legendre coefficients and moments are equivalent; in other words, the  $k^{\text{th}}$  moment of  $f(\mu_0)$  is derived from the first  $k$  Legendre coefficients of  $f(\mu_0)$ .
- (b) The orthogonal polynomials  $\{Q_0, \dots, Q_n\}$  (and hence the  $n$  roots  $\{\mu_1, \dots, \mu_n\}$ ) may be derived from the first  $2n$  moments of  $f(\mu_0)$ .

Therefore, in order to obtain the scattering angles ( $\mu_i$ ) and probabilities ( $\omega_i$ ) of  $f_d(\mu_0)$  accurate to order  $2n-1$ , knowledge of the exact angular distribution is not required. We only need to know  $f_0, \dots, f_{2n-1}$  or  $M_0, \dots, M_{2n-1}$  to obtain  $f_d(\mu_0)$ . Therefore, the generalized quadrature that has been developed is valid for the whole class of functions having the same first  $2n$  Legendre coefficients or moments; i.e., the same Legendre expansion:

$$f(\mu_0) \approx f^*(\mu_0) = \sum_{\ell=0}^{2n-1} \frac{2\ell+1}{2} f_\ell P_\ell(\mu_0) . \quad (2-20)$$

In particular, the discrete distribution ( $f_d(\mu_0)$ ) derived using Gauss quadrature is itself one function in this class. We show that  $f_d(\mu_0)$  has the same coefficients,  $f_\ell$ , as  $f^*(\mu_0)$  with the simple equation sequence below:

$$f_\ell = \int_{-1}^{+1} f^*(\mu_0) P_\ell(\mu_0) d\mu_0 , \quad \ell=0, 2n-1 \quad (2-21a)$$

$$= \sum_{i=1}^n \omega_i P_\ell(\mu_i) \quad (2-21b)$$

$$= \sum_{i=1}^n \omega_i \int_{-1}^{+1} \delta(\mu_0 - \mu_i) P_\ell(\mu_0) d\mu_0 \quad (2-21c)$$

$$= \int_{-1}^{+1} f_d(\mu_0) P_\ell(\mu_0) d\mu_0 . \quad (2-21d)$$

In developing the Gauss quadrature, we were given a prerequisite (Restriction I) that the weight function  $f(\mu_0)$  was everywhere greater than zero. Although the actual angular distribution  $f(\mu_0)$  is everywhere positive by definition, the truncated expansion  $f^*(\mu_0)$  may not be. However, since only the first  $2n$  moments of a class of functions are needed to develop the quadrature, it is not required that all the functions of this class be non-negative; in

fact, there are infinitely many which are not. However, it is necessary that at least one function in this class be non-negative (Emmett, 1975).

We have discussed how negative cross section values may result due to the truncation of an infinite Legendre series. However, it is also possible that a given set of Legendre coefficients may result in negative cross sections because they do not represent a physically possible (everywhere positive) angular distribution. Irving et al. (1966) performed a check on Legendre coefficients from several published sources and found a surprisingly large number of instances where the coefficients were impossible. What are the mathematical criteria that must be satisfied in order that there exist an everywhere positive distribution having a given set of Legendre coefficients? It was shown by Irving et al. that  $f^*(\mu_0)$  represents (or originated from) an everywhere positive function if we can find an  $f_d(\mu_0)$ , where the weights are all greater than zero and the roots lie between (-1,+1). The failure of either of these two conditions expresses the fact that the given coefficients or moments of  $f^*(\mu_0)$  are not those of an everywhere positive function.

The first condition on  $f_d(\mu_0)$ , that  $\omega_i \geq 0$ , is replaced in the MORSE code system by the requirement that

$$N_k > 0 \text{ for } k=1, n-1 . \quad (2-22)$$

Since

$$\omega_i = \left\{ \sum_{k=1}^{n-1} Q_k^2(\mu_i) / N_k \right\}^{-1} \quad (2-17)$$

then we are guaranteed that all the  $\omega_i$  will be non-negative if all the  $N_k$  are greater than zero. In addition, Appendix B shows that if the  $N_k$  are all positive, then the orthogonal polynomial sequence  $\{Q_0, \dots, Q_n\}$  will be unique, and the weight function is at least "well-behaved". Stroud and Secrest (1966) also mention that for positive  $N_i$ , the zeros  $\mu_1, \dots, \mu_n$  of the polynomial  $Q_n(\mu_0)$  will be real and distinct and that they will separate the zeros of  $Q_{n+1}(\mu_0)$ . However, in order to guarantee that the zeros lie between  $(-1, +1)$ , we must be dealing with the coefficients of a non-negative weight function.

Radau Quadrature. The generalized Radau quadrature technique is very analogous to--and may be considered an extension of--the Gauss quadrature method. In effect, we seek to replace  $f^*(\mu_0)$  with a discrete distribution

$$f_d(\mu_0) = \sum_{i=1}^{n-1} \omega_i \delta(\mu_0 - \mu_i) + \omega_n \delta(\mu_0 - 1), \quad (2-23)$$

where  $f_d(\mu_0)$  must meet the same three requirements mentioned for Gauss quadrature, along with a fourth requirement that one of the direction cosines lie at  $\mu_0 = 1$ . In order to satisfy these requirements, the Legendre coefficients for each group-to-group

transfer are converted to angles and probabilities of scattering at those angles by the use of a generalized Radau quadrature:

Given a non-negative weight function,  $f(x) \geq 0$  (Restriction I), we want

$$\int_{-1}^{+1} f(x) g(x) dx + \sum_{i=1}^{n-1} \omega_i g(x_i) + \omega_n g(1) \quad (\text{Restriction II}) \quad (2-24)$$

to hold for all  $g(x)$  where  $g(x)$  is a polynomial of degree  $\leq 2n-2$  (this is one degree less than for Gauss quadrature since we have pre-assigned one of the parameters). A set of  $x_i$ 's and  $\omega_i$ 's that satisfy Equation (2-24) must be found. As explained in Appendix B, we determine a set of polynomials,  $Q_i$ , which is orthogonal with respect to an altered weight function.

$$\bar{\omega}(x) = \omega(x)(1 - x) \quad (2-25)$$

such that

$$\int_{-1}^{+1} Q_i(x) Q_j(x) \bar{\omega}(x) dx = \delta_{ij} N_i, \quad (2-26)$$

where  $N_i$  is the normalization constant. The moments of the altered weight function  $M_i$ ,  $i=0, 2n-3$ , determine the orthogonal polynomials  $Q_i$ ,  $i=1, n-1$ . The  $n-1$  discrete abscissas,  $x_i$ , are given by the roots of  $Q_{n-1}$ ,

$$Q_{n-1}(x_i) = 0, \quad (2-27)$$

and the corresponding probabilities are

$$\omega_i = \left\{ (1 - x_i) \sum_{k=0}^{n-2} Q_k^2(x_i) / N_k \right\}^{-1} \quad \text{for } i=1, n-1, \quad (2-28)$$

and

$$\omega_n = 1 - \sum_{i=1}^{n-1} \omega_i. \quad (2-29)$$

In the process of deriving the orthogonal polynomials, some restrictions on the moments of the altered weight function are obtained. As in the Gauss quadrature case, these restrictions arise if both the original distribution and the derived point distribution are to be everywhere positive. Two of these restrictions are:

- 1)  $N_i > 0$  for  $i=1, n-2$  and
- 2) The roots of  $Q_{n-1}(\mu_0)$  must all lie in the interval  $-1 < \mu_i < 1$ .

The above restrictions ensure that the  $\omega_i$ ,  $i=1, n-1$  are all positive and that the  $\mu_i$  are within the correct scattering range for Monte Carlo selection. However, they do not guarantee that the weight ( $\omega_n$ ) corresponding to the direction cosine of  $\mu_n = 1$  is positive. Therefore, for Radau quadrature, we have a third requirement:

- 3)  $\omega_n > 0$

(in Gauss quadrature, we recall that only the first two restrictions are needed to insure that all the weights are positive).

Advantages and Disadvantages of the Discrete Angle Representation. The reference by Carter and Forest (1976) discusses and compares three multigroup methods for sampling the scattering angle

after a group-to-group scattering event. Each of the methods uses the coefficients of a truncated Legendre expansion as a working base. These methods include (1) a direct sampling of the truncated Legendre series, (2) sampling from a discrete distribution of angles and probabilities which conserves all the moments of a truncated Legendre polynomial (the technique used in MORSE), and (3) sampling from a step function with bounds that are computed to conserve the first few moments of the Legendre expansion. However, each of the methods has distinct comparative advantages and disadvantages with regards to storage requirement, sampling, and modeling of the density function. We repeat below only those conclusions of Carter and Forest which concern the MORSE sampling techniques.

Advantages:

- (1) Only positive weights are used in the random walk.
- (2) The sampling of the scattering angle is computationally fast.
- (3) The standard flux estimators are positive (however, the point detector estimator may give negative fluxes or unrealistic fluxes during the first few collisions for highly directional extraneous sources).

Disadvantages:

- (1) Ray effects are present for the first few collisions.
- (2) Subroutines are needed to compute the discrete angles and probabilities.

- (3) For low-order truncations, a few discrete angles may not closely represent density functions unless they are highly localized.

The disadvantage of ray effects can be minimized somewhat by increasing the number of discrete sampling angles (and this in turn usually requires that the order of the Legendre expansion be increased). Increasing the number of sampling angles also has the effect of decreasing the statistical variance of the solution. For example, a third order Legendre expansion input into MORSE will provide a discrete scattering distribution of two scattering angles and two weights with Gauss quadrature, or three angles and three weights with Radau quadrature. Since both quadrature sets have two "free" angles (Radau quadrature has one angle "prefixed" at  $\mu_0 = 1$ ) which hopefully closely represents or adequately samples the density functions, then this would imply similarly low standard deviations on the response of the analog detectors. However, if we have MORSE calculate only two angles and two weights with Radau quadrature using the same  $P_3$  expansion, then only one angle is free to represent the density function. In such a case, the standard deviations may increase significantly.

One possibility for increasing the number of scattering angles without increasing the order of the Legendre expansion (or assuming a value of zero for higher-order moments) is to combine the angles and weights from both quadrature methods. That is, for a  $P_3$  expansion,

we may use the two angles and weights from Gauss quadrature, the three angles and weights from Radau quadrature computed with a preset angle at  $\mu_0 = 1$ , and the three angles and weights from Radau quadrature with a preset angle at  $\mu_0 = -1$ . After linearly combining each set of weights into one cumulative probability distribution, a total of eight discrete angles may be sampled. The accuracy of such a technique has not as yet been verified either theoretically or computationally but would have the advantage of decreasing ray effects, and perhaps that of decreasing the variance of a solution.

#### Comparison Between Radau Quadrature and the Extended Transport Cross-Section Correction

The extended transport cross-section correction (Morel, 1979) attempts to approximate a highly forward peaked cross section ( $\sigma(\mu_0)$ ) with the sum of a relatively low-order expansion and a delta function:

$$\sigma(\mu_0) = \sum_{\ell=0}^{\infty} \frac{2\ell+1}{4\pi} \sigma_{\ell} P_{\ell}(\mu_0) \quad (2-30)$$

$$= \sum_{\ell=0}^{2n-2} \frac{2\ell+1}{4\pi} \sigma_{\ell}^* P_{\ell}(\mu_0) + \frac{\alpha}{2\pi} \delta(\mu_0 - 1) . \quad (2-31)$$

The quantities  $\sigma_{\ell}^*$  and  $\alpha$  are obtained by first expanding the delta function in a series of Legendre polynomials

$$\delta(\mu_0 - 1) = \sum_{\ell=0}^{\infty} \frac{2\ell+1}{2} P_{\ell}(\mu_0) , \quad (2-32)$$

and substituting the expansion into Equation (2-31). This gives

$$\sigma(\mu_0) \approx \sum_{\ell=0}^{\infty} \frac{2\ell+1}{4\pi} (\sigma_{\ell}^* + \alpha) P_{\ell}(\mu_0) , \quad (2-33)$$

where we have arbitrarily set  $\sigma_{\ell}^* = 0.0$  for  $\ell \geq 2n - 1$ . If Equation (2-33) is to be equivalent to Equation (2-30) up to order  $2n-1$ , we require that

$$\sigma_{\ell}^* + \alpha = \sigma_{\ell} , \quad \ell=0, 2n-1 . \quad (2-34)$$

Since  $\sigma_{2n-1}^* = 0.0$ , then

$$\alpha = \sigma_{2n-1} \quad (2-35)$$

and

$$\sigma_{\ell}^* = \sigma_{\ell} - \sigma_{2n-1} , \quad \ell=0, 2n-2 . \quad (2-36)$$

Now, delta function scattering for within-group cross sections is equivalent to no scattering at all. Thus, we can delete the delta function from Equation (2-31) to obtain

$$\sigma(\mu_0) \approx \sum_{\ell=0}^{2n-2} \frac{2\ell-1}{4\pi} \sigma_{\ell}^* P_{\ell}(\mu_0) \equiv \sigma^*(\mu_0) . \quad (2-37)$$

Morel (1979) refers to  $\sigma^*(\mu_0)$  as the  $P_{2n-2}$  transport-corrected expansion corresponding to  $\sigma(\mu_0)$ . The lowest order expansion of  $\sigma^*(\mu_0)$ , or the  $P_1$  transport-corrected  $P_0$  expansion, is the classical transport-corrected cross section:

$$\sigma_0^* = \sigma_0 - \sigma_1 = \sigma_0(1 - \bar{\mu}) = \sigma_{tr} . \quad (2-38)$$

It should also be noted that  $\sigma^*(\mu_0)$  is smaller in magnitude and less forward peaked than  $\sigma(\mu_0)$ . Although  $\sigma^*(\mu_0)$  and  $\sigma(\mu_0)$  are dissimilar in appearance, they are however, equivalent to order  $2n-2$  in the sense that they yield identical  $P_{2n-1}$  solutions.

Let us here remark that the coefficients  $\sigma_\ell^*$  do not usually represent, or could not have originated from, an everywhere positive distribution. That is, if the coefficients  $\sigma_\ell^*$  are used as input for the MORSE code system, some of them will usually be rejected (this problem does not arise in  $P_n$  calculations). Therefore,  $\sigma^*(\mu_0)$  is often physically unrealistic even though the original function  $\sigma(\mu_0)$  is a positive distribution.

The extended transport correction subtracts from  $\sigma(\mu_0)$  a delta function of magnitude  $\alpha = \sigma_{2n-1}$  to obtain  $\sigma^*(\mu_0)$ . Now, if  $\sigma(\mu_0)$  is actually the sum of a delta function and some other function  $\xi$ , then the value of  $\sigma_\ell$  will gradually approach  $\alpha$  as  $\ell \rightarrow \infty$ . But in setting  $\alpha = \sigma_{2n-1}$ , we are assuming that  $\sigma^*(\mu_0)$  with order  $2n-2$  actually converges completely to  $\xi$ . In using the extended transport correction, it is difficult to decide what expansion order to use for  $\sigma^*(\mu_0)$  in order to retain sufficient accuracy in the calculations. Since the expansion order is determined by setting  $\alpha$  equal to some particular coefficient  $\sigma_{2n-1}$ , the question one really asks is how large or small to make  $\alpha$ .

We would expect that within-group cross sections would have a higher probability of scattering at angles near  $\mu_0 = 1$  than group-to-group cross sections. It follows (assuming elastic scattering) that the expansion coefficients of a within-group cross section would tend to remain close to  $\sigma_0$  (an extreme example would be a pure delta function with all its coefficients equal to  $\sigma_0$ ) whereas the group-to-group coefficients would approach zero much more rapidly (an extreme case would be isotropic scattering with  $f_0 = 1$  and all the other coefficients equal to zero). Therefore, within-group cross sections would require a relatively high  $\alpha$  and group-to-group cross sections a relatively low  $\alpha$ .

In order to fix  $\alpha$  correctly, we turn to Radau quadrature. We recall that Radau quadrature uses the normalized coefficients  $f_\ell$  of a truncated expansion

$$f(\mu_0) \approx \sum_{\ell=0}^{2n-2} \frac{2\ell+1}{2} f_\ell P_\ell(\mu_0) \quad (2-39)$$

to produce a discrete distribution with positive weights or probabilities for scattering at angles  $\mu_i$ :

$$f_d(\mu_0) = \sum_{i=1}^{n-1} \omega_i \delta(\mu_0 - \mu_i) + \omega_n \delta(\mu_0 - 1) . \quad (2-40)$$

The probability of scattering at  $\mu_0 = 1$  is equal to  $\omega_n$ . As shown in Equations (2-21a) through (2-21d), the discrete distribution ( $f_d$ ), if expanded in terms of Legendre polynomials, will have the

same first  $2n-2$  coefficient as  $f(\mu_0)$ . The coefficients are given by

$$f_\ell = \sum_{i=1}^{n-1} \omega_i P_\ell(\mu_i) + \omega_n, \quad \ell=0, 2n-2. \quad (2-41)$$

If we substitute Equation (2-41) into (2-39), we have

$$\sigma(\mu_0) \approx \frac{\sigma_0}{2\pi} \sum_{\ell=0}^{2n-2} \frac{2\ell+1}{2} f_\ell P_\ell(\mu_0) \quad (2-42a)$$

$$\approx \frac{\sigma_0}{2\pi} \sum_{\ell=0}^{2n-2} \frac{2\ell+1}{2} \left[ \sum_{i=1}^{n-1} \omega_i P_\ell(\mu_i) + \omega_n \right] P_\ell(\mu_0) \quad (2-42b)$$

$$\begin{aligned} & \approx \sum_{\ell=0}^{2n-2} \frac{2\ell+1}{4\pi} \left[ \sigma_0 \sum_{i=1}^{n-1} \omega_i P_\ell(\mu_i) \right] P_\ell(\mu_0) \\ & + \frac{\sigma_0 \omega_n}{2\pi} \sum_{\ell=0}^{2n-2} \frac{2\ell+1}{2} P_\ell(\mu_0). \end{aligned} \quad (2-42c)$$

If we note the similarities between Equation (2-42c) and (2-31), we have

$$\sigma(\mu_0) \approx \sum_{\ell=0}^{2n-2} \frac{2\ell+1}{4\pi} \sigma_\ell^* P_\ell(\mu_0) + \frac{\alpha}{2\pi} \delta(\mu_0 - 1), \quad (2-43a)$$

where

$$\sigma_\ell^* = \sigma_0 \sum_{i=1}^{n-1} \omega_i P_\ell(\mu_i) \quad (2-43b)$$

and

$$\alpha = \sigma_0 \omega_n. \quad (2-43c)$$

Two important points about Equations (2-43a) through (2-43c) are that the coefficients  $\sigma_\ell^*$  represent an everywhere positive distribution and the equations are exact up to order  $2n-2$  since

$$\sigma_\ell^* + \alpha = \sigma_\ell \quad \text{for } \ell=0, 2n-2. \quad (2-44)$$

Therefore, Radau quadrature is an exact method for breaking up a cross section into the sum of a delta function and a low-order, physically acceptable expansion. This is in contrast to the conventional transport correction which produces a low-order, physically unacceptable expansion by setting  $\sigma_{2n-1} = \alpha$ .

In order to illustrate the effectiveness of the Radau quadrature technique in performing the transport cross section correction, sample calculations were performed on a set of  $P_{12}$  electron cross section expansions (see Morel, 1979, for cross sections). Table 2-1 compares the ratio  $\sigma_0^*/\sigma_0$  for the conventional and Radau-based cross section corrections at several energies. Note that both transport

Table 2-1  
Delta Function Corrected Electron Cross Sections

<u>Energy (MeV)</u>	<u><math>\sigma_0^*/\sigma_1</math></u>	<u>Standard</u>	<u>Radau</u>
0.01	0.652	0.490	
0.10	0.132	0.141	
1.00	0.013	0.022	

corrections severely reduce the total magnitude of the cross sections at the higher energies, and therefore, greatly reduced running times can be expected in the MORSE calculations.

## CHAPTER III

### GENERATION OF CHARGED-PARTICLE MULTIGROUP CROSS SECTIONS USING THE FOKKER-PLANCK APPROXIMATION

In this chapter we shall introduce the second and primary research objective of this work; that of modifying MORSE to perform charged-particle Fokker-Planck calculations using appropriate multi-group Legendre cross section data. The first phase of the research has been introduced in Chapter II.

The Boltzmann equation models a full range of different types of particle interactions. The Fokker-Planck equation, however, is a simpler model which assumes that "grazing" collisions are the predominant interaction mechanism. Grazing collisions entail small losses in energy and small angles of scatter. The attraction and repulsion of charged particles is governed by the coulomb force; such interactions are forward peaked and are therefore prime candidates for the Fokker-Planck approximation. Tanenbaum (1967) suggested that "the Fokker-Planck term is a good approximation for long-range forces, such as the coulomb interaction between charged particles, and a poor approximation for short-range forces, such as the interaction of hard spheres".

Most of the applications of the Fokker-Planck approximation have been directed toward solving energetic charged-particle transport in controlled thermonuclear fusion schemes. Two applications in the inertial confinement scheme are the study of

- (1) the suprathermal electron energy deposition produced during the pellet implosion process, and
- (2) the outward propagation of the supersonic burn-wave caused by the reaction products redepositing their energy in the pellet; e.g., from a 3.5 MeV alpha particle produced in a deuterium-tritium reaction.

Many different methods have evolved over the past decade to solve the Fokker-Planck equation. Corman et al. (1975) devised a low-storage computer program which utilized a multigroup method to handle the energy dependence and a "flux-limited" diffusion coefficient to approximate the spatial dependence of the Fokker-Planck equation. However, the program was not suitable for problems with extreme source discontinuities in space or where detailed behavior within a mean free path of the source was important. Antal and Lee (1976) attempted to simulate charged particle mass and energy deposition in a plasma using  $S_n$  techniques. The characteristic finite difference equations were derived to conserve both mass and energy. However, one disadvantage of the method was that angular deflections were ignored. Moses (1977) solved the charged particle transport equation with a time-dependent particle tracking technique which approximated the trajectories of the charged particles, from creation to thermalization, as straight lines. Even though the integral tracking technique ignored angular deflections, it was sufficiently accurate to describe the slowing down of the larger thermonuclear

reaction products. Haldy and Ligou (1977) were able to take into account scattering anisotropy with their modified moment method, but were limited to infinite medium problems. One of the more extensive formalisms for obtaining a solution to the Fokker-Planck equation was developed by Mehlhorn and Duderstadt (1980). Difference relations for the Fokker-Planck collision term were derived and then implemented in a discrete ordinates code called TIMEX. The conservation of both particles and energy were continuously monitored in the code and both angular dispersion and velocity diffusion were accounted for.

Mehlhorn and Duderstadt admitted, however, that their method was not the most efficient way to perform Fokker-Planck calculations inasmuch as it required internal modification of the codes. They noted that in order to take advantage of, and directly utilize all of the varied and powerful discrete ordinates codes currently available for neutron transport, it would be much more productive to generate "effective Fokker-Planck cross sections" that could be used as input to the codes. Just such an enhancement was developed by J. E. Morel (1981) at Sandia National Laboratories. He succeeded in accommodating the angular dispersion and energy loss effects of the Fokker-Planck approximation into appropriate multigroup Legendre polynomial expansions which could be input directly into discrete ordinate codes without internal modification. This eliminated the need to develop a redundant or separate set of Fokker-Planck discrete ordinate codes to parallel those codes used for neutron transport.

Chapter I contained a brief discussion of some of the relative advantages and disadvantages of the Monte Carlo versus discrete ordinates method. The primary advantage of multigroup Monte Carlo, and in particular the MORSE code system, is its ability to perform three-dimensional forward or adjoint calculations for coupled neutron-photon transport. Since adjoint capability for coupled electron-photon transport currently does not exist with continuous energy Monte Carlo, the generation of effective Fokker-Planck cross sections for use in MORSE would provide an approximate, yet hopefully very reliable solution for adjoint electron-photon transport. Unfortunately, the Fokker-Planck Legendre expansions derived by Morel for discrete ordinate codes are not acceptable for use in MORSE; that is, the code system will reject them since they do not represent (or do not originate from) an everywhere positive distribution. Thus, the purpose of this work is to determine a new general purpose algorithm for generating the Fokker-Planck cross section coefficients so as to treat charged-particle transport with MORSE.

The derivation of the Fokker-Planck equation is shown in Appendix A. In summarizing the derivation, we start with one form of the Boltzmann equation

$$\begin{aligned}
 & \nabla \cdot \vec{\Omega} \psi(\vec{r}, \mu, E) + \sigma_t(\vec{r}, E) \psi(\vec{r}, \mu, E) \\
 & = \int_0^\infty \int_0^{2\pi} \int_{-1}^{+1} \sigma_s(\vec{r}, E' \rightarrow E, \mu_0) \psi(\vec{r}, \mu', E') d\mu' d\phi' dE' + Q(\vec{r}, \mu, E)
 \end{aligned} \tag{3-1}$$

(the terms of the equation are defined at the beginning of Appendix A). The equation assumes that the direction of the particles is defined by only one variable,  $\mu$ , the deflection cosine. For discrete ordinate codes, this means that only one-dimensional geometries with an axis of symmetry, such as a slab or sphere, are considered (see Chapter 1 of Bell and Glasstone, 1970). Since the elastic scattering cross section is coupled in both energy loss ( $E' - E$ ) and scattering angle ( $\theta_0 = \cos^{-1} \mu_0$ ), then the Boltzmann may be rearranged to form

$$\nabla \cdot \bar{\Omega} \psi + \sigma_a \psi = \Gamma_B \psi + Q , \quad (3-2a)$$

where

$$\begin{aligned} \Gamma_B \psi = & \int_0^{2\pi} \int_{-1}^{+1} [\sigma_s(\bar{r}, E', \mu_0) \psi(\bar{r}, \mu', E') \\ & - \sigma_s(\bar{r}, E, \mu_0) \psi(\bar{r}, \mu, E)] d\mu' d\phi' . \end{aligned} \quad (3-2b)$$

The term  $\Gamma_B \psi$  is known as the Boltzmann scattering operator. In the Fokker-Planck approximation, the integrand of  $\Gamma_B \psi$  is first expanded in a Taylor series expansion about  $\theta_0 = 0$ . If we retain only up to the second-order terms of the expansion, and then perform a fair amount of algebraic manipulation, we obtain the expression

$$\nabla \cdot \bar{\Omega} \psi + \sigma_a \psi = \Gamma_{FP} \psi + Q , \quad (3-3a)$$

where the integral operator of the Boltzmann equation has been replaced by the Fokker-Planck differential operator:

$$r_{FP} \psi = \frac{\alpha}{2} \frac{\partial}{\partial \mu} [(1 - \mu^2) \frac{\partial}{\partial \mu} \psi] + \frac{\partial}{\partial E} \beta \psi + \frac{1}{2} \frac{\partial^2}{\partial E^2} \gamma \psi \quad (3-3b)$$

with

$$\alpha = 2\pi \int_{-1}^{+1} \sigma_s(\bar{r}, E, \mu_0) (1 - \mu_0) d\mu_0, \quad (3-3c)$$

$$\beta = \int_0^{\infty} \sigma_s(\bar{r}, E + E') (E - E') dE', \quad (3-3d)$$

$$\gamma = \int_0^{\infty} \sigma_s(\bar{r}, E + E') (E - E')^2 dE'. \quad (3-3e)$$

The terms  $\alpha$ ,  $\beta$ , and  $\gamma$  are usually referred to as the momentum transfer, the stopping power, and the mean-square stopping power, respectively.

If the integrand of  $r_B \psi$ , and in particular the angular flux ( $\psi$ ), varies smoothly as a function of the expanded variables, then the Fokker-Planck operator will successfully approximate the Boltzmann operator in the region of small  $\theta_0$ . For forward peaked scattering, the scattering cross section has little angular support; that is, the probability of scattering at large angles is relatively small in comparison with scattering at small angles. As the cross sections become more forward peaked, the region of angular support decreases, and the relative contribution of small angle scatters to the solution of the Boltzmann increases. In such a case the Fokker-Planck solution will gradually converge to the Boltzmann solution.

Morel (1981) points out that it is often difficult to establish the reliability or accuracy of the Fokker-Planck equation within firm limits since the angular flux may not always be sufficiently smooth. In some problems, the derivatives of the angular flux with respect to energy may be either unbounded or extremely large. However, Morel states that "experience has shown that good results for scalar quantities (angle and energy integrated), such as energy and charge deposition profiles, can be expected in charged-particle calculations. However, results for detailed differential quantities are generally inadequate. The Fokker-Planck equation is very useful in spite of this deficiency because it is the scalar rather than the differential quantities that are most often of applied interest."

#### Theoretical Basis for the Decoupled Cross Section

As mentioned previously, Mehlhorn and Duderstadt (1980) replaced the quadrature forms of the Boltzmann integral operator in discrete ordinate codes, with difference equations representing the differential quantities of the Fokker-Planck operator. Morel's approach was to define cross sections in terms of the Fokker-Planck functions. The key to his approach was in discerning that the same Fokker-Planck equation (Equation (3-3)) may be derived by using a cross section decoupled in angle and energy, rather than a coupled cross section.

Let us reexpress the differential operator (Equation (3-3b)) as

$$\Gamma_{FP} \psi = \Gamma_{FP}^{\alpha} \psi + \Gamma_{FP}^{\epsilon} \psi, \quad (3-4a)$$

where  $\Gamma_{FP}^\alpha \psi$  redistributes in angle with no energy loss:

$$\Gamma_{FP}^\alpha \psi = \frac{\alpha}{2} \frac{\partial}{\partial \mu} [(1 - \mu^2) \frac{\partial}{\partial \mu} \psi] \quad (3-4b)$$

and  $\Gamma_{FP}^e \psi$  redistributes in energy with no directional change:

$$\Gamma_{FP}^e \psi = \frac{\partial}{\partial E} \beta \psi + \frac{1}{2} \frac{\partial^2}{\partial E^2} \gamma \psi. \quad (3-4c)$$

Such a decoupling of the Fokker-Planck collision term suggests that we may also define a composite, decoupled cross section of the form

$$\sigma_s(E' \rightarrow E, \mu_0) = \sigma^\alpha(E, \mu_0) \delta(E' - E) + \sigma^e(E' \rightarrow E) \frac{1}{2\pi} \delta(\mu_0 - 1) \quad (3-5)$$

which when inserted into the Boltzmann equation achieves the same result as the coupled cross section. The term  $\sigma^\alpha(E, \mu_0) \delta(E' - E)$  permits directional change only, and the term  $\sigma^e(E' \rightarrow E) \delta(\mu_0 - 1)/2\pi$  allows only energy loss.

The derivation of the Fokker-Planck equation using the decoupled cross section is also shown in Appendix A, and is very similar to the derivation for the coupled cross section. Inserting Equation (3-5) into (3-1) and rearranging slightly produces the Boltzmann scattering operators

$$\Gamma_B^\alpha \psi = \int_0^{2\pi} \int_{-1}^{+1} \sigma^\alpha(E, \mu_0) [\psi(\mu') - \psi(\mu)] d\mu' d\phi' \quad (3-6a)$$

and

$$r_B^e \psi = \int_0^\infty [\sigma^e(E' \rightarrow E) \psi(E') - \sigma^e(E \rightarrow E') \psi(E)] dE' . \quad (3-6b)$$

We approximate  $r_B^\alpha \psi$  and  $r_B^\beta \psi$  by expanding the integrands above about  $\mu_0 = 0$ . After simplifying, we obtain  $r_{FP}^\alpha \psi$  (Equation (3-4b)), where

$$\alpha = 2\pi \int_{-1}^{+1} \sigma^\alpha(\bar{r}, E, \mu_0)(1 - \mu_0) d\mu_0 , \quad (3-7)$$

and we obtain  $r_{FP}^\beta \psi$  (Equation (3-4c)), where

$$\beta = \int_0^\infty \sigma^e(E \rightarrow E')(E - E') dE' \quad (3-8a)$$

and

$$\gamma = \int_0^\infty \sigma^e(E \rightarrow E')(E - E')^2 dE' \quad (3-8b)$$

respectively.

Morel's approach was to define multigroup expansion coefficients for the composite, decoupled cross section in terms of the Fokker-Planck functions ( $\alpha$ ,  $\beta$ , and  $\gamma$ ) and certain  $S_n$  parameters (the order of the quadrature set and the energy group structure). Since the Fokker-Planck and Boltzmann equation approximate one another with forward-peaked scattering, it follows that the Boltzmann solution calculated using these coefficients would "converge to the desired

Fokker-Planck solution as the  $S_n$  space-angle-energy mesh was refined" (Morel, 1981).

The use of decoupled cross sections in charged particle transport is not new. Such a cross section has been used in continuous or analog Monte Carlo programs for many years. Although the actual basis for using the decoupled cross section is its theoretical linkage to the derivation of the Fokker-Planck equation, the decoupled cross section is usually considered as simply a model of the physical interaction processes involved in charged particle transport.

#### Physical Basis for the Decoupled Cross Section

Let us focus qualitatively on the interactions of charged particles: ionization, scattering, various types of radiative losses, and others, all of which are due primarily to coulomb forces. The mechanisms by which a charged particle loses its kinetic energy, or is deflected from its original path, involve four principle types of interaction: inelastic collisions with atomic electrons, inelastic collisions with a nucleus, elastic collisions with a nucleus, and elastic collisions with atomic electrons. Each will be discussed briefly in turn. More detailed and quantitative discussions on the interaction of radiation with matter may be obtained in references by Evans (1955) and Segre (1964). The information below is primarily taken from Evans.

Inelastic Collisions with Atomic Electrons. Inelastic collisions with bound atomic electrons are usually the primary mechanism by which charged particles lose their energy in passing through an absorber. Upon entering the absorber, the charged particle immediately interacts simultaneously with many electrons. These orbital electrons (primarily valence electrons) receive an impulse from the coulomb force (attraction or repulsion) as the particle passes by and as a result, energy is transferred to the electron. This does not mean that each atom receives a small energy transfer. Either no energy is transferred at all, or else an energy approximately equal to an excitation or ionization energy of the atom is transferred; i.e., the energy available to the atom must be greater than the minimum excitation potential. Because of the small mass of the electron, the energy transfer may be relatively large and the electron will experience a transition to an excited state (excitation) or to an unbound state (ionization). If the atom is ionized, then the liberated electron and the corresponding positive ion constitute a primary ion pair. Also, the liberated ion is itself a charged particle (called a delta ray) and will produce secondary ionization while being brought to rest.

Head-on collisions would naturally produce the largest impulse to the electron, and therefore, the largest energy transfer. In a classical sense, the probability of a given energy transfer in an inelastic collision varies inversely with the square of the energy

loss. Therefore, "soft" collisions, in which the energy loss is small, are strongly favored over "hard" collisions, in which the energy loss is large. Since hard collisions are very infrequent, they contribute very little to the most probable energy loss. However, because the struck electron in a hard collision is given a relatively large amount of kinetic energy, an appreciable fraction (roughly one-half) of the energy lost by primary particles occurs in such a collision. This means that the average energy loss will exceed the most probable energy loss.

Since heavy charged particles (not electrons) have a mass much larger than the orbital electrons, the deflection of these charged particles is extremely small. Heavy charged particles passing through matter have essentially straight paths--apart from the rare event of a nuclear collision where a large angle scattering occurs--and slow down in an almost continuous manner. This introduces the concept of range. That is, a monoenergetic beam of heavy charged particles, in passing through some small thickness of material, will continuously lose energy until all of the particles are "stopped" (i.e., reached thermal energies). The distance traveled to the point of "stopping" is the range.

Inelastic Collision with a Nucleus. If a charged particle approaches the nucleus in a close, noncapture encounter, the incoming particle will experience a deflection (i.e., an acceleration) due to

the coulomb fields. In the quantum mechanical model, there is a small but finite probability (which increases as a function of incident particle energy) that a photon will be emitted each time a particle experiences such a deflection. Because the probability or cross section is so small, usually no photon is emitted. However, in the few collisions which are accompanied by photon emission, a relatively large amount of energy is released, and the collisions are called radiative. The photon emission is termed bremsstrahlung.

In a classical sense, the total bremsstrahlung per atom varies as the square of the atomic number and inversely with the square of the mass of the incident particle. Due to the strong dependence on the mass of the incident particle, bremsstrahlung is almost completely negligible for all charged particles other than electrons. And as mentioned previously, energy loss by radiation at low energies is much less than that by ionization, but at high energies, loss by radiation may predominate.

In a radiative collision, the initial momentum of the incident electron becomes shared between the residual electron, the atomic nucleus, and the emitted photon. Although the photon may receive any fraction of the total initial kinetic energy of the electron and can be emitted in any direction, usually its share of the momentum is small compared with that of the deflected electron. Thus, for radiative collisions of moderate energy, the momentum is primarily conserved between the nucleus and the deflected electron. And since

relatively little momentum is transferred to the photon, the angular deflections of the incident electron are seldom significant.

Radiative loss may also occur in electron-electron interactions. However, the electron-electron bremsstrahlung is usually accounted for by changing the  $Z^2$  dependence of electron-nucleus bremsstrahlung to  $(Z^2 + Z)$ .

Elastic Collision with a Nucleus. An important practical difference between the ionization behavior of heavy charged particles and electrons arises from the fact that the trajectories of electrons in matter are rather tortuous and nonlinear. The actual path length of an electron passing through two points may be significantly longer than the distance between these points measured on a straight line. Hence, electrons of the same energy are not all stopped by the same thickness of material (in contrast to heavy charged particles) and the concept of range has limited applicability. One cause of the irregular trajectories of electrons is the elastic collisions with the nucleus, or "Rutherford scattering"; that is, the electrostatic repulsion or screened coulomb force from the nucleus will deflect the charged particle without any photon emission or excitation of the nucleus. The charged particle loses only that amount of kinetic energy necessary to conserve momentum between the two particles. In an elastic electron-molecule collision, the average energy transferred to the molecule is small. However, such collisions may give

rise to large changes in the direction of the colliding particles and thus produce large transfers in momentum.

Incident electrons have a relatively high probability of experiencing nuclear elastic scattering. The nuclear scattering increases with  $Z^2$  while the inelastic electronic scattering increases only with  $Z$ , the number of electrons per atom. In hydrogen, the cross sections for scattering by the two different processes are about equal. In higher  $Z$  elements, the nuclear scattering will increase and predominate over the electronic scattering by roughly a factor of  $Z$ .

As is characteristic of other charged particle interactions, elastic cross sections are forward peaked. So although the deflections of many single scatters may be small, the cumulative effect of many small nuclear scatters (multiple scattering) for any one electron may be significant. The theoretical treatment of multiple scattering, in fact, attempts to evaluate the statistical average of many elastic nuclear deflections. Also, it is often satisfactory for computational purposes to combine the angular effects of inelastic electronic scattering and multiple scattering. This is usually done by replacing the  $Z^2$  dependence in multiple scattering formulas with the term  $(Z^2 + Z)$ , since the probability of electron-electron scatter increases in proportion to  $Z$ .

Elastic Collision with Atomic Electrons. Incident particles which have kinetic energies below the first electronic excitation

potential of the medium through which they travel are often called subexcitation particles. It is these particles (with energies <100 eV) which primarily participate in elastic scattering events with atomic electrons. The subexcitation particles transfer only that amount of energy which is necessary to conserve momentum and energy.

Summary. The decoupled cross section consists of an energy loss only term and a directional change only term. Of the four charged particle interactions mentioned above, only elastic nuclear scattering contributes significantly to the angular term, while the other interaction types are primarily energy loss mechanisms.

#### Coefficients for $\sigma^\alpha$

We have established thus far that the composite, decoupled cross section

$$\sigma_S(E' \rightarrow E, \mu_0) = \sigma^\alpha(E, \mu_0) \delta(E' - E) + \sigma^e(E' \rightarrow E) \frac{1}{2\pi} \delta(\mu_0 - 1) \quad (3-9)$$

has a theoretical as well as a physical basis; that is, when the scattering is highly forward peaked, the decoupled cross section may be used to derive the Fokker-Planck equation. In the derivation, we noted that  $r_B^\alpha$  and  $r_{FP}^\alpha$  will approximate one another as  $\sigma^\alpha$  becomes increasingly peaked about  $\mu_0 = 1$ . Similarly,  $r_B^e$  and  $r_{FP}^e$  will approximate each other as  $\sigma^e$  becomes increasingly peaked about  $E' = E$ . This convergence of the Boltzmann and Fokker-Planck scattering operators with forward peaked scattering is an important property of

our formalism and brings us to the actual development of the expansion coefficients for our multigroup cross sections.

For this development, we require for each energy group, probabilities of transfer to all other groups. Since the angular redistribution term ( $\sigma^\alpha(E, \mu_0) \delta(E' - E)$ ) of the decoupled cross section permits no energy loss,  $\sigma^\alpha$  must correspond to a within-group cross section. Conversely, since the energy redistribution term ( $\sigma^e(E' \rightarrow E) \delta(\mu_0 - 1)/2\pi$ ) is a delta function in angle,  $\sigma^e$  must correspond to a group-to-group transfer. We will discuss both the past work by Morel (1981) and the new developments for each cross section in turn.

Morel's Method for Determining Coefficients for  $\sigma^\alpha$ . We first define a set of Legendre coefficients ( $\sigma_\ell^\alpha$ ) for the within-group cross section ( $\sigma^\alpha$ ) such that

$$\sigma^\alpha(E, \mu_0) = \sum_{\ell=0}^{\infty} \frac{2\ell + 1}{4\pi} \sigma_\ell^\alpha P_\ell(\mu_0) . \quad (3-10)$$

The coefficients of the expansion are determined by forcing the Boltzmann and Fokker-Planck operators to be equivalent when operating on polynomials of degree  $L$  or less. If we assume the angular flux is expressible as a polynomial of degree  $L$  or less,

$$\psi(\mu) = \sum_{\ell=0}^L \frac{2\ell + 1}{4\pi} \phi_\ell P_\ell(\mu) \quad (3-11)$$

then we are in effect requiring that

$$\Gamma_B^\alpha \psi = \Gamma_{FP}^\alpha \psi . \quad (3-12)$$

We recall that

$$\Gamma_B^\alpha \psi = \int_0^{2\pi} \int_{-1}^{+1} \sigma^\alpha(E, \mu_0) [\psi(\mu') - \psi(\mu)] d\mu_0 d\phi_0 . \quad (3-13)$$

Replacing  $\psi(\mu')$  and  $\sigma^\alpha(E, \mu_0)$  with their respective Legendre expansions gives

$$\begin{aligned} \Gamma_B^\alpha \psi &= \sum_{\ell=0}^L \frac{2\ell + 1}{4\pi} \phi_\ell \sum_{m=0}^{\infty} \frac{2m + 1}{4\pi} \sigma_m^\alpha \int_{-1}^{+1} P_m(\mu_0) P_\ell(\mu') d\mu_0 d\phi_0 \\ &\quad - \sigma_0^\alpha \psi(\mu) . \end{aligned} \quad (3-14)$$

To perform the remaining integration, we insert for  $P_\ell(\mu')$ , the addition theorem for spherical harmonics (Bell and Glasstone, 1970)

$$P_\ell(\mu') = P_\ell(\mu) P_\ell(\mu_0) + 2 \sum_{r=1}^{\ell} \frac{(\ell - r)!}{(\ell + r)!} P_\ell^r(\mu) P_\ell^r(\mu_0) \cos[r(\phi - \phi_0)] . \quad (3-15)$$

After integrating with respect to  $\phi_0$ , all but the first term of the identity goes to zero and Equation (3-14) becomes

$$\begin{aligned} \Gamma_B^\alpha \psi &= \sum_{\ell=0}^L \frac{2\ell + 1}{4\pi} \phi_\ell P_\ell(\mu) \sum_{m=0}^{\infty} \frac{2m + 1}{2} \sigma_m^\alpha \int_{-1}^{+1} P_m(\mu_0) P_\ell(\mu_0) d\mu_0 \\ &\quad - \sigma_0^\alpha \psi(\mu) \end{aligned} \quad (3-16)$$

$$= \sum_{\ell=0}^L \frac{2\ell + 1}{4\pi} \phi_\ell (\sigma_\ell^\alpha - \sigma_0^\alpha) P_\ell(\mu) . \quad (3-17)$$

Let us now consider  $\Gamma_{FP}^\alpha \psi$ . Recall that

$$\Gamma_{FP}^\alpha \psi = \frac{\alpha}{2} \frac{\partial}{\partial \mu} [(1 - \mu^2) \frac{\partial}{\partial \mu} \psi] , \quad (3-18a)$$

where  $\alpha$  carries units of steradians/cm and is known as the momentum transfer:

$$\alpha = \int_{-1}^{+1} \sigma^\alpha(E, \mu_0) (1 - \mu_0) d\mu_0 . \quad (3-18b)$$

Inserting the Legendre expansion for  $\psi(\mu)$  as before and using the identity

$$(1 - \mu^2) P'_\ell(\mu) = -\ell \mu P_\ell(\mu) + \ell P'_{\ell-1}(\mu) \quad (3-19)$$

then Equation (3-18a) becomes

$$\Gamma_{FP}^\alpha \psi = \frac{\alpha}{2} \sum_{\ell=0}^L \frac{\ell(2\ell+1)}{4\pi} \phi_\ell [-\mu P'_\ell(\mu) - P_\ell(\mu) + P'_{\ell-1}(\mu)] . \quad (3-20)$$

Using another well-known recurrence relation for the Legendre polynomials

$$-\mu P'_\ell(\mu) + P'_{\ell-1}(\mu) = -\ell P_\ell(\mu) , \quad (3-21)$$

we obtain the final expression

$$\Gamma_{FP}^\alpha \psi = \sum_{\ell=0}^L \frac{2\ell+1}{4\pi} \phi_\ell [(-\frac{\ell\alpha}{2}) (\ell+1)] P_\ell(\mu) . \quad (3-22)$$

Now, as stipulated in Equation (3-12), we require that  $\Gamma_B^\alpha \psi$  be equal

to  $\Gamma_{FP}^\alpha \psi$ . Therefore, we equate the coefficients of their respective expansions found in Equations (3-17) and (3-22):

$$\sigma_\ell^\alpha - \sigma_0^\alpha = -\frac{\ell\alpha}{2} (\ell + 1) , \quad \ell = 1, L . \quad (3-23)$$

If we choose  $\sigma_L = 0$  so as to minimize the resulting value for  $\sigma_0^\alpha$ , Equation (3-23) becomes

$$\sigma_\ell^\alpha = \frac{\alpha}{2} [L(L + 1) - \ell(\ell + 1)] , \quad \ell = 0, L . \quad (3-24)$$

The above expression is the equation developed by Morel to define the Legendre coefficients for the within-group cross section. Equation (3-24) shows that we only need an expansion of degree  $L$  for  $\sigma^\alpha$  in order for  $\Gamma_B^\alpha$  and  $\Gamma_{FP}^\alpha$  to be equivalent when operating on polynomials of degree  $L$  or less.

Some comments regarding the behavior of  $\sigma^\alpha$  are appropriate:

1. The momentum transfer ( $\alpha$ ) is exact regardless of the expansion order ( $L$ ). This is easily demonstrated with the equation sequence below:

$$\alpha = 2\pi \int_{-1}^{+1} \sigma^\alpha(E, \mu_0) (1 - \mu_0) d\mu_0 \quad (3-25a)$$

$$= \sigma_0^\alpha - \sigma_1^\alpha \quad (3-25b)$$

$$= \frac{\alpha}{2} (L) (L + 1) - \frac{\alpha}{2} [L(L + 1) - 2] = \alpha . \quad (3-25c)$$

2.  $\sigma^\alpha$  becomes increasingly forward peaked with increasing expansion order. Using the Fokker-Planck equation to redefine the average cosine of the scattering angle, we have

$$\bar{\mu}_0 = \sigma_1^\alpha / \sigma_0^\alpha \quad (3-26a)$$

$$= \frac{L(L+1) - 2}{L(L+1)} = 1 - \frac{2}{L(L+1)} . \quad (3-26b)$$

The average cosine goes to unity at the approximate rate of  $1/L^2$ .

3.  $\sigma_0^\alpha$  increases without bounds as  $L$  increases:

$$\sigma_0^\alpha = \frac{\alpha}{2} L(L+1) . \quad (3-27)$$

Let us synthesize the three comments above by expressing the momentum transfer as

$$\alpha = \sigma_0^\alpha (1 - \bar{\mu}_0) . \quad (3-28)$$

The above equation dictates that as  $\mu_0$  approaches unity, then for  $\alpha$  to remain a constant,  $\sigma_0^\alpha$  must become unbounded. This relationship, along with the fact that  $r_B^\alpha$  better approximates  $r_{FP}^\alpha$  as  $\sigma^\alpha$  becomes more forward peaked, infers that  $r_{FP}^\alpha$  corresponds to a type of continuous-deflection approximation. Morel states that the Fokker-Planck operator "effectively causes particles to scatter continuously while incurring a differential deflection in each scattering event".

It follows then, that the Fokker-Planck cross section expansions as given by Equation (3-24) cause particles to "continuously deflect with the mean deflection per unit path length given by the momentum transfer".

An additional important aspect of the Fokker-Planck expansions discussed by Morel is that they are "spherical-harmonic equivalent". By this it is meant that one-dimensional slab geometry  $S_N$  solutions for the Boltzmann equation

$$\nabla \cdot \Omega \psi + \sigma_a \psi = \Gamma_B^\alpha \psi + Q, \quad (3-29)$$

obtained using Gauss quadrature sets of order  $N$  in conjunction with  $\sigma^\alpha$  expansions of degree  $(N-1)$ , are equivalent to the spherical harmonics solutions of order  $(N-1)$  with Mark boundary conditions for the Fokker-Planck equation

$$\nabla \cdot \Omega \psi + \sigma_a \psi = \Gamma_{FP}^\alpha \psi + Q. \quad (3-30)$$

Therefore, if the Fokker-Planck expansions are to be input to a discrete-ordinates/ $S_N$  code, it is advantageous to use Gauss quadrature sets of order  $N$  with cross section expansions of degree  $(N-1)$ .

We reaffirm that  $\Gamma_B^\alpha$  and  $\Gamma_{FP}^\alpha$  are approximations to each other and are equal only in the limit as  $\bar{\mu}_0$  goes to 1. Although both operators are linear, positive, and mirror to an extent physical reality, the process of forcing them to be equal, when in reality they are

not, causes  $\sigma^\alpha$  to be nonphysical. Since cross sections model probabilities of interaction, they must by definition be everywhere positive. A cross section  $\sigma(\mu_0)$  must be positive over the entire interval  $(-1, +1)$  spanned by the cosine of the polar angle ( $\mu_0 = \cos \theta_0$ ). However, we do not usually deal with actual cross sections in codes, but with approximate representations in the form of truncated Legendre polynomial expansions. The truncated expansions often times do become negative over the cosine interval, but it is usually sufficient if they originated from, or converge in the limit as the expansion becomes infinite, to an everywhere positive function. By stating that Morel's expansion is nonphysical, we do not mean to infer that the expansion is useless or of little worth--because it is still spherical-harmonic equivalent. We simply mean that the coefficients are representative of a cross section which is negative somewhere over the interval  $(-1, +1)$  (i.e., no fully positive cross section will have expansion coefficients identical with those of Morel's expansion). Although nonphysical, Morel's expansion does converge in the limit to a positive function,  $\delta(\mu_0 - 1)$ , but in a nonuniform fashion; that is, the lower order coefficients converge faster than the higher order coefficients.

We now demonstrate, using the Gauss quadrature technique discussed in Chapter II and Appendix B, that Morel's Fokker-Planck expansion is a truncated version of a physically unrealistic cross section, and as such is not amenable to the scattering algorithm in

MORSE. We define  $f^*(\mu_0)$  as the truncated expansion of  $f(\mu_0)$  where

$$f(\mu_0) \approx f^*(\mu_0) = \sum_{\ell=0}^{2n-1} \frac{2\ell+1}{2} f_\ell P_\ell(\mu_0) . \quad (3-31)$$

In this case,  $f_\ell$  represents the normalized coefficients corresponding to  $\sigma_\ell^\alpha$ . We recall that the Gauss quadrature technique seeks to replace  $f^*(\mu_0)$  with a discrete distribution,  $f_d(\mu_0)$ ,

$$f_d(\mu_0) = \sum_{i=1}^n \omega_i \delta(\mu_0 - \mu_i) , \quad (3-32)$$

where the weights ( $\omega_i$ ) are all greater than zero and the roots ( $\mu_i$ ) lie between (-1, +1). The failure of either of these two conditions indicates that the given coefficients ( $f_\ell$ ) or moments ( $M_\ell$ ) of  $f^*(\mu_0)$  are not those of an everywhere positive function. The nonnegativity requirement on the weights may be shown to yield the following restriction or lower limit on the value of  $f_2$ :

$$f_2 > \frac{1}{2} (3f_1^2 - 1) = P_2(f_1) = P_2(\bar{\mu}_0) . \quad (3-33)$$

At this point, let us note that if a delta function, located at  $\mu_0 = f_1$ , is expanded in terms of Legendre polynomials, we have

$$f_\ell = \int_{-1}^{+1} \delta(\mu_0 - f_1) P_\ell(\mu_0) d\mu_0 = P_\ell(f_1) . \quad (3-34)$$

Therefore, the lower bound for the coefficient  $f_2$  of an everywhere positive function is the same as the coefficient  $f_2$  of a delta function expansion at  $\mu_0 = f_1$ . Now Morel's equation for  $f_2$  (obtained

from Equations (3-23) and (3-25b)) is

$$f_2 = -2f_0 + 3f_1. \quad (3-35)$$

Combining the above equation with the restriction on  $f_2$  obtained from the quadrature technique (Equation (3-33)) gives

$$(f_1 - 1)^2 < 0. \quad (3-36)$$

Since the term  $(f_1 - 1)^2$  can never be negative, it follows that the Fokker-Planck coefficients ( $\sigma_2^\alpha, \sigma_3^\alpha, \dots$ ) do not originate from an everywhere positive function and are therefore not acceptable to the MORSE code. For example, setting  $L = 3$  in Morel's expression for  $\sigma_\lambda^\alpha$  (Equation (3-24)) gives the following normalized Fokker-Planck coefficients:  $f_0 = 1, f_1 = 5/6, f_2 = 1/2$ , and  $f_3 = 0$ . Using these coefficients as input for the Gauss quadrature subroutines of MORSE results in an error message stating that  $f_2$  is bad and that the acceptable values for  $f_2$  are between 0.54167 ( $= P_2(5/6)$ ) and 1. Since  $f_2$  is bad, the code proceeds to calculate a single direction and weight for  $f_d(\mu_0)$  using only  $f_0$  and  $f_1$ . The discrete direction corresponds to  $\bar{\mu}_0 = f_1 = 5/6$ , and it is of course the same direction that would have been obtained if the original weight function were  $\delta(\mu_0 - 5/6)$  instead of the Fokker-Planck expression. Therefore, only the first two coefficients of the Fokker-Planck expansion are acceptable in MORSE. We are limited to a  $P_1$  expansion of the Fokker-Planck equation.

Triangular Impulse Function Representation for  $\sigma^\alpha$ . We desire to obtain a new set of Legendre expansion coefficients to approximate  $\sigma^\alpha$  which are both physically acceptable and suitable for input to MORSE. One highly important requirement for the new expansion is that it retain the same  $\sigma_0^\alpha$  and  $\sigma_1^\alpha$  as given by Morel's expansion

$$\sigma_0^\alpha = \frac{\alpha}{2} L(L + 1) \cdot f_0 , \quad (3-37)$$

$$\sigma_1^\alpha = \frac{\alpha}{2} [L(L + 1) - 2] = \sigma_0^\alpha f_1 . \quad (3-38)$$

This is to insure that  $r_B^\alpha$  remains equivalent to  $r_{FP}^\alpha$  in the diffusion limit (i.e., they are equivalent when operating on polynomials of degree less than or equal to 1). Since  $\sigma_2^\alpha$  is bad, retaining the first two coefficients is the best we can do. However, there exist an infinite number of expansions with the same  $\sigma_0^\alpha$  and  $\sigma_1^\alpha$ . Therefore, the other coefficients ( $\sigma_2^\alpha, \sigma_3^\alpha, \dots$ ) must be chosen so that they are in some sense "close" to Morel's coefficients.

An obvious choice for the new expansion would be a delta function at  $\bar{\mu}_0$ . It is certainly everywhere positive and retains  $\sigma_0^\alpha$  and  $\sigma_1^\alpha$  as its first two coefficients:

$$\sigma_0^\alpha \int_{-1}^{+1} \delta(\mu_0 - \bar{\mu}_0) d\mu_0 = \sigma_0^\alpha \cdot f_0 , \quad (3-39)$$

$$\sigma_0^\alpha \int_{-1}^{+1} \delta(\mu_0 - \bar{\mu}_0) \mu_0 d\mu_0 = \sigma_0^\alpha \bar{\mu}_0 = \sigma_1^\alpha . \quad (3-40)$$

An additional advantage is that the coefficients of the delta function are precisely at the edge of physical acceptability (see Equation (3-33)) and are therefore the closest in value to Morel's coefficients. However, delta functions are not amenable to the scattering algorithm in MORSE. The Gauss quadrature technique attempts to find a set of polynomials  $Q_i(x)$  orthogonal with respect to the delta function such that

$$\int_{-1}^{+1} Q_i(\mu_0) Q_j(\mu_0) \delta(\mu_0 - \bar{\mu}_0) d\mu_0 = \delta_{ij} N_i \quad (3-41)$$

or

$$Q_i(\bar{\mu}_0) Q_j(\bar{\mu}_0) = \delta_{ij} N_i . \quad (3-42)$$

It is easily seen that if  $i \neq j$ , then either  $Q_i(\bar{\mu}_0)$  or  $Q_j(\bar{\mu}_0)$  must be zero since the Kronecker delta is zero. If  $i = j$ , then we have  $Q_i^2(\bar{\mu}_0) = N_i$  or  $Q_j^2(\bar{\mu}_0) = N_j$ . It follows that either  $N_i$  or  $N_j$  must also be zero and this is unacceptable. From a computational viewpoint, we acknowledge that delta functions are not always rejected by the quadrature routines. This is because we do not actually input delta functions to the code, but truncated expansions of those delta functions, with coefficients which are slightly altered due to round-off. But as may be expected, the computation becomes more ill-conditioned as the expansion degree is increased and the coefficients are made more exact.

A second choice for the new expansion might be a rectangular impulse function centered at  $\bar{\mu}_0$  with some finite width  $h$ . But an obvious question is how large or small to make  $h$ .

A third choice for the new expansion for  $\sigma^\alpha$ , and the one which we have elected to use, is a triangular impulse function (TIF). As depicted in Figure (3-1), the TIF is forward peaked with positive slope  $m$  and intercept  $b$ , and it equals zero at  $\mu_S$ . We will now compute the normalized Legendre coefficients ( $f_0, f_1, f_2, \dots$ ) for TIF where  $f_0 = 1$  and  $f_1 = \bar{\mu}_0$ . In general,

$$f_\ell = \int_{\mu_S}^1 (m\mu_0 + b) P_\ell(\mu_0) d\mu_0 . \quad (3-43)$$

For  $\ell = 0$ ,

$$f_0 = 1 = \int_{\mu_S}^1 (m\mu_0 + b) d\mu_0 \quad (3-44a)$$

$$= \frac{m}{2} + b - \frac{m}{2} \mu_S^2 - b\mu_S . \quad (3-44b)$$

Since

$$TIF(\mu_S) = 0 = m\mu_S + b , \quad (3-45a)$$

then

$$\mu_S = -b/m \quad (3-45b)$$

and Equation (3-44b) becomes

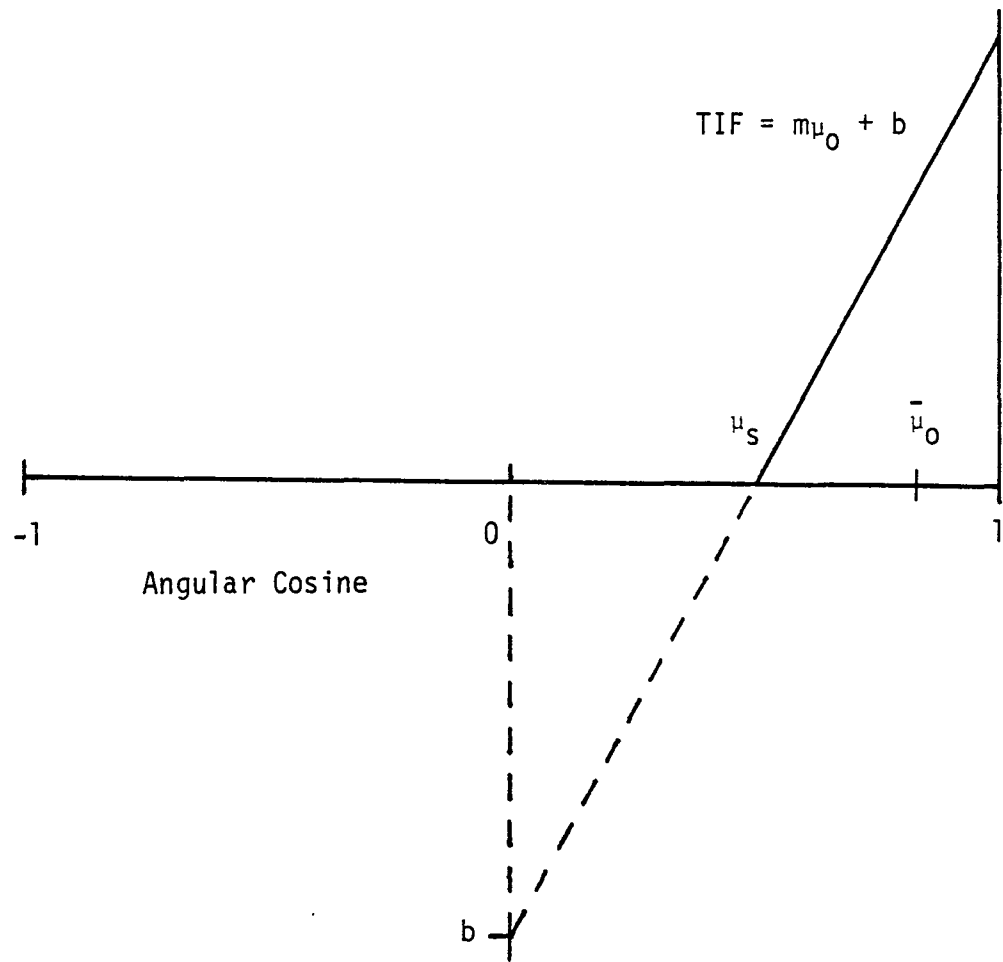


Figure (3-1). Triangular impulse function.

$$f_0 = 1 = \frac{m}{2} + b + \frac{b^2}{m} . \quad (3-46)$$

For  $\ell = 1$ ,

$$f_1 = \bar{\mu}_0 = \int_{\mu_S}^1 \mu_0 (m\mu_0 + b) d\mu_0 \quad (3-47a)$$

$$= \frac{m}{3} + \frac{b}{2} - \frac{b^3}{6m^2} . \quad (3-47b)$$

Equation (3-46) and (3-47b) give us two equations and two unknowns (m and b). Solving for the two unknowns gives

$$m = \frac{2}{9} \frac{1}{(1 - \bar{\mu}_0)^2} \quad (3-48)$$

and

$$b = m(2 - 3 \bar{\mu}_0) . \quad (3-49)$$

And since  $\mu_S = -b/m$ , then

$$\mu_S = (3\bar{\mu}_0 - 2) . \quad (3-50)$$

For  $\ell = 2$  and above, the coefficients are given by

$$f_\ell = m \left\{ \frac{P_{\ell-2}(\mu_S)}{(2\ell - 1)(2\ell + 1)} - \frac{2P_\ell(\mu_S)}{(2\ell - 1)(2\ell + 3)} + \frac{P_{\ell+2}(\mu_S)}{(2\ell + 1)(2\ell + 3)} \right\} . \quad (3-51)$$

The new cross section expansion,  $\sigma^\alpha$ , is obtained by multiplying each of the normalized expansion coefficients ( $f_0, f_1, f_2, \dots$ ) by

Morel's  $\sigma_0^\alpha$  (Equation (3-37)). Because the triangular impulse function retains the same first two coefficients as Morel's expansion, it also retains many of the same functional characteristics, i.e., the momentum transfer remains exact, the TIF becomes increasingly forward peaked with increasing expansion order  $L$ , and as  $\bar{\mu}_0$  approaches unity, then the scalar magnitude becomes unbounded.

The most important property characterizing  $\sigma^\alpha$  is that  $r_B^\alpha$  converges to  $r_{FP}^\alpha$  as  $\mu_0$  goes to 1. We will demonstrate this convergence property for the triangular impulse function. Listed for comparison in Table 3-1 are the coefficients of three different Fokker-Planck expansions: Morel's exact expansion, a delta function at  $\bar{\mu}_0$ , and the TIF, for  $L = 3$  to 8. We note, as previously stipulated, that each set of expansions has the same first two coefficients, and that the last coefficient of Morel's expansion is always zero. Also, for any particular  $L$ , the coefficients for the delta function expansion drop less rapidly than Morel's coefficients but more rapidly than the TIF coefficients; this is reasonable since the delta function lies on the border between physical/nonphysical cross sections. Of importance, however, is the fact that as  $L$  increases, or as  $\bar{\mu}_0$  goes to 1, then the coefficients of the three different expansions converge to each other. For example, the third coefficient ( $\sigma_2^\alpha$ ) differs by 12.7, 1.25, and 0.32 percent at  $L = 3, 5$ , and 7, respectively. It follows that the three expansions become equivalent in the Fokker-Planck limit.

Table 3-1  
Comparison of Coefficients for Various Fokker-Planck Expansions

$L = 3, \bar{\mu}_0 = 5/6$

MFP	6	5	3	0
DF	6	5	3.25	1.18
TIF	6	5	3.38	1.69

$L = 4, \bar{\mu}_0 = 9/10$

MFP	10	9	7	4	0
DF	10	9	7.15	4.73	2.08
TIF	10	9	7.23	5.06	2.93

$L = 5, \bar{\mu}_0 = 14/15$

MFP	15	14	12	9	5	0
DF	15	14	12.1	9.49	6.42	3.20
TIF	15	14	12.15	9.72	7.05	4.47

$L = 6, \bar{\mu}_0 = 20/21$

MFP	21	20	18	15	11	6	0
DF	21	20	18.07	15.35	12.03	8.35	4.52
TIF	21	20	18.11	15.52	12.50	9.34	6.32

$L = 7, \bar{\mu}_0 = 27/28$

MFP	28	27	25	22	18	13	7	0
DF	28	27	25.05	22.26	18.78	14.79	10.49	6.11
TIF	28	27	25.08	22.39	19.15	15.58	11.95	8.49

$L = 8, \bar{\mu}_0 = 35/36$

MFP	36	35	33	30	26	21	15	8	0
DF	36	35	33.04	30.21	26.61	22.41	17.76	12.86	7.90
TIF	36	35	33.06	30.31	26.90	23.05	18.96	14.86	10.95

Definitions: MFP - Morel's Fokker-Planck Expansion  
 DF - Delta Function Expansion at  $\bar{\mu}_0$   
 TIF - Triangular Impulse Function

We recall that the Fokker-Planck coefficients,  $\sigma_\ell^\alpha$ , where

$$\sigma_\ell^\alpha - \sigma_0^\alpha = -\frac{\ell\alpha}{2} (\ell + 1) , \quad \ell = 1, L , \quad (3-23)$$

were found by equating  $\Gamma_B^\alpha$  with a second order accurate  $\Gamma_{FP}^\alpha$ . In order to show a more rigorous proof of convergence for TIF, let us first derive a more accurate expression for  $\sigma_\ell^\alpha$ . We begin with the identity

$$\sigma_\ell^\alpha = 2\pi \int_{-1}^{+1} \sigma^\alpha(E, \mu_0) P_\ell(\mu_0) d\mu_0 . \quad (3-52)$$

Since

$$P_\ell(\mu_0) = \sum_{n=0}^{\ell} \frac{(-1)^n (\ell + n)!}{2^n (n!)^2 (\ell - n)!} (1 - \mu_0)^n \quad (3-53)$$

(see Gradshteyn and Ryzhik, 1965), then

$$\sigma_\ell^\alpha = 2\pi \sum_{n=0}^{\ell} \frac{(-1)^n (\ell + n)!}{2^n (n!)^2 (\ell - n)!} \int_{-1}^{+1} \sigma^\alpha(E, \mu_0) (1 - \mu_0)^n d\mu_0 \quad (3-54)$$

or

$$\sigma_\ell^\alpha = \sum_{n=0}^{\ell} \frac{(-1)^n \alpha^n (\ell + n)!}{2^n (n!)^2 (\ell - n)!} , \quad (3-55a)$$

where we have defined the different moments of the momentum transfer as

$$\alpha^n = 2\pi \int_{-1}^{+1} \sigma^\alpha(E, \mu_0) (1 - \mu_0)^n d\mu_0 . \quad (3-55b)$$

From the above equation we find that for  $n=0$ ,  $\alpha^0 = \sigma_0^\alpha$ , and Equation (3-55a) may then be rearranged as

$$\sigma_\ell^\alpha - \sigma_0^\alpha = \sum_{n=1}^{\ell} \frac{(-1)^n \alpha^n (\ell + n)!}{2^n (n!)^2 (\ell - n)!} . \quad (3-56)$$

This expression is exact. Note that the first term of the summation is the standard Fokker-Planck formula derived by Morel. Although the derivation is much too tedious to present here, Equation (3-56) may also be derived by first obtaining  $r_{FP}^\alpha$  exact to infinite order:

$$r_{FP}^\alpha \psi = \sum_{n=1}^{\infty} \frac{\alpha^n (A_n \psi)}{2^n (n!)^2} , \quad (3-57a)$$

where  $\alpha^n$  is given by Equation (3-55b), and where

$$A_n \psi = \frac{\partial^n}{\partial \mu^n} \left[ (1 - \mu^2)^n \frac{\partial^n \psi}{\partial \mu^n} \right] \quad (3-57b)$$

$$= \sum_{\ell=0}^{\infty} \frac{2\ell + 1}{4\pi} \phi_\ell [(-1)^n \frac{(\ell + n)!}{(\ell - n)!}] P_\ell(\mu) , \quad (3-57c)$$

and by then setting  $r_B^\alpha \psi$  equal to  $r_{FP}^\alpha \psi$ . Having obtained an exact equation for  $\sigma_\ell^\alpha$  in terms of  $\alpha^n$ , we proceed with the demonstration of convergence. We first compute the higher order moments of the momentum transfer for the TIF in terms of  $\alpha^1$ :

$$\alpha^n = 2\pi \int_{-1}^{+1} \sigma^\alpha(E, \mu_0) (1 - \mu_0)^n d\mu_0 \quad (3-58a)$$

$$= \sigma_0^\alpha \int_{\mu_S}^1 (m\mu_0 + b) (1 - \mu_0)^n d\mu_0 \quad (3-58b)$$

$$= \sigma_0^\alpha (1 - \mu_S)^{n+1} \left\{ \frac{m + b}{n + 1} - \frac{m(1 - \mu_S)}{n + 2} \right\} \quad (3-58c)$$

$$= \frac{2\sigma_0^\alpha 3^n (1 - \mu_0)^n}{(n + 1)(n + 2)} \quad (3-58d)$$

$$= \frac{(6\alpha) (3^{n-1}) (1 - \mu_0)^{n-1}}{(n + 1)(n + 2)}. \quad (3-58e)$$

Substituting Equation (3-58e) into (3-56) and extracting the first term of the summation gives

$$\sigma_\ell^\alpha - \sigma_0^\alpha = -\frac{\alpha}{2} (\ell) (\ell + 1) + 6\alpha \sum_{n=2}^{\ell} \frac{(-1)^n (\ell + n)! 3^{n-1} (1 - \bar{\mu}_0)^{n-1}}{2^n (n!)^2 (\ell - n)! (n + 1)(n + 2)} \quad (3-59)$$

It is easily seen in the above equation that in the limit as  $\bar{\mu}_0$  goes to 1, all of the higher order summation terms go to zero and only the standard Fokker-Planck equation remains.

The rate of convergence may be determined by analyzing the equation for the normalized coefficients (obtained by inserting Equation (3-58d) into (3-55a)):

$$f_\ell = \sum_{n=0}^{\infty} \frac{(-1)^n 2 \cdot 3^n (1 - \bar{\mu}_0)^n (\ell + n)!}{2^n (n!)^2 (n + 1)(n + 2)(\ell - n)!}. \quad (3-60)$$

Since the cosine of the average scattering angle is given by

$$\bar{\mu}_0 = 1 - \frac{2}{L(L+1)} \quad (3-26b)$$

then

$$f_\ell = \sum_{n=0}^{\ell} \frac{(-2)^n 3^n (\ell + n)!}{L^n (L+1)^n (n!)^2 (n+1) (n+2) (\ell - n)!} \quad (3-61a)$$

$$= 1 - \frac{\ell(\ell+1)}{L(L+1)} + \frac{3}{8} \frac{(\ell+2)(\ell+1)(\ell)(\ell-1)}{L^2(L+1)^2} \dots \quad (3-61b)$$

If  $\ell$  is small and  $L$  is large, then the ratio of the  $(n+1)$  term to the  $n$ th term goes as approximately  $-1/L^2$ . If  $\ell = L$ , then the ratio of successive terms goes as approximately  $-1/n^2$ . Therefore, the lower order coefficients converge at a faster rate than the higher order coefficients.

We showed previously in Table (3-1) that the difference between the lower order coefficients of Morel's expansion and those of the TIF, was smaller than the difference between corresponding higher order coefficients. That is, the difference between corresponding coefficients diverges with increasing  $\ell$ . However, this "reluctance" of  $f_\ell$  to converge, where  $\ell$  is large, does not significantly affect the accuracy of the solution. It is instructive to consider the  $S_n$  scattering source expressed below

$$S(\mu_i) = \sum_{\ell=0}^{N-1} \frac{2\ell+1}{4\pi} \sigma_\ell \phi_\ell P_\ell(\mu_i), \quad i = 1, N \quad (3-62)$$

where we have used a truncated cross section expansion of degree  $(N-1)$  in conjunction with a Gaussian quadrature set of order  $N$ . In

using a quadrature set of order  $N$ , we are also assuming that the angular flux may be adequately represented by a polynomial of degree  $(N-1)$  or less; if not, the coefficients of  $\psi$  obtained through Gauss quadrature

$$\phi_\ell = 2\pi \int_{-1}^{+1} \psi(\mu) P_\ell(\mu) d\mu = \sum_{k=1}^N \psi_k P_\ell(\mu_k) w_k \quad (3-63)$$

will not be exact. In analyzing the scattering source, we wish to portray the cross section coefficients as being weighted by the flux coefficients. Since the flux coefficients decrease in value with increasing  $\ell$ , then each succeeding term of the summation in Equation (3-62) contributes less to the scattering source. Therefore, for any particular value of  $\ell$ , if  $\phi_\ell$  is very small, then the contribution of  $\sigma_\ell$  is diminished accordingly, and it will not matter significantly if  $\sigma_\ell$  is inexact. It follows from this analysis that we would expect the TIF expansions to produce approximately the same results as Morel's expansions.

#### Coefficients for $\sigma^e$

We recall that the group-to-group transfer cross section must be defined from the term of the decoupled cross section which allows redistribution in energy but no angular change:  $\sigma^e(E' \rightarrow E) \delta(\mu_0 - 1)/2\pi$ . The Legendre expansion coefficients of a delta function at  $\mu_0 = 1$  are equal to  $P_\ell(1) = 1$ . Therefore,  $\sigma^e$  must be a truncated delta-function expansion with coefficients of equal magnitude.

For convenience, Morel decomposed  $\sigma^e$  into the sum of two cross sections

$$\sigma^e(E' \rightarrow E) = \sigma^\beta(E' \rightarrow E) + \sigma^\gamma(E' \rightarrow E) . \quad (3-64)$$

The cross sections  $\sigma^\beta$  and  $\sigma^\gamma$  correspond to the differential operators containing  $\beta$  and  $\gamma$ , or  $r_{FP}^\beta$  and  $r_{FP}^\gamma$ , respectively (see Equations (3-3b) and (3-3e)). Morel explains that both  $r_{FP}^\beta$  and  $r_{FP}^\gamma$  correspond to a type of continuous scattering approximation.  $r_{FP}^\beta$  corresponds to the well-known continuous slowing down approximation wherein particles lose energy continuously with the energy loss per unit path length given by the stopping power.  $r_{FP}^\gamma$  causes particles to both up-scatter and downscatter in equal numbers so that the overall energy loss is zero. The mean square stopping power determines the amount of mean-square energy change experienced by the particles per unit path length. This "diffusion" in energy space introduces energy-loss straggling into the calculation.

Morel defined the multigroup cross sections corresponding to  $\sigma^\beta$  and  $\sigma^\gamma$  as follows:

$$\begin{aligned} \sigma_{g+k}^\beta &= \frac{\beta(E_g)}{E_g - E_k}, & \text{for } k = g + 1, \text{ if } \beta(E_g) \geq 0, \text{ and} \\ & & \text{for } k = g - 1, \text{ if } \beta(E_g) < 0, \\ &= 0 & \text{for all other values of } k, \end{aligned} \quad (3-65)$$

and

$$\sigma_{g \rightarrow k}^Y = \frac{\gamma(E_g)}{2(E_g - E_k)^2}, \quad \text{for } k = g - 1 \text{ and } k = g + 1, \\ = 0 \quad \text{for all other values of } k. \quad (3-66)$$

The variable  $E_g$  denotes the group midpoint energy of group  $g$  and  $\sigma_{g \rightarrow k}$  is defined as the probability per unit path length that a particle will scatter through zero degrees from group  $g$  to group  $k$ . Since a particle cannot upscatter in the first group nor downscatter in the last group, we complete the definitions for the multigroup cross sections by setting  $\sigma^Y = 0$  for the first and last groups,  $\sigma^\beta = 0$  for the first group if  $\beta(E_1) < 0$ , and  $\sigma^\beta = 0$  for the last (NG) group if  $\beta(E_{NG}) > 0$ .

For problems involving a lower cutoff energy (i.e., an energy deposition calculation), Morel also defines an effective absorption cross section for the last group (see Equation (3-65)):

$$\sigma_a^* = \frac{\beta(E_{NG})}{E_{NG} - E_f}, \quad (3-67)$$

where  $E_f$  denotes the midpoint energy of a fictitious group below the last one. The absorption cross section effectively transfers particles from the last group to thermal energies and deposits their remaining energy on the spot.

Let us restate some of the analysis and conclusions drawn by Morel concerning the multigroup cross sections:

1. The multigroup coefficients are based on energy rather than particle conservation requirements.

$$\sum_k g \rightarrow k (E_g - E_k) = \beta(E_g) \quad (3-68)$$

is always correct, but the mean-square stopping power

$$\sum_k \sigma_{g \rightarrow k}^e (E_g - E_k)^2 = \gamma(E_g) + \beta(E_g) (E_g - E_{g+1}) \quad (3-69)$$

converges to  $\gamma(E_g)$  only in the limit as the group width goes to zero.

3. With a uniform energy group width, the multigroup treatment for  $r_{FP}^\beta$  is equivalent to a standard first order backward-difference approximation, and the treatment for  $r_{FP}^\gamma$  is equivalent to a standard second order center-difference approximation.

4. The use of a truncated delta function expansion, in conjunction with the multigroup cross section for  $\sigma^e$ , is valid for  $S_n$  calculations if the cross section expansion is of degree  $(N-1)$  and the Gauss quadrature set is of order  $N$ . Quadrature sets other than the Gauss quadrature set may not be sufficiently accurate to treat delta function scattering.

5. Since  $r_{FP}^\gamma$  introduces upscatter into a calculation, and since the computational cost of treating upscatter is relatively high, then it may be advantageous to neglect the  $r_{FP}^\gamma$  term for problems without upscatter.

Since Morel's coefficients for  $\sigma^e$  represent an everywhere positive function, no new expansion was derived as in the case for  $\sigma^\alpha$ . But as explained earlier, delta function expansions are not suitable for input to the quadrature scattering algorithms present in MORSE. This problem was easily remedied however, by inserting some Fortran statements into the code to check for those expansions characterized by having all of its coefficients close to 1. If such an expansion was found, it was then known to approximate a delta function and a single scattering direction at  $\mu_0 = 1$  and a weight of 1 were set for that group-to-group transfer. The new coding statements are shown at the beginning of Subroutine ANGLES in Appendix C.

### Computational Results and Analysis

In the two previous sections of this chapter, we have discussed Morel's multigroup treatment of  $\sigma^\alpha$  and  $\sigma^e$ , as well as a new approximation in the form of a triangular impulse function for  $\sigma^\alpha$ . For convenience, we will label Morel's Fokker-Planck expansion for  $\sigma^\alpha$  as MFP and the new expansion as TIF. The MFP has the important and highly desirable characteristic of being spherical-harmonic equivalent, but it converges to the Fokker-Planck operator,  $r_{FP}^\alpha$ , from the negative region of phase space (it is nonphysical with respect to angle). Conversely, the TIF is not spherical-harmonic equivalent, except in the diffusion limit, but it approaches  $r_{FP}^\alpha$  from the

positive region of phase space. Nevertheless, the TIF and MFP, each with the same order of expansion  $L$ , should approximate each other when the angular flux is adequately represented by an expansion of degree  $L$  or less.

In this section, we will compare the MFP and TIF cross section expansions from a computational standpoint via energy and charge deposition calculations using the ONETRAN (a one-dimensional finite element  $S_n$  code; see Hill, 1975) and MORSE codes. The computations were performed for 1-MeV electrons isotropically incident on cold slabs of aluminum. The slab thicknesses were chosen to correspond to approximately one-sixth range (12.5 mil), one-third range (25 mil), and two-thirds range (50 mil), denoted as Problems 1, 2, and 3, respectively. Fifty evenly-spaced groups were used, ranging from 1 MeV down to 0.1 MeV, and the source strength was normalized to unity. An effective absorption cross section (see Equation (3-67)) was defined for the last energy group since the range of the electrons in that group was small relative to the slab dimensions and the residual energy would be deposited locally. The cross section expansions, TIF and MFP, were each given the same  $\sigma_0^\alpha$  and  $\sigma_1^\alpha$ , and were each input as  $P_7$  expansions. For the ONETRAN code, this means that a Gaussian  $S_8$  quadrature set must be used to effectively treat the delta function scattering and to obtain spherical-harmonic equivalency. For the MORSE code, it means that we may extract up to four discrete directions (NSCT = 1, 2, 3, or 4) and weights from which to sample

scattering angles. If we elect to compute only one discrete direction and weight from the  $P_7$  expansion, then we are using only the first two coefficients of the expansion, and this corresponds to inputting a delta function at  $\bar{\mu}_0 = \sigma_1^\alpha / \sigma_0^\alpha$ . Recall that a delta function at  $\bar{\mu}_0$  lies on the border between the physical (TIF) and the non-physical (MFP) expansions, and as such, is the best we can do in approximating the MFP. Also, since no upscattering occurs at the energies of interest, the full second order approximation for  $\sigma^e$  was not needed in the calculation, and only the first order continuous slowing down approximation was used.

Using the identical test case described above, Morel (1981) analyzed his Fokker-Planck expansions by comparing the ONETRAN results against "exact" solutions from a one-dimensional coupled electron-photon Monte Carlo transport code called TIGER (Halbleib and Vandevender, 1974). However, the TIGER code had to first be modified to solve the Fokker-Planck equation instead of the coupled electron-photon Boltzmann equation. This was done by removing energy loss straggling effects (disallowed sampling from the Landau distribution), thereby restricting the calculation to the continuous slowing down approximation. The scattering angle in TIGER is sampled from a Legendre expansion derived from Goudsmit-Saunderson multiple scattering theory. The coefficients of the expansion contain the term  $(\sigma_0 - \sigma_\ell)$  which was replaced by the Fokker-Planck equivalent,  $\alpha\ell(\ell + 1)/2$ . Morel's comparison of the ONETRAN-MFP results and the "exact"

solutions from TIGER will be presented along with the TIF and MFP comparison. The energy deposition values calculated by TIGER and MORSE for each spatial zone have a relative standard deviation of less than two percent.

There are other items pertaining to these computations which have been adequately discussed by Morel and need not be repeated in detail here: the equations relating the multigroup stopping powers, the flux, and the effective absorption cross section to charge and energy deposition, as well as the expressions for the nonrelativistic momentum transfer ( $\alpha(E)$ ) and the relativistic stopping power ( $\beta(E)$ ) required to compute the cross sections. Also, for information regarding the input format of the cross section libraries, since it is code specific, the reader is referred to the available code documentation.

Figure (3-2) shows three sets of curves which represent Morel's energy deposition profiles as a function of slab penetration for Problems 1, 2, and 3. The profiles were calculated by TIGER (denoted by "Monte Carlo" in the legend) and ONETRAN-MFP (denoted by " $S_N$ " in the legend). The energy deposition profiles appear to be in excellent agreement. Figures (3-3) through (3-5) show similar profiles for MORSE-TIF (NSCT = 1) and ONETRAN-MFP, and as expected, the agreement also appears to be quite good (note that the ordinate axis in Figure (3-4) is expanded).

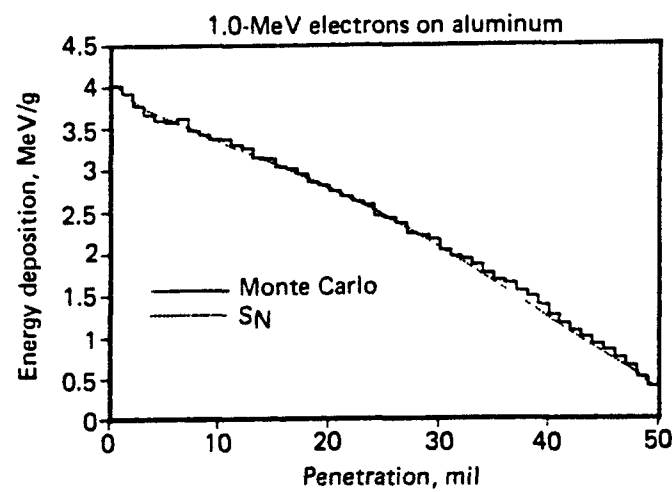
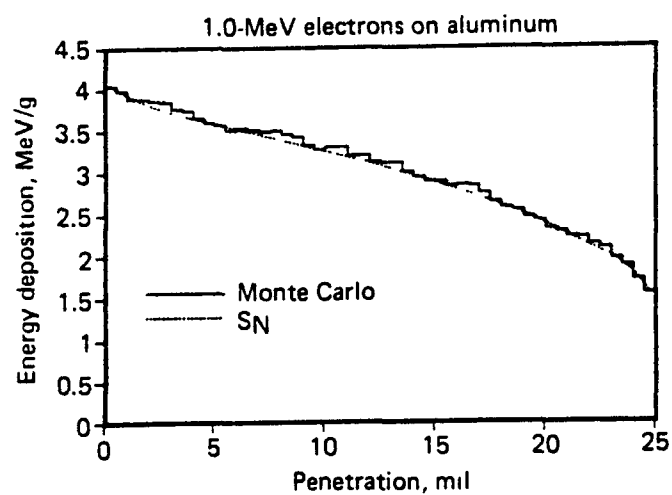
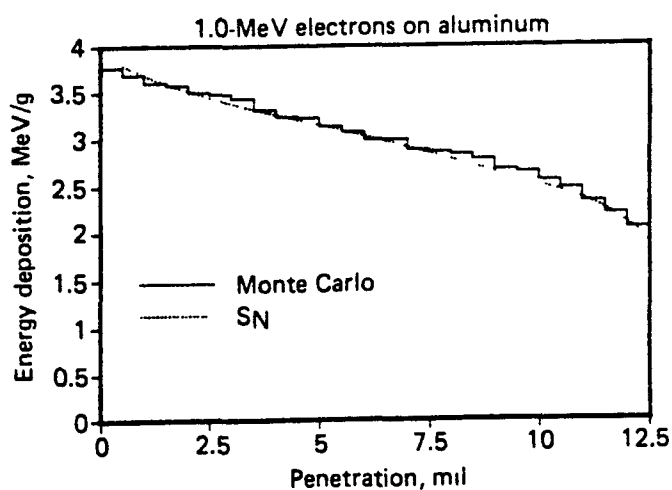


Figure (3-2). Energy deposition profile comparison for Problems 1, 2, and 3 (top to bottom).

## 1.0 MeV Electrons on Aluminum

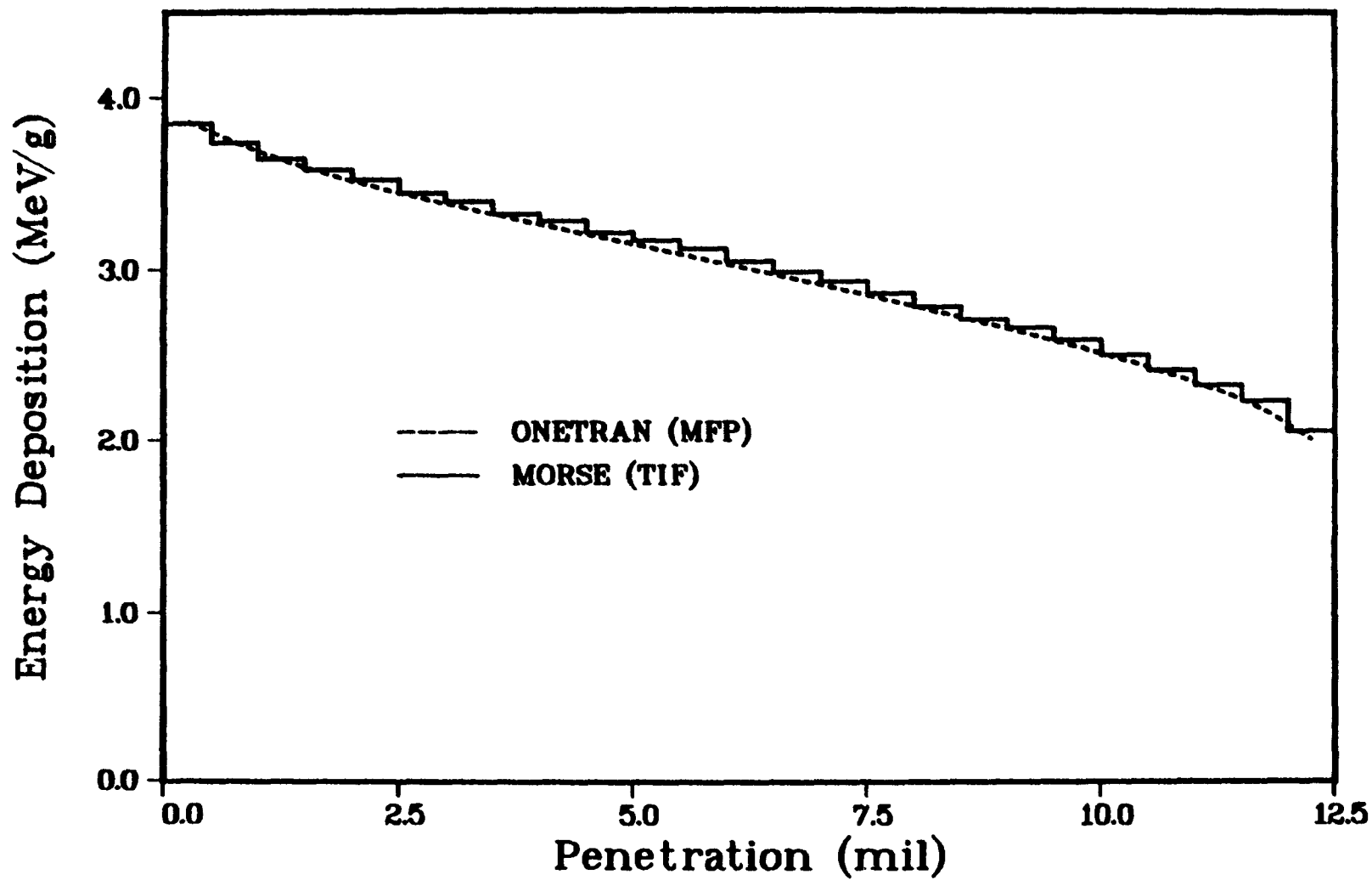


Figure (3-3). Energy deposition profile comparison for Problem 1.

### 1.0 MeV Electrons on Aluminum

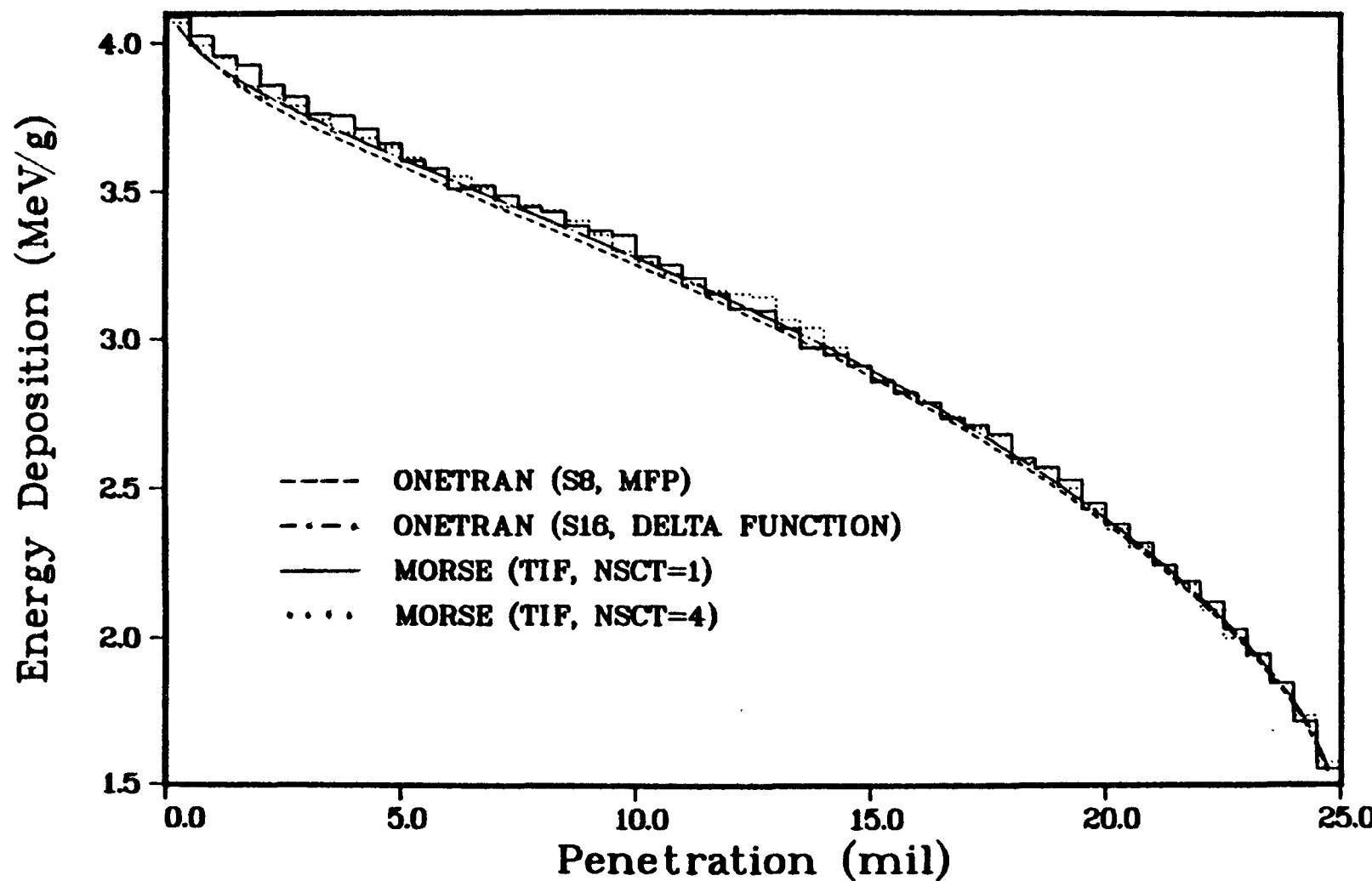


Figure (3-4). Energy deposition profile comparison for Problem 2.

## 1.0 MeV Electrons on Aluminum

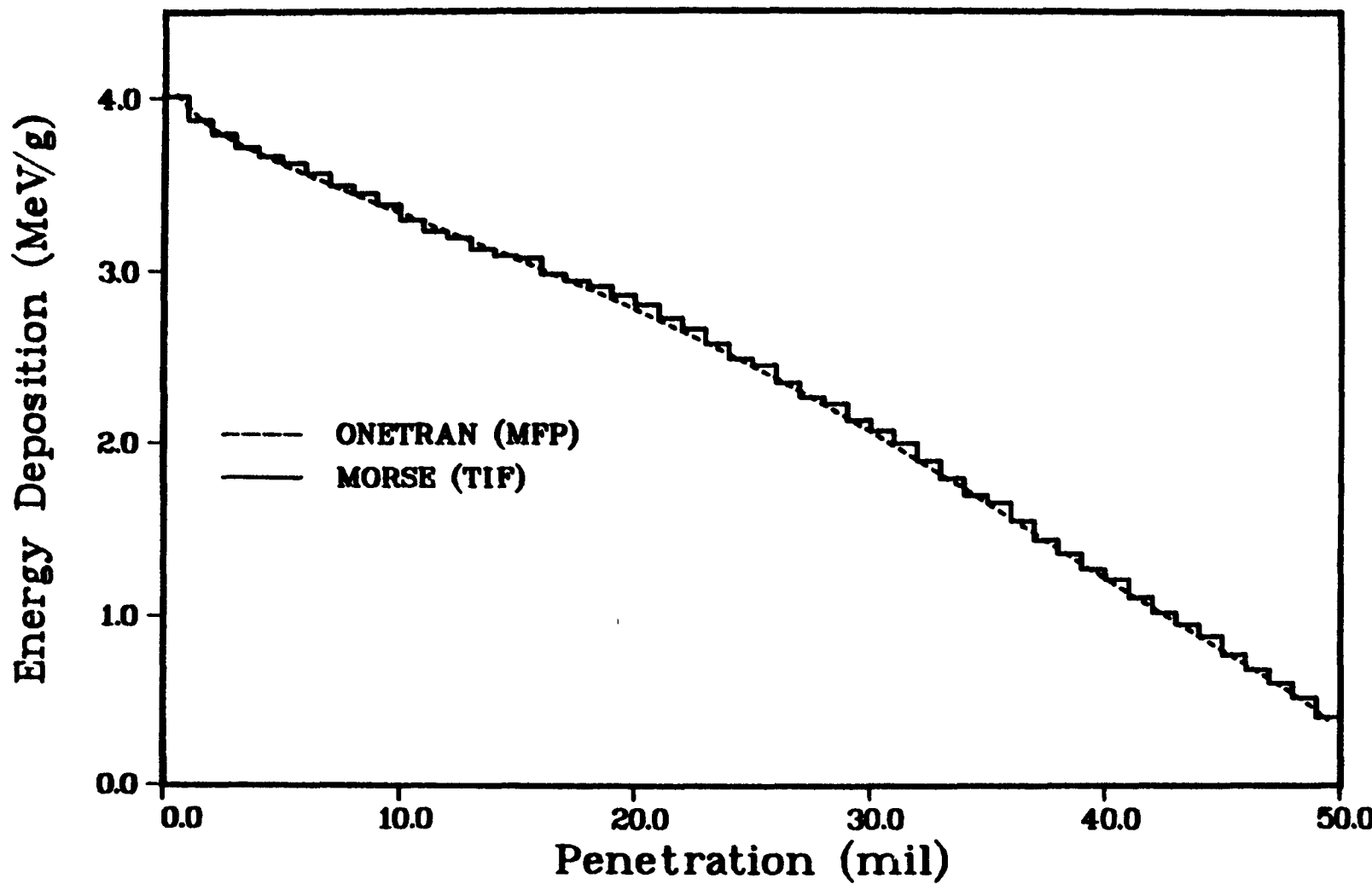


Figure (3-5). Energy deposition profile comparison for Problem 3.

A more quantitative analysis of the agreement between TIGER, ONETRAN-MFP, and MORSE-TIF may be obtained from the bulk energy deposition values shown in Table (3-2).

Table (3-2)

Bulk Energy Deposition

	<u>ONETRAN-MFP</u>	<u>MORSE-TIF</u>	<u>TIGER</u>
Problem 1	0.255	$0.258 \pm 0.2\%$	$0.258 \pm 1.0\%$
Problem 2	0.512	$0.519 \pm 0.1\%$	$0.518 \pm 0.5\%$
Problem 3	0.795	$0.802 \pm 0.2\%$	$0.806 \pm 0.5\%$

The data shows that the ONETRAN bulk energy deposition values lie approximately 0.8 to 1.4 percent lower than the TIGER and MORSE values. This difference, though admittedly very small, is persistent and is in part due to convergence of the  $S_N$  solution rather than statistical error. Although the solution is basically converged as far as the energy group structure is concerned, Morel showed that increasing the number of energy groups does raise the ONETRAN profile slightly.

The same analysis holds true for increasing the  $S_N$  quadrature and expansion order. To show this, ONETRAN calculations were performed for the TIF, as well as the MFP, for each test case. The TIF and MFP were both input as  $P_7$  expansions in an  $S_8$  calculation, and the resulting difference in the solutions was usually close enough to be indiscernible on a plot. This is what we expected from our theoretical analysis. And since a delta function (located at the  $\bar{\mu}_0$

corresponding to a  $P_7$  MFP) is on the physical/nonphysical border between the MFP and TIF, its solution should likewise be very close to the others. However, it was found that if the quadrature order was increased from an  $S_8$  to an  $S_{16}$ , and the expansion order of the same delta function was increased to a  $P_{15}$ , then the energy deposition curve would shift upwards (this effect is shown in Figure (3-4) for Problem 2). We would ultimately expect that if the quadrature order was increased to  $S_\infty$ , and the expansion order increased to infinity to represent the delta function exactly, then the ONETRAN curve would converge to the MORSE-TIF (NSCT = 1) profile. This conclusion follows from the fact that using MORSE with one allowed discrete scattering cosine, at some  $\mu_0$ , is equivalent to an  $S_\infty$  calculation with a delta function cross section at the same  $\mu_0$ .

Also shown in Figure (3-4) is an energy deposition profile from a MORSE-TIF (NSCT = 4) calculation. Setting the number of allowed scattering angles to four permits the code to use all eight moments of the  $P_7$  TIF expansion, instead of just the first two moments in the case where NSCT = 1. From the plot, it is difficult to statistically resolve any significant difference in the NSCT = 1 and NSCT = 4 solutions. This would indicate that the MORSE solutions using the TIF and delta function cross sections are essentially equivalent.

In addition to energy deposition calculations, charge deposition for Problems 1, 2, and 3 was also determined for comparison purposes. Figure (3-6) shows Morel's charge deposition profiles from

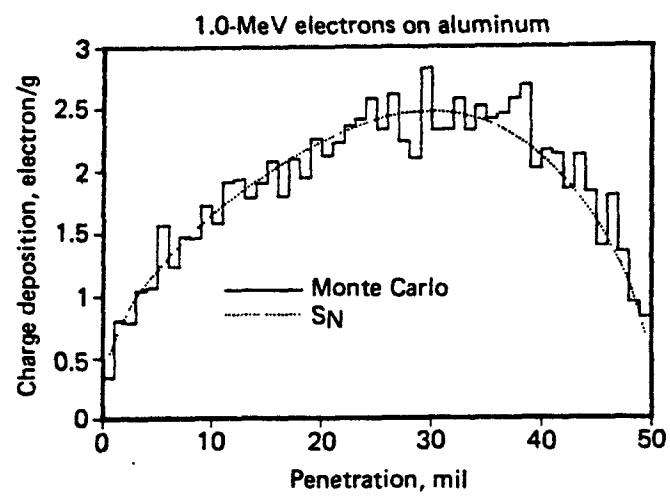
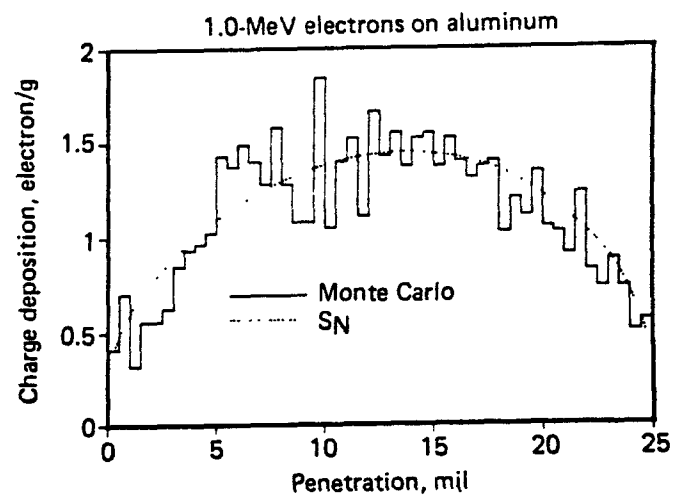
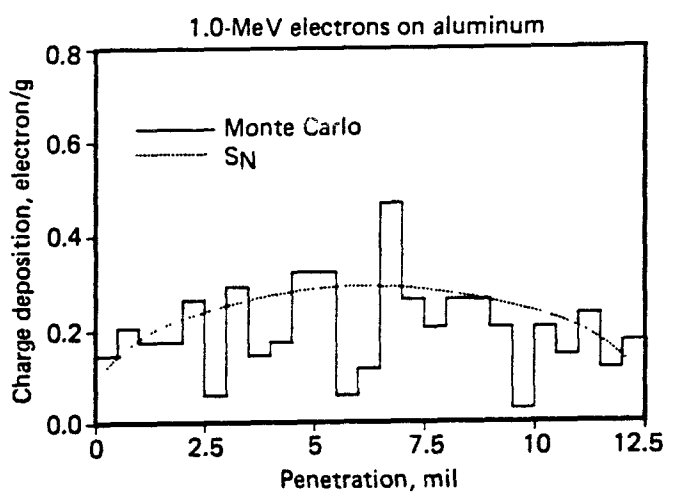


Figure (3-6). Charge deposition profile comparison for Problems 1, 2, and 3 (top to bottom).

ONETRAN-MFP and TIGER as a function of penetration. The TIGER profile for Problem 1 is a poor representation due to the large amounts of statistical error. The same profiles for Problems 2 and 3 achieved better statistics and permit more meaningful analysis. Figures (3-7) through (3-9) show charge deposition profile comparisons for ONETRAN-MFP and MORSE-TIF (NSCT = 1). A larger number of particle histories was generated in the MORSE calculation to enhance its statistics somewhat over the TIGER calculations. The agreement between the charge deposition profiles from the various codes is still very good, though clearly the statistical error is more severe than for the energy deposition profile comparisons. The reason for the poorer statistical agreement among the charge deposition profiles is that the particles may contribute to the charge deposition only when they have reached the lowest energy group, whereas particles have a finite probability of contributing to the energy deposition at every collision.

The bulk charge electron deposition values are given in Table (3-3).

Table (3-3)  
Bulk Charge Electron Deposition

	<u>ONETRAN-MFP</u>	<u>MORSE-TIF</u>	<u>TIGER</u>
Problem 1	0.020	$0.022 \pm 2.4\%$	$0.017 \pm 3\%$
Problem 2	0.198	$0.202 \pm 0.8\%$	$0.193 \pm 1\%$
Problem 3	0.643	$0.649 \pm 0.5\%$	$0.651 \pm 1\%$

## 1.0 MeV Electrons on Aluminum

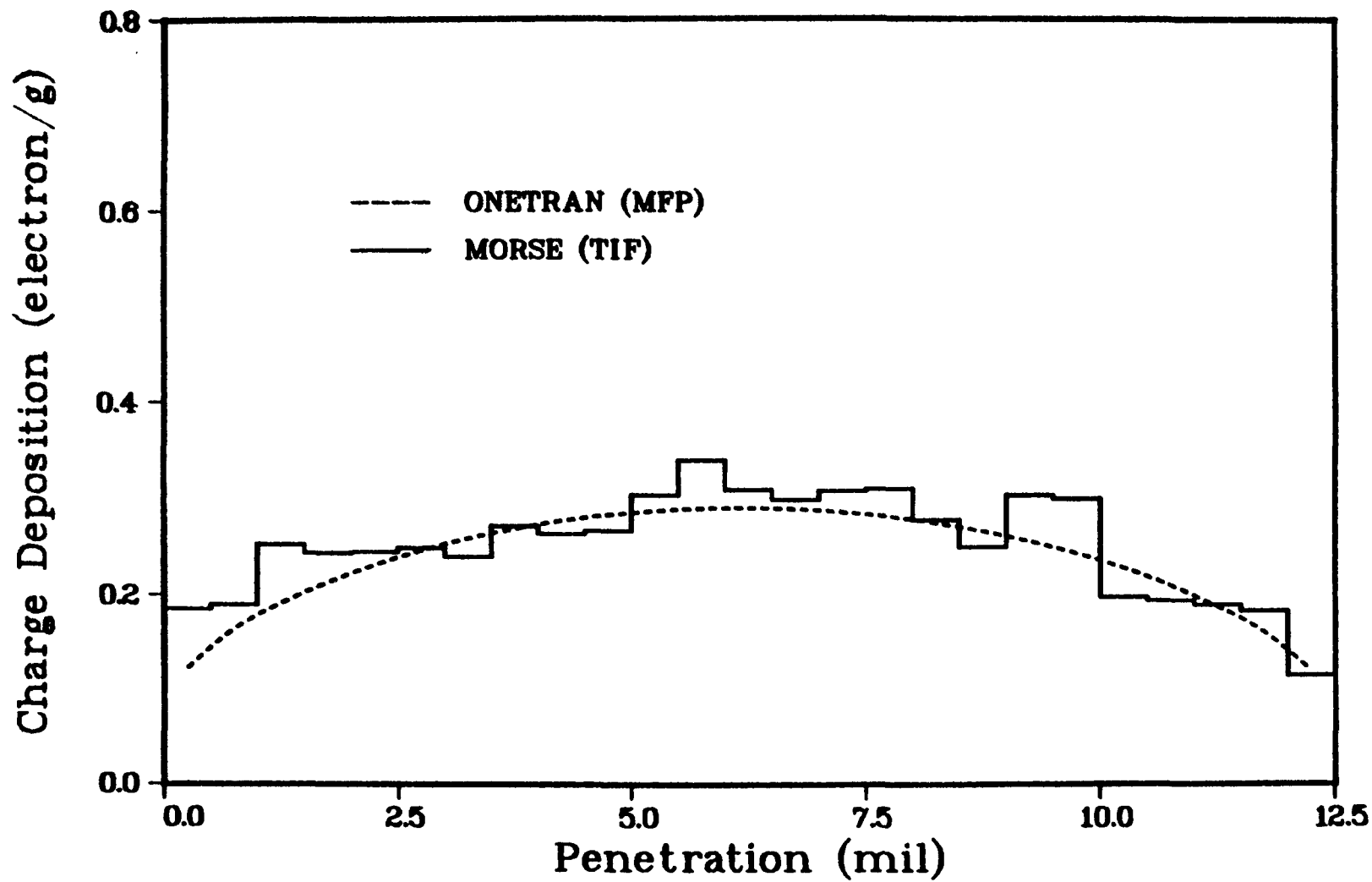


Figure (3-7). Charge deposition profile comparison for Problem 1.

## 1.0 MeV Electrons on Aluminum

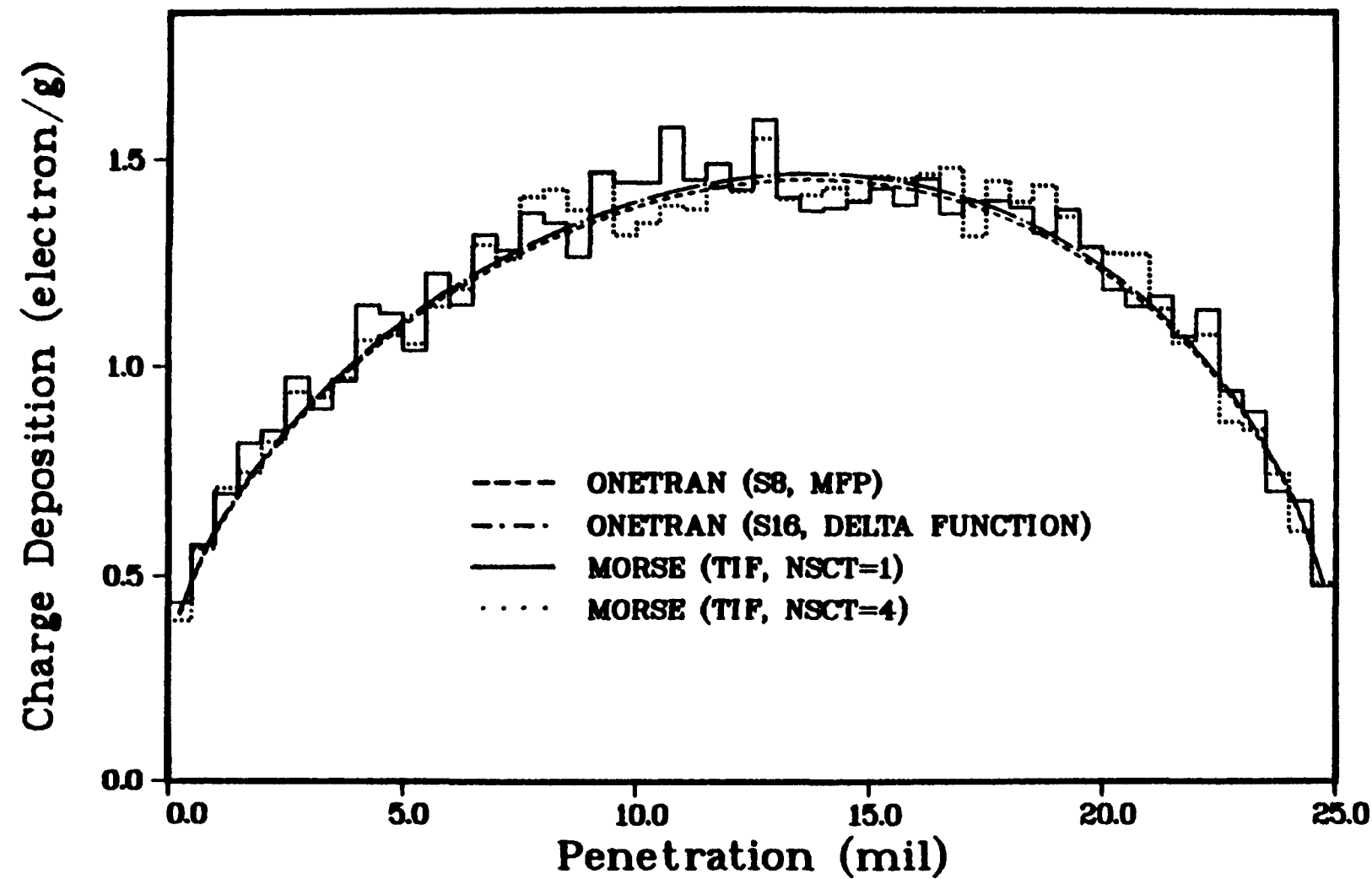


Figure (3-8). Charge deposition profile comparison for Problem 2.

### 1.0 MeV Electrons on Aluminum

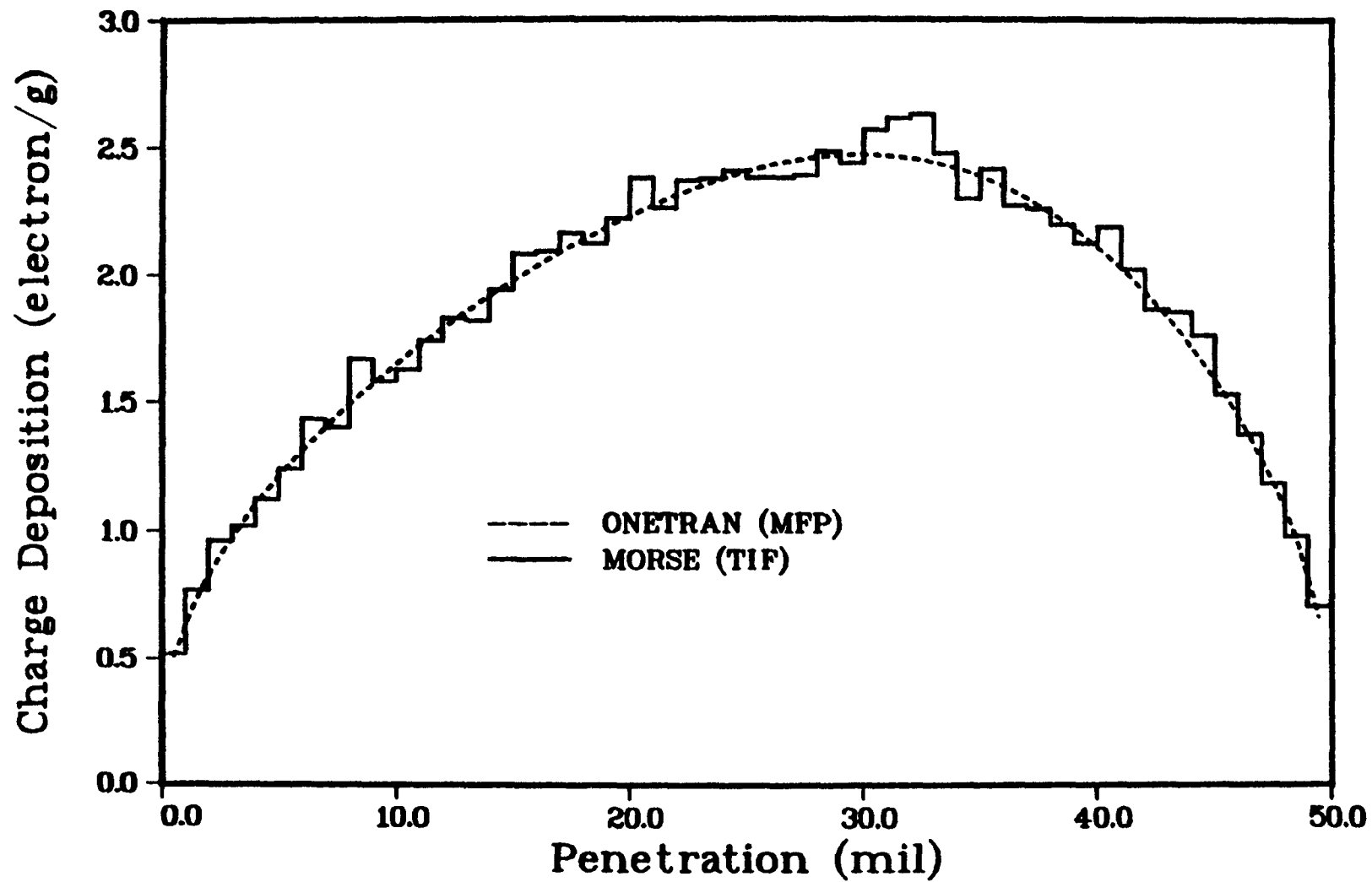


Figure (3-9). Charge deposition profile comparison for Problem 3.

The ONETRAN and TIGER values differ by approximately 17.7, 2.6, and 1.3 percent for Problems 1, 2, and 3, respectively. The MORSE and TIGER values differ by approximately 29.4, 4.7, and 0.3 percent for the same problems. These percent differences, between the TIGER values, and those from ONETRAN and MORSE, appear to decrease with increasing thickness. Morel proposes that the poor estimate of charge deposition in Problem 1 is due to range or energy-loss straggling. This straggling effect permits particles to thermalize over path lengths much shorter or longer than the actual range, and is an inherent characteristic of the multigroup approximation to the CSDA (continuous slowing down approximation) operator. The range straggling effects decrease with decreasing energy group widths.

The ONETRAN-TIF profile was not shown along with the ONETRAN-MFP profile in any of the figures for charge deposition because the solutions matched so closely. However, the MORSE-TIF profiles are shown for both NSCT = 1 and NSCT = 4 in Figure (3-8), and the agreement is very good. This close agreement of solutions from a particular code, independent of whether the cross section input is MFP, delta function, or TIF, is strong evidence for the interchangeability of these cross sections.

Figure (3-8) also contains a charge deposition curve from an  $S_{16}$  ONETRAN calculation with a  $P_{15}$  delta function input. The delta function is positioned at the mean scattering angle characterizing the  $P_7$  MFP. The charge deposition curve is seen to shift up from the

ONETRAN-MFP curve and again emphasizes that the difference in the bulk charge electron values between ONETRAN-MFP and MORSE-TIF (though small) is primarily due to  $S_n$  convergence.

Figure (3-10) shows a comparison of the reflected current spectrum between ONETRAN-MFP and TIGER for Problem 2. Figure (3-11) shows a similar comparison of the transmitted current spectrum for various group structures.

Referencing Figure (3-10) first, the ONETRAN-MFP reflected current spectrum shows good agreement with the TIGER spectrum except at the source energy end of the spectrum where the ONETRAN curve takes an upswing. This high energy peak is characteristic of the ONETRAN solution only, and is not found in either the MORSE or TIGER solutions. The cause of the peak is that the full-range Gauss quadrature set does not completely satisfy the Marshak boundary condition. The peak height is reduced by increasing the quadrature order, or it may even be eliminated by using a special half-range quadrature set developed by Morel (1983). Figure (3-12) shows the reflected current spectrum comparison for ONETRAN and MORSE with various input cross sections. Note specifically the difference in the peak heights between the  $S_8$  and  $S_{16}$  ONETRAN solutions. Since  $S_n$  calculations conserve particles, a result of increasing the quadrature order and thereby reducing the high energy peak is that particles are now forced to transmit through the slab or be absorbed. And that is why the  $S_{16}$  ONETRAN calculations shifted the energy and charge deposition

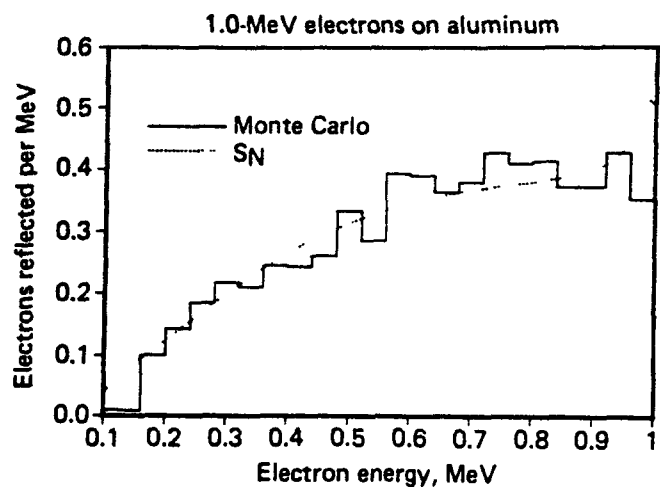


Figure (3-10). Reflected current spectrum comparison for Problem 2.

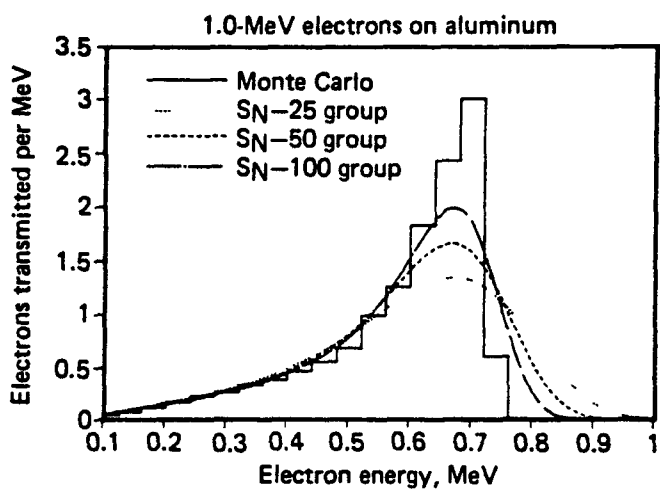


Figure (3-11). Transmitted current spectrum comparison with various group structures for Problem 2.

## 1.0 MeV Electrons on Aluminum

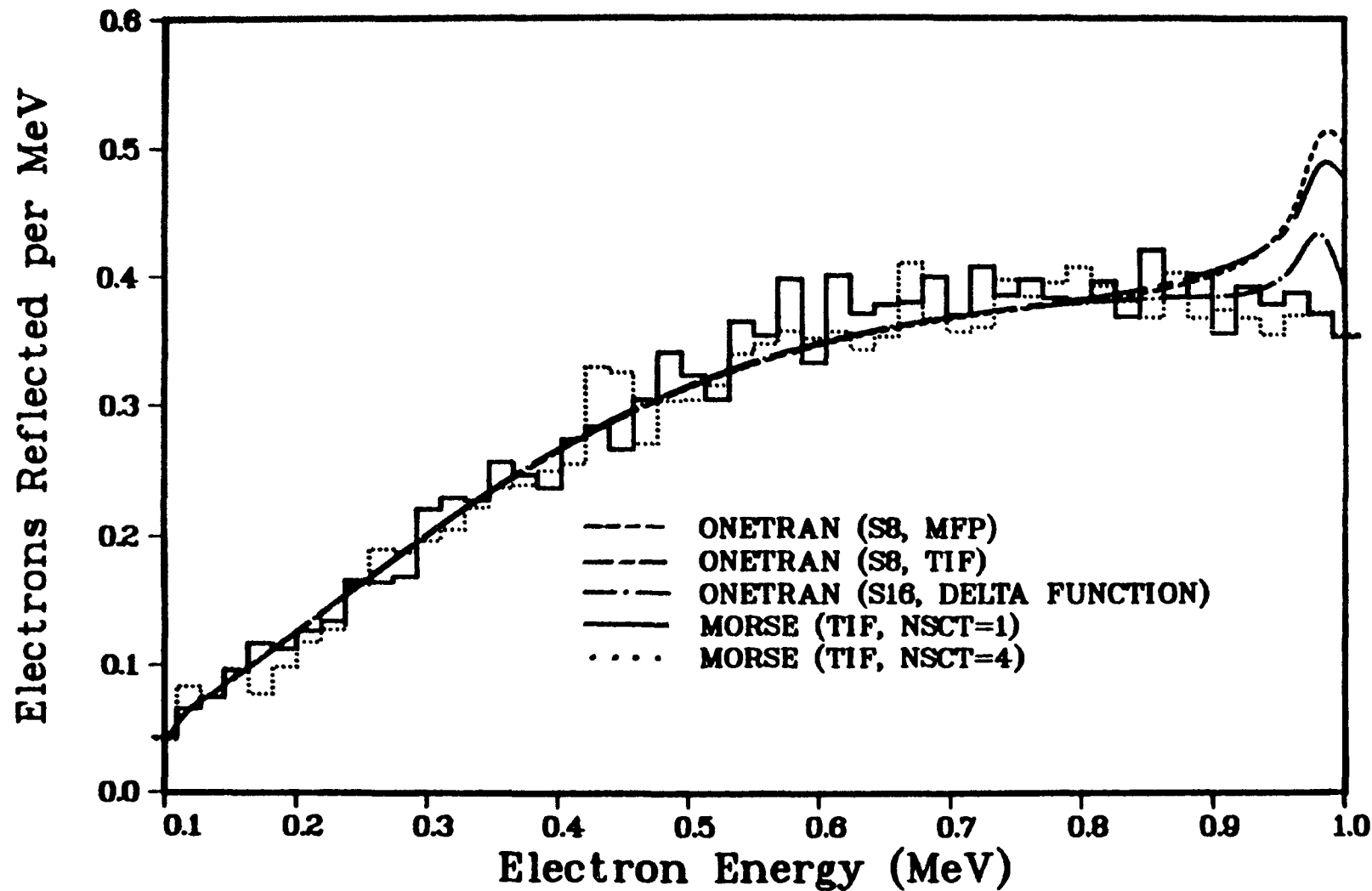


Figure (3-12). Reflected current spectrum comparison for Problem 2.

profiles upwards slightly from the  $S_8$  profiles. Further increases in quadrature order would enhance the convergence of the ONETRAN solution to the MORSE solution.

Additional information may be gained by referring back to the transmitted current spectrum comparison shown in Figure (3-11).

Obviously, the TIGER and ONETRAN-MFP profiles agree very poorly. Morel analyzed the spectra comparisons and discussed their significance. We will briefly summarize some of this findings and conclusions below.

1. The TIGER and ONETRAN curves do show good agreement at low energies--this is necessary to account for good charge deposition profile agreement.
2. The spectrum integral represents the total number of particles transmitted, and the energy-weighted integral represents the total amount of energy transmitted. These quantities remain relatively unchanged in comparing one curve to another which accounts for the good energy deposition profile agreement.
3. The broadening effect exhibited by the discrete ordinates curves is generally more pronounced at larger distances from the source than at smaller distances.
4. The spectral broadening is due to energy-loss straggling originating from the multigroup approximation. Decreasing the energy group width enhances convergence, as seen in

Figure (3-11). However, the rate of convergence is inversely related to the slope or rate of change of the true energy spectrum. For example, a rapidly varying spectrum denotes slow convergence of the  $S_n$  solution.

Since MORSE also uses the same multigroup cross section data as ONETRAN, we would expect the MORSE-TIF transmitted spectrum to copy the ONETRAN-MFP solution (rather than the TIGER solution). This analysis is substantiated by Figure (3-13) showing the transmitted current spectrum comparisons for Problem 2 using ONETRAN and MORSE. The spectral agreement is excellent and does not seem to depend on the type of cross section used. The MORSE spectra exhibits the same broadening effect from energy loss straggling as the discrete ordinates spectra.

We have thus far shown that our treatment of the angular operator,  $\Gamma_{Fp}^\alpha$ , in developing the TIF cross section, is equivalent computationally to the MFP and is compatible with the scattering algorithm in MORSE. The Fokker-Planck approximation using the triangular impulse function retains the same benefits and weaknesses as the previous cross section set developed by Morel; i.e., accurate solutions may be obtained for energy and charge deposition, but the accuracy of the differential spectra is dependent on its distance from the source.

The development of the new set of Fokker-Planck cross sections for use in MORSE results in both three-dimensional capability as well

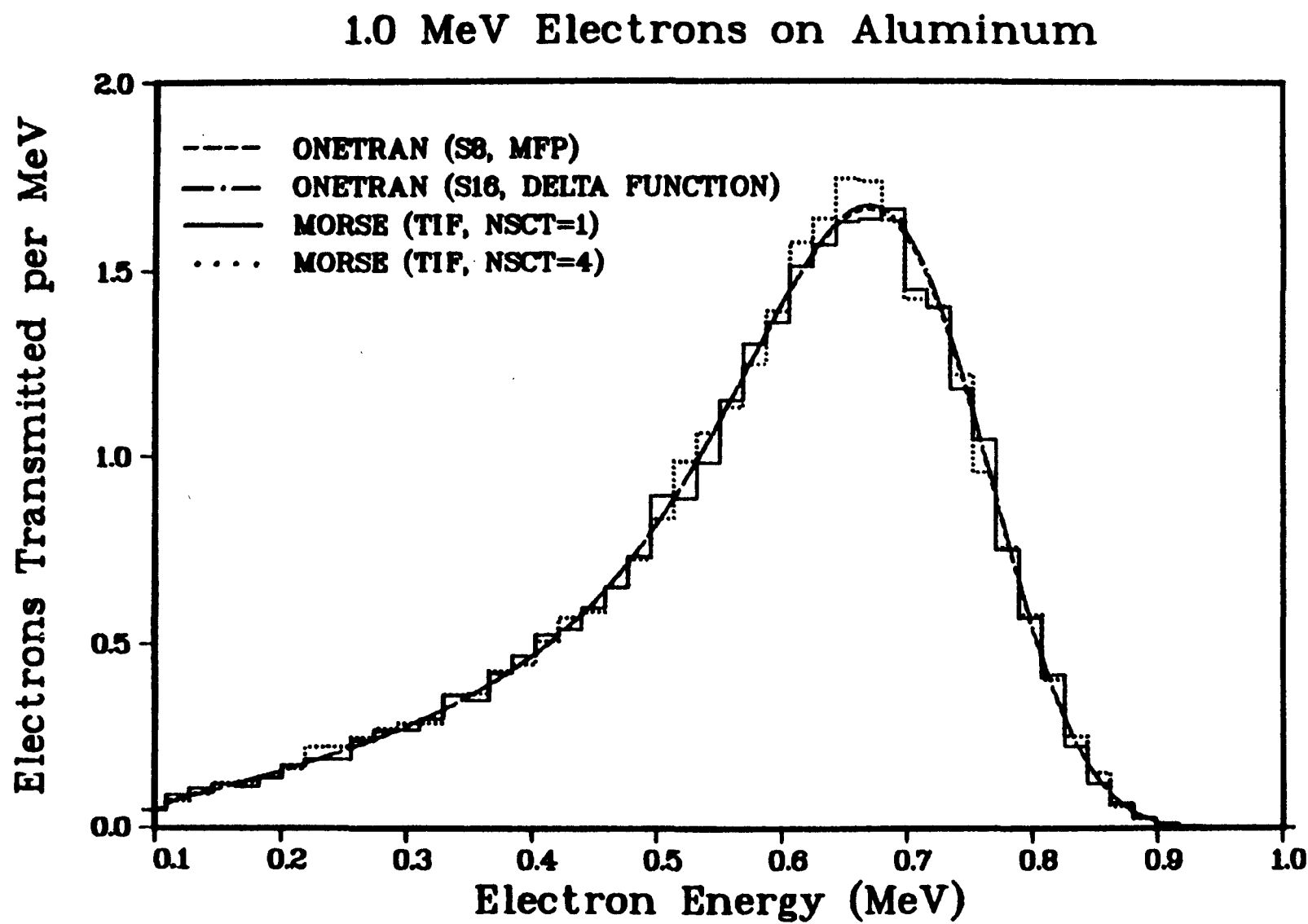


Figure (3-13). Transmitted current spectrum comparison for Problem 2.

as a forward or adjoint option for problem solving. This greatly increases the versatility of the code and the number of applications to which the Fokker-Planck approximation could conceivably be applied. To demonstrate this versatility, we have performed an adjoint calculation to calculate energy deposition in the core of a sphere. The geometry was chosen to be one-dimensional in angle so that comparisons with ONETRAN could be obtained (recall that two-dimensional quadrature sets do not have sufficient accuracy to treat the delta function scattering in the energy operator). The problem was similar in many aspects to the previous slab calculations. A 1.0 MeV electron flux was isotropically incident on a sphere of cold aluminum. The radius of the sphere was approximately one-third the range of a source particle. The inner core of the sphere was arbitrarily set to one-tenth the sphere radius. Fifty evenly-spaced energy groups were used over the energy range from 1.0 to 0.1 MeV. Again, we will dismiss with many of the details of the calculation and simply refer the reader to ample documentation on the codes and adjoint formalism: Halbleib and Morel (1980), Renken (1970), Hansen and Sandmeier (1965).

Table (3-4) shows the forward and adjoint energy deposition results for the spherical inner core from ONETRAN-MFP and MORSE-TIF.

Table (3-4)

Bulk Core Energy Deposition  
(MeV x 10<sup>-5</sup>)

	<u>Forward</u>	<u>Adjoint</u>
ONETRAN-MFP	1.037	1.058
MORSE-TIF	1.045 ± 2.5%	1.017 ± 1.4%

The agreement is very good. The ONETRAN and MORSE forward solutions compare very well, and the MORSE forward and adjoint solutions agree to within the statistical error. The ONETRAN forward and adjoint solutions, though approximately equal, do not show exact agreement, because the adjoint  $S_n$  equation in curvilinear coordinates is not exactly adjoint to the forward  $S_n$  equation. However, the adjoint and forward solutions do converge in the limit as the quadrature order is increased with a constant spatial mesh and group structure.

## APPENDIX A

### DERIVATION OF THE FOKKER-PLANCK EQUATION

The following derivation of a second-order accurate Fokker-Planck equation follows closely the derivation of Morel (1981) and somewhat that of Wang and Guth (1951). The derivation is appropriate for problems with:

1. one-dimensional slab or spherical geometry,
2. an isotropic transport medium (a medium with no preferred direction for particle travel; crystalline structures or certain plasma configurations are examples of anisotropic medias), and
3. forward-peaked elastic scattering.

In order to fully define the working variables, the derivation begins with the general time-dependent integro-differential form of the Boltzmann transport equation (Emmett, 1975). The Boltzmann equation describes a bookkeeping process that sets the net storage of particles within a differential element of phase space ( $d\bar{r}, dE, d\bar{\Omega}$ ) equal to the particle gains minus the particle losses within that differential element. One familiar form of the Boltzmann is:

$$\frac{1}{v} \frac{\partial}{\partial t} \psi(\bar{r}, E, \bar{\Omega}, t) + \bar{\Omega} \cdot \nabla \psi(\bar{r}, E, \bar{\Omega}, t) + \sigma_t(\bar{r}, E) \psi(\bar{r}, E, \bar{\Omega}, t) = Q(\bar{r}, E, \bar{\Omega}, t) + \iint dE' d\bar{\Omega}' \sigma_s(\bar{r}, E' \rightarrow E, \bar{\Omega}' \rightarrow \bar{\Omega}) \psi(\bar{r}, E', \bar{\Omega}', t), \quad (A-1)$$

where

$(\bar{r}, E, \bar{\Omega}, t)$  = the general multidimensional phase space,

$\bar{r}$  = position vector,

$E$  = the particle kinetic energy,

$v$  = the particles speed corresponding to its kinetic energy,  $E$ ,

$\bar{\Omega}$  = a unit vector which describes the particles direction of motion,

$t$  = time variable,

$\psi(\bar{r}, E, \bar{\Omega}, t)$  = the time-dependent angular flux,

$\psi(\bar{r}, E, \bar{\Omega}, t) dE d\bar{\Omega}$  = the number of particles that cross a unit area normal to the  $\bar{\Omega}$  direction per unit time at the space point  $\bar{r}$  and time  $t$  with energies in  $dE$  about  $E$  and with directions that lie within the differential solid angle  $d\bar{\Omega}$  about the unit vector  $\bar{\Omega}$ ,

$\frac{1}{v} \frac{\partial}{\partial t} \psi(\bar{r}, E, \bar{\Omega}, t) dE d\bar{\Omega}$  = the net storage (gains minus losses) per unit volume and time at the space point  $\bar{r}$  and time  $t$  of particles with energies in  $dE$  about  $E$  and with directions which lie in  $d\bar{\Omega}$  about  $\bar{\Omega}$ ,

$\bar{\Omega} \cdot \nabla \psi(\bar{r}, E, \bar{\Omega}, t) dE d\bar{\Omega}$  = net convective loss per unit volume and time at the space point  $\bar{r}$  and time  $t$  of particles with energies in  $dE$  about  $E$  and directions which lie in  $d\bar{\Omega}$  about  $\bar{\Omega}$ ,

$\sigma_t(\bar{r}, E)$  = the total cross section at the space point  $\bar{r}$  for particles of energy  $E$ ,

$\sigma_t(\bar{r}, E) \psi(\bar{r}, E, \bar{\Omega}, t) dE d\bar{\Omega}$  = collision loss per unit volume and time at the space point  $\bar{r}$  and time  $t$  of particles with energies in  $dE$  about  $E$  and directions which lie in  $d\bar{\Omega}$  about  $\bar{\Omega}$ ,

$\sigma_s(\bar{r}, E' \rightarrow E, \bar{\Omega}' \rightarrow \bar{\Omega}) dE d\bar{\Omega}$  = the differential scattering kernel which describes the probability per unit path length that a particle with an initial energy  $E'$  and an

initial direction  $\bar{\Omega}'$  undergoes a scattering collision at  $\bar{r}$  which places it into a direction that lies in  $d\bar{\Omega}$  about  $\bar{\Omega}$  with a new energy in  $dE$  about  $E$ ,

$\iint \sigma_s(\bar{r}, E' \rightarrow E, \bar{\Omega}' \rightarrow \bar{\Omega}) \psi(\bar{r}, E', \bar{\Omega}', t) dE' d\bar{\Omega}'$  = inscattering gain per unit volume and time at the space point  $\bar{r}$  and time  $t$  of particles with energies in  $dE$  about  $E$  and directions which lie in  $d\bar{\Omega}$  about  $\bar{\Omega}$ ,

$Q(\bar{r}, E, \bar{\Omega}, t) dE d\bar{\Omega}$  = source particles emitted per unit volume and time at the space point  $\bar{r}$  and time  $t$  with energies in  $dE$  about  $E$  and directions which lie in  $d\bar{\Omega}$  about  $\bar{\Omega}$ .

A simplified version of the Boltzmann equation (Bell and Glasstone, 1970), which neglects time dependence, and is limited to one-dimensional slab and spherical geometries, is shown below:

$$\nabla \cdot \bar{\Omega} \psi(\bar{r}, \mu, E) + \sigma_t(\bar{r}, E) \psi(\bar{r}, \mu, E) = \int_0^\infty \int_0^{2\pi} \int_{-1}^{+1} \sigma_s(\bar{r}, E' \rightarrow E, \mu_0) \psi(\bar{r}, \mu', E') d\mu' d\phi' dE' + Q(\bar{r}, \mu, E), \quad (A-2a)$$

where

$$\bar{\Omega}' = \bar{\Omega}'(\mu', \phi') = \bar{\Omega}'(\cos \theta', \phi') , \quad (A-2b)$$

$$\bar{\Omega} = \bar{\Omega}(\mu, \phi) = \bar{\Omega}(\cos \theta, \phi) , \quad (A-2c)$$

and

$$\mu_0 = \mu' \mu + [(1 - \mu'^2)(1 - \mu^2)]^{1/2} \cos(\phi' - \phi) . \quad (A-2d)$$

The variables  $(\theta, \phi)$  are shown in the standard phase space coordinate system illustrated in Figure (A-1). The two unit direction vectors,

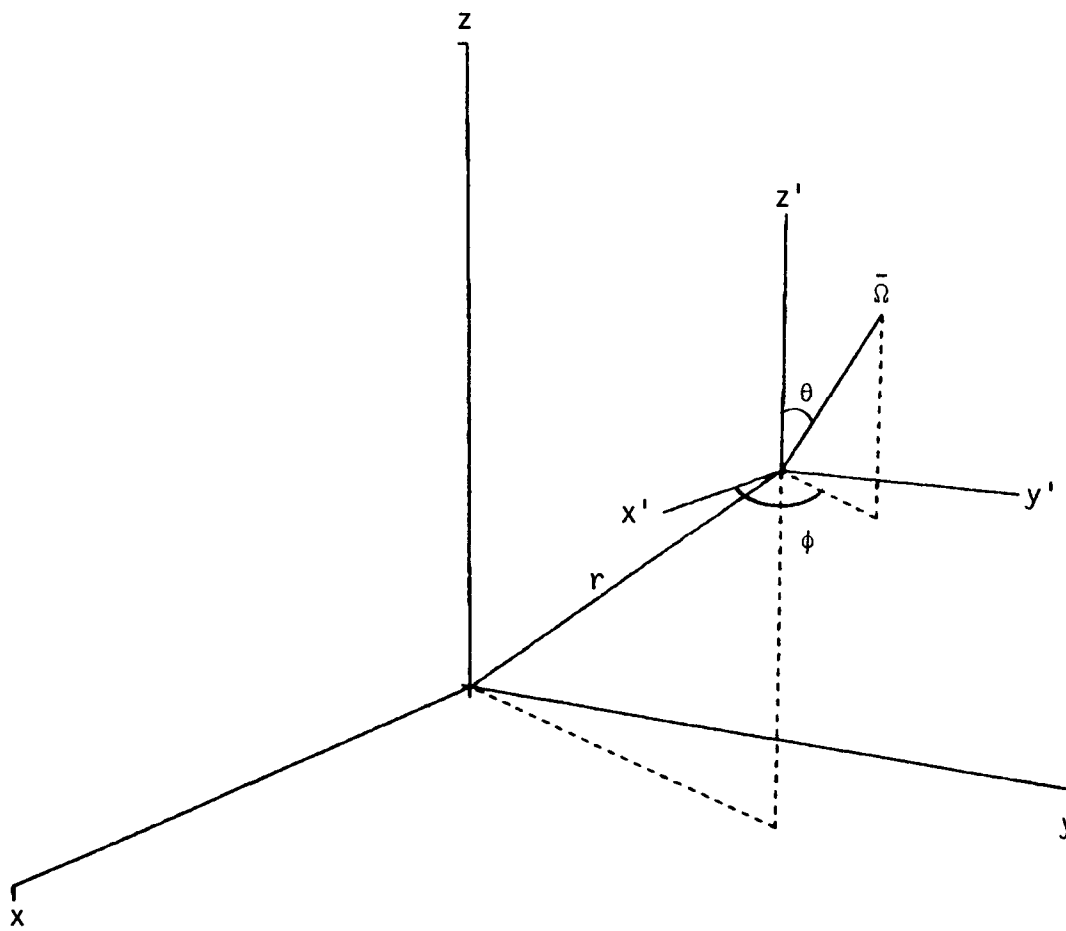


Figure (A-1). Standard phase-space coordinate system.

$\vec{\Omega}'$  and  $\vec{\Omega}$ , and their inclusive angle  $\theta_0$  ( $= \cos^{-1} \mu_0$ ) are shown in a direction-space coordinate system illustrated in Figure (A-2a). Also shown in Figure (A-2a) is a spherical triangle formed from  $\vec{\Omega}'$ ,  $\vec{\Omega}$ , and from a unit vector along the z-axis. Equation (A-2d) was derived by using the law of cosines for the sides of a spherical triangle, where  $\theta_0$ ,  $\theta'$ , and  $\theta$  represent the sides.

There are two ways of deriving the Fokker-Plank equation depending on how one defines the scattering cross section.

#### Method One

One of the basic assumptions for this derivation is that inelastic scattering is either ignored or irrelevant. Since with elastic scattering, energy loss ( $E' - E$ ) and scattering angle ( $\mu_0$ ) are directly coupled, the differential scattering cross section may be expressed as

$$\sigma_s(\vec{r}, E' \rightarrow E, \mu_0) = \sigma_s(\vec{r}, E', \mu_0) \delta(E - E_s) \quad (A-3a)$$

with

$$E_s = E_s(E', \mu_0) \quad (A-3b)$$

or

$$\sigma_s(\vec{r}, E' \rightarrow E, \mu_0) = \sigma_s(\vec{r}, E' \rightarrow E) \delta(\mu_0 - \mu_s) \quad (A-3c)$$

with

$$\mu_s = \mu_s(E', E) . \quad (A-3d)$$

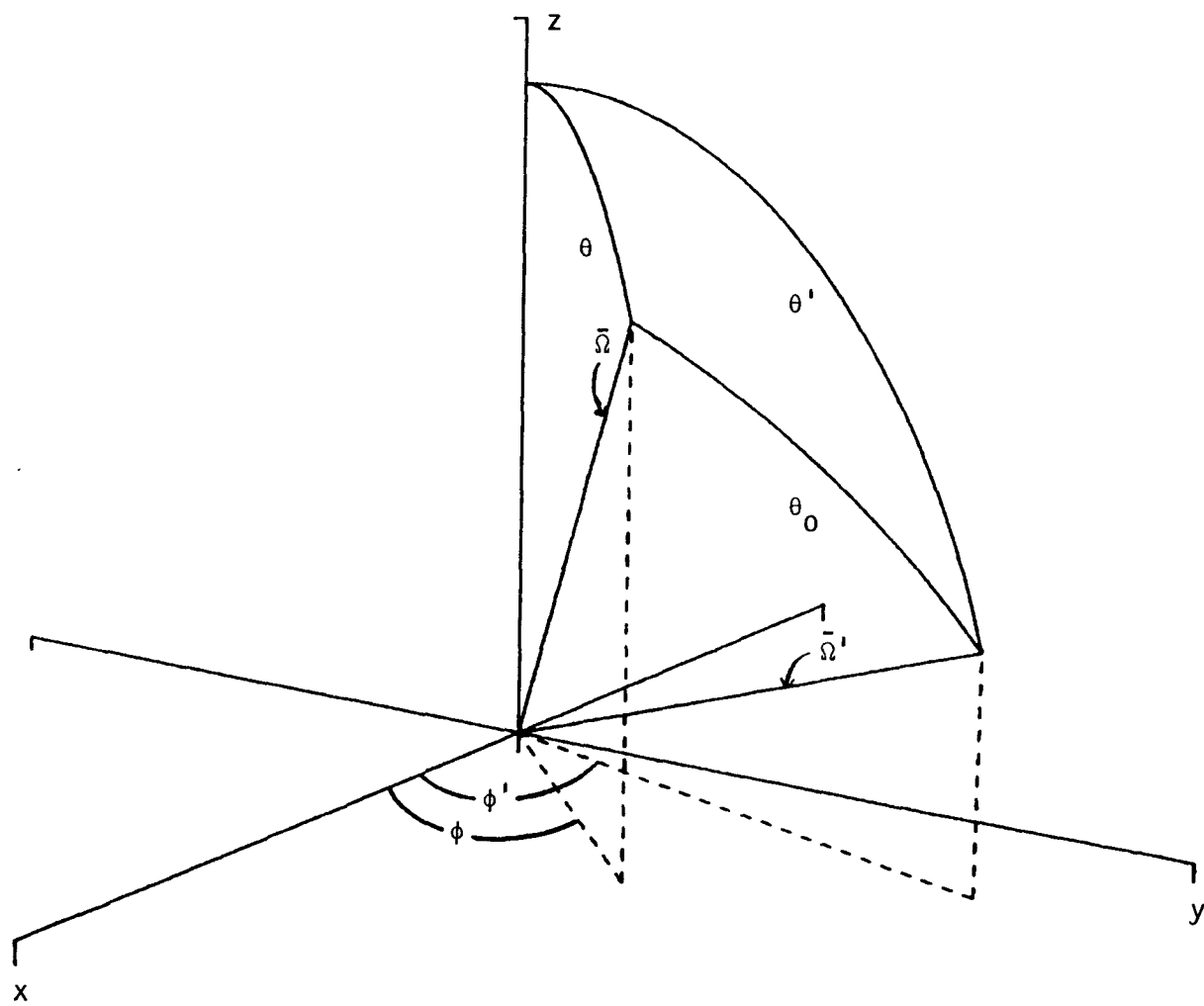


Figure (A-2a). Direction-space coordinate system.

Because of the direct coupling,  $E_S = E'$  when  $\mu_0 = 1$  (Equation (A-3b)) or  $\mu_S = 1$  when  $E' = E$  (Equation (A-3d)).

Substituting Equation (A-3a) into Equation (A-2a), and integrating over the variable ( $E'$ ) gives

$$\nabla \cdot \bar{\Omega} \psi(\bar{r}, \mu, E) + \sigma_t(\bar{r}, E) \psi(\bar{r}, \mu, E) = \int_0^{2\pi} \int_{-1}^{+1} [\sigma_s(\bar{r}, E', \mu_0) \psi(\bar{r}, \mu', E')] d\mu' d\phi' + Q(\bar{r}, \mu, E) . \quad (A-4a)$$

where

$$E = E_S(E', \mu_0) . \quad (A-4b)$$

Since the total cross section is the sum of the absorption and scattering cross section,

$$\begin{aligned} \sigma_t(\bar{r}, E) \psi(\bar{r}, \mu, E) &= \sigma_a \psi + \sigma_s \psi \\ &= \sigma_a \psi + \int_0^{2\pi} \int_{-1}^{+1} \sigma_s(\bar{r}, E, \mu_0) \psi(\bar{r}, \mu', E) d\mu' d\phi' , \end{aligned} \quad (A-5)$$

Equation (A-4a) may be rearranged in the following form:

$$\nabla \cdot \bar{\Omega} \psi(\bar{r}, \mu, E) + \sigma_a(\bar{r}, E) \psi(\bar{r}, \mu, E) = \Gamma_B \psi + Q(\bar{r}, \mu, E) , \quad (A-6a)$$

where

$$\begin{aligned} \Gamma_B \psi &= \int_0^{2\pi} \int_{-1}^{+1} [\sigma_s(\bar{r}, E', \mu_0) \psi(\bar{r}, \mu', E')] \\ &\quad - \sigma_s(\bar{r}, E, \mu_0) \psi(\bar{r}, \mu, E) d\mu' d\phi' . \quad (A-6b) \end{aligned}$$

The term  $(\Gamma_B \psi)$  is known as the Boltzmann scattering operator. It is this integral operator that is replaced with a differential operator in the Fokker-Planck approximation.

The scattering operator  $(\Gamma_B \psi)$  represents the inscatter minus the outscatter at a position  $\bar{r}$ , energy  $E$  and angle  $\mu$ . Because  $\sigma_S$  is forward peaked, the significant contributions to Equation (A-6b) are made when the quantities  $(E' - E)$ ,  $(\mu' - \mu)$ , and  $(\phi' - \phi)$  are small. Since the angular flux  $(\psi)$  is relatively smooth as a function of  $E$  and  $\mu$ , then  $\psi$  will not change much as  $(E' \rightarrow E)$  and  $(\mu' \rightarrow \mu)$ . Also, the explicit dependence of the cross section  $(\sigma_S)$  on  $E'$  varies slowly. However, with regard to  $\mu_0$ , the differential cross section may vary dramatically.

For reasons which will become obvious later on, it will facilitate the derivation if we change the variables of integration in Equation (A-6b) from  $\mu'$  and  $\phi'$  to  $\mu_0$  and  $\phi_0$ . This change of variables is carried out by exchanging  $(d\mu' d\phi')$  with  $(J d\mu_0 d\phi_0)$  where  $J$  represents the absolute value of the Jacobian. Geometrically, this change of variables is brought about by the sequential direction-space coordinate transformations shown in Figures (A-2a), (A-2b), and (A-2c). The coordinate system  $(x', y', z')$  in Figure (A-2b) was formed from the coordinate system  $(x, y, z)$  in Figure (A-2a) by rotating the  $x$ - $y$  plane about the  $z$ -axis through an angle  $\phi$ . Then the coordinate system  $(x'', y'', z'')$  in Figure (A-2c) was formed from  $(x', y', z')$  by rotating the  $x'$ - $z'$  plane about the  $y'$  axis through an

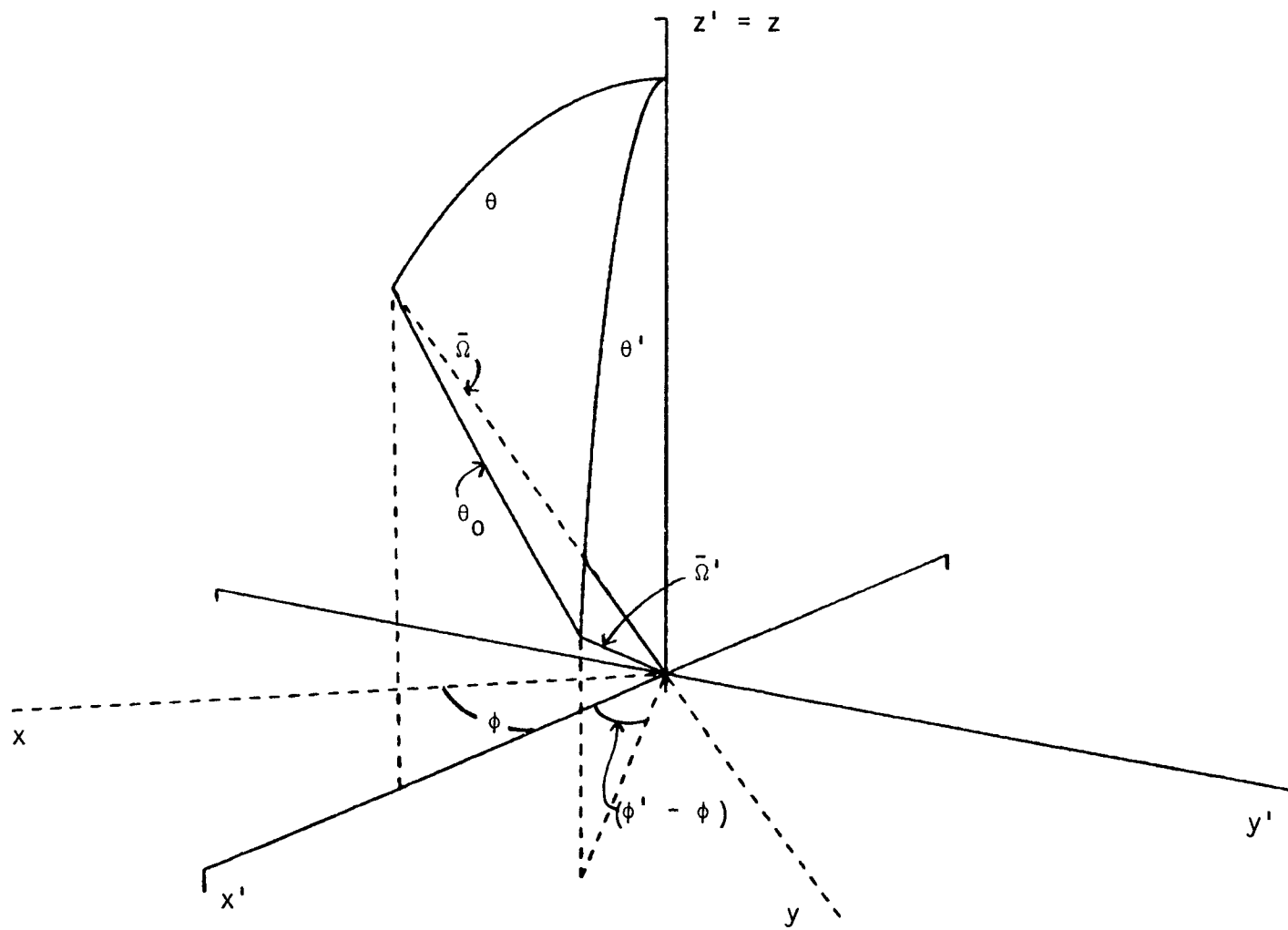


Figure (A-2b). Direction-space coordinate system.

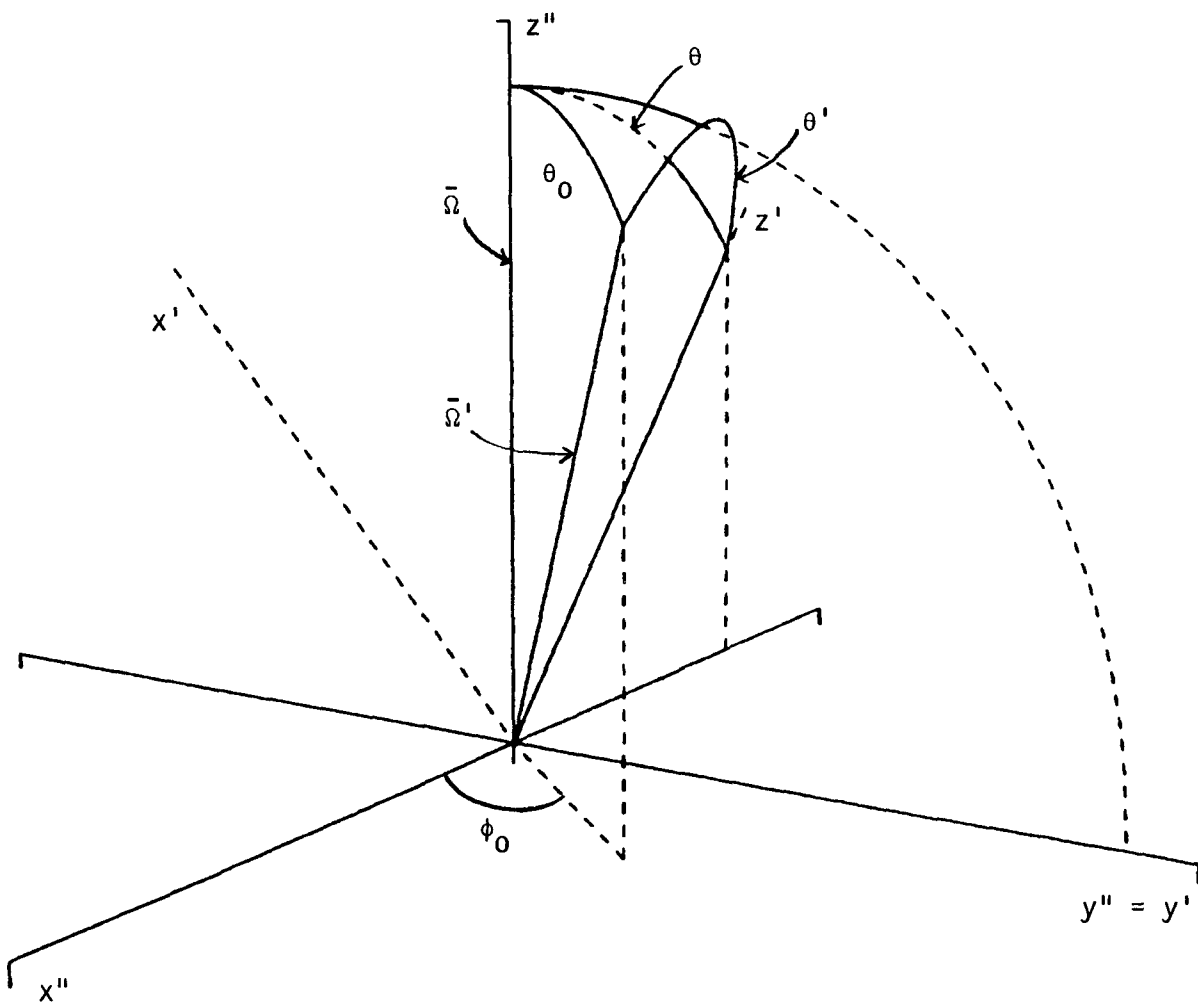


Figure (A-2c). Direction-space coordinate system.

angle  $\theta$ . Since the Jacobian of any number of plane rotations equals 1, then Equation (A-6b) becomes

$$\Gamma_B \psi = \int_0^{2\pi} \int_{-1}^{+1} [\sigma_s(\bar{r}, E', \mu_0) \psi(\bar{r}, \mu', E') - \sigma_s(\bar{r}, E, \mu_0) \psi(\bar{r}, \mu, E)] d\mu_0 d\phi_0 . \quad (A-7)$$

The variable  $\mu'$  is put in terms of  $\mu$  and  $\mu_0$  by using the law of cosines for the spherical triangle pictured in Figure (A-2c):

$$\mu' = \mu\mu_0 + [(1 - \mu^2)(1 - \mu_0^2)]^{1/2} \cos(\pi - \phi_0) , \quad (A-8a)$$

$$= \mu\mu_0 - [(1 - \mu^2)(1 - \mu_0^2)]^{1/2} \cos \phi_0 . \quad (A-8b)$$

The next step in the derivation is to expand the  $E'$  and  $\mu'$  dependence of  $\sigma_s(r, E', \mu_0) \psi(r, \mu', E')$  about  $\theta_0 = 0$ . We note that  $E' = E$  and  $\mu' = \mu$  (see Equation (A-8b)) when  $\theta_0 = 0$ . Although  $\mu_0$  is also a function of  $\theta_0$ , we do not expand its dependence.

Therefore, suppressing the  $\bar{r}$  dependence and keeping only up to and including the second-order terms, we obtain the Taylor series expansion

$$\begin{aligned} \sigma_s(E', \mu_0) \psi(\mu', E') &= \sigma_s(E, \mu_0) \psi(\mu, E) \\ &+ \left[ \frac{\partial}{\partial E'} \sigma_s(E', \mu_0) \psi(\mu', E') \frac{\partial E'}{\partial \theta_0} \right]_{\theta_0=0} (\theta_0) \\ &+ \sigma_s(E, \mu_0) \left[ \frac{\partial}{\partial \mu'} \psi(\mu', E') \frac{\partial \mu'}{\partial \theta_0} \right]_{\theta_0=0} (\theta_0) \end{aligned}$$

$$\begin{aligned}
& + \left[ \frac{\partial^2}{\partial E^1 \partial E^1} \sigma_S(E^1, \mu_0) \psi(\mu^1, E^1) \left( \frac{\partial E^1}{\partial \theta_0} \right)^2 \right. \\
& \quad \left. + \frac{\partial}{\partial E^1} \sigma_S(E^1, \mu_0) \psi(\mu^1, E^1) \frac{\partial^2 E^1}{\partial \theta_0^2} \right]_{\theta_0=0} \frac{\theta_0^2}{2} \\
& + \sigma_S(E, \mu_0) \left[ \frac{\partial^2}{\partial \mu^1 \partial \mu^1} \psi(\mu^1, E^1) \left( \frac{\partial \mu^1}{\partial \theta_0} \right)^2 + \frac{\partial}{\partial \mu^1} \psi(\mu^1, E^1) \frac{\partial^2 \mu^1}{\partial \theta_0^2} \right]_{\theta_0=0} \frac{\theta_0^2}{2} .
\end{aligned} \tag{A-9}$$

Rearranging gives

$$\sigma_s(E', \mu_0) \psi(\mu', E') - \sigma_s(E, \mu_0) \psi(\mu, E) = I_1 + I_2 , \quad (A-10a)$$

where the left-hand side of the equation is now the integrand for  $\Gamma_B \psi$  in Equation (A-7), and where  $I_1$  and  $I_2$  are given below:

$$I_1 = \sigma_s(\varepsilon, \mu_0) \left\{ \frac{\partial}{\partial \mu} \psi(\mu, \varepsilon) \left[ \left[ \frac{\partial \mu'}{\partial \theta_0} \right]_{\theta_0=0} (\theta_0) + \left[ \frac{\partial^2 \mu'}{\partial \theta_0^2} \right]_{\theta_0=0} \frac{\theta_0^2}{2} \right] + \frac{\partial^2}{\partial \mu^2} \psi(\mu, \varepsilon) \left[ \left( \frac{\partial \mu'}{\partial \theta_0} \right)^2 \right]_{\theta_0=0} \frac{\theta_0^2}{2} \right\} \quad (A-10b)$$

and

$$I_2 = \frac{\partial}{\partial E} \sigma_s(E, \mu_0) \psi(\mu, E) \left[ \left[ \frac{\partial E'}{\partial \theta_0} \right]_{\theta_0=0} (\theta_0) + \left[ \frac{\partial^2 E'}{\partial \theta^2} \right]_{\theta_0=0} \frac{\theta_0^2}{2} \right] \\ + \frac{\partial^2}{\partial E^2} \sigma_s(E, \mu_0) \psi(\mu, E) \left[ \left( \frac{\partial E'}{\partial \theta_0} \right)^2 \right]_{\theta_0=0} \frac{\theta_0^2}{2}. \quad (A-10c)$$

Equations (A-10b) and (A-10c) contain partials of  $\mu'$  and  $E'$  with respect to  $\theta_0$  which must now be evaluated at  $\theta_0 = 0$ . Recalling that

$$\mu' = \mu \cos \theta_0 - (1 - \mu^2)^{1/2} \sin \theta_0 \cos \phi_0, \quad (A-8b)$$

then

$$\left. \frac{\partial \mu'}{\partial \theta_0} \right|_{\theta_0=0} = -(1 - \mu^2)^{1/2} \cos \phi_0, \quad (A-11a)$$

$$\left. \frac{\partial^2 \mu'}{\partial \theta_0^2} \right|_{\theta_0=0} = -\mu \quad (A-11b)$$

and

$$\left. \left( \frac{\partial \mu'}{\partial \theta_0} \right)^2 \right|_{\theta_0=0} = (1 - \mu^2) \cos^2 \phi_0. \quad (A-11c)$$

For the partials of  $E'$  with respect to  $\theta_0$ , a Taylor expansion of  $E'$  about  $\theta_0 = 0$  gives

$$E' - E = \left[ \frac{\partial E'}{\partial \theta_0} \right]_{\theta_0=0} (\theta_0) + \left[ \frac{\partial^2 E'}{\partial \theta_0^2} \right]_{\theta_0=0} \frac{\theta_0^2}{2} + \dots \quad (A-12a)$$

and the square of that expansion becomes

$$(E' - E)^2 = \left[ \frac{\partial E'}{\partial \theta_0} \right]_{\theta_0=0}^2 \theta_0^2 + 2 \left[ \frac{\partial E'}{\partial \theta_0} \right] \left[ \frac{\partial^2 E'}{\partial \theta_0^2} \right]_{\theta_0=0} \frac{\theta_0^3}{2} + \dots. \quad (A-12b)$$

Substituting Equations (A-11a) through (A-12b) into  $I_1$  and  $I_2$  gives

$$I_1 = \sigma_s(E, \mu_0) \left\{ \left[ -\theta_0 (1 - \mu^2)^{1/2} \cos \phi_0 - \frac{\theta_0^2 \mu}{2} \right] \frac{\partial}{\partial \mu} \psi(\mu, E) \right. \\ \left. + \frac{\theta_0^2}{2} (1 - \mu^2) \cos^2 \phi_0 \frac{\partial^2}{\partial \mu^2} \psi(\mu, E) \right\} \quad (A-13a)$$

and

$$I_2 = \left[ \frac{\partial}{\partial E} \sigma_s(E, \mu_0) \psi(\mu, E) \right] (E' - E) + \frac{1}{2} \left[ \frac{\partial^2}{\partial E^2} \sigma_s(E, \mu_0) \psi(\mu, E) \right] \\ \cdot (E' - E)^2. \quad (A-13b)$$

Since we have replaced the integrand in  $\Gamma_B \psi$  (in Equation (A-7)) with an approximate expression ( $I_1 + I_2$ ), we now have

$$\Gamma_B \psi \approx \Gamma_{FP} \psi = \int_0^{2\pi} \int_{-1}^{+1} I_1 d\mu_0 d\phi_0 + \int_0^{2\pi} \int_{-1}^{+1} I_2 d\mu_0 d\phi_0, \quad (A-14)$$

where  $\Gamma_{FP} \psi$  is referred to as the Fokker-Planck scattering operator. However,  $\Gamma_{FP} \psi$  is yet to be developed into a familiar and usable form. For convenience, let us define the integral of  $I_1$  as  $I'_1$ , and the integral of  $I_2$  as  $I'_2$ . Looking first only at  $I_1$ , and integrating with respect to  $\phi_0$  over the limits 0 to  $2\pi$  gives

$$I'_1 = \left[ \pi \left( \frac{1 - \mu^2}{2} \right) \frac{\partial^2 \psi}{\partial \mu^2} - \pi \mu \frac{\partial \psi}{\partial \mu} \right] \int_{-1}^{+1} \sigma_s(E, \mu_0) \theta_0^2 d\mu_0 \quad (A-15a)$$

or

$$I'_1 = \frac{\pi}{2} \frac{\partial}{\partial \mu} \left[ (1 - \mu^2) \frac{\partial}{\partial \mu} \psi \right] \int_{-1}^{+1} \sigma_s(E, \mu_0) \theta_0^2 d\mu_0. \quad (A-15b)$$

Since

$$\theta_0^2 \approx 2(1 - \mu_0) \quad (A-16)$$

then the equation may be rearranged as follows:

$$I_1' = \frac{\alpha}{2} \frac{\partial}{\partial \mu} \left[ (1 - \mu^2) \frac{\partial}{\partial \mu} \psi \right], \quad (A-17a)$$

where

$$\alpha = 2\pi \int_{-1}^{+1} \sigma_s(E, \mu_0) (1 - \mu_0) d\mu_0. \quad (A-17b)$$

Looking now only at  $I_2$  (Equation (A-13b)), the integral ( $I_2$ ) becomes

$$I_2' = \int_0^{2\pi} \int_{-1}^{+1} \left\{ \left[ \frac{\partial}{\partial E} \sigma_s \psi \right] (E' - E) + \frac{1}{2} \left[ \frac{\partial^2}{\partial E^2} \sigma_s \psi \right] (E' - E)^2 \right\} d\mu_0 d\phi_0. \quad (A-18)$$

The above equation contains the term ( $E' - E$ ) where  $E$  is the final energy after in-scattering occurs from energy  $E'$ . We recall that

$$E' - E = \frac{\partial E'}{\partial \theta_0} \Big|_{\theta_0=0} \theta_0 + \frac{1}{2} \frac{\partial^2 E'}{\partial \theta_0^2} \Big|_{\theta_0=0} \theta_0^2 + \dots' \quad (A-12a)$$

where

$$E = E_s(E', \theta_0). \quad (A-4b)$$

Equation (A-4b) is an implicit function of  $E'$  in terms of  $E$  and  $\theta_0$ .

Since  $E$  (or  $E_s$ ) is a constant, the first and second total derivatives of  $E_s$  equal zero:

$$\frac{dE_s(E', \theta_0)}{d\theta_0} = \frac{\partial E_s(E', \theta_0)}{\partial E'} \frac{\partial E'}{\partial \theta_0} + \frac{\partial E_s(E', \theta_0)}{\partial \theta_0} = 0 \quad (A-19)$$

and

$$\frac{d^2 E_s(E', \theta_0)}{d \theta_0^2} = \frac{\partial E_s(E', \theta_0)}{\partial E'} \frac{\partial^2 E'}{\partial \theta_0^2} + \frac{\partial^2 E_s(E', \theta_0)}{\partial E'^2} \left( \frac{\partial E'}{\partial \theta_0} \right)^2 + \frac{\partial^2 E_s(E', \theta_0)}{\partial \theta_0^2} = 0. \quad (A-20)$$

If we evaluate the two expressions above at  $\theta_0 = 0$ , and note that  $E = E'$  at  $\theta_0 = 0$ , we obtain

$$\frac{\partial E'}{\partial \theta_0} \Big|_{\theta_0=0} = - \frac{\partial E_s(E', \theta_0)}{\partial \theta_0} \Big|_{\theta_0=0} \quad (A-21)$$

and

$$\frac{\partial^2 E'}{\partial \theta_0^2} \Big|_{\theta_0=0} = - \frac{\partial^2 E_s(E', \theta_0)}{\partial \theta_0^2} \Big|_{\theta_0=0}. \quad (A-22)$$

Substituting Equations (A-21) and (A-22) into (A-12a) gives

$$E' - E = - \frac{\partial E_s(E', \theta_0)}{\partial \theta_0} \Big|_{\theta_0=0} \theta_0 - \frac{\partial^2 E_s(E', \theta_0)}{\partial \theta_0^2} \Big|_{\theta_0=0} \frac{\theta_0^2}{2} - \dots. \quad (A-23)$$

We note that an expansion of  $(E - E_s(E, \theta_0))$  is identical to the right-hand side of Equation (A-23); thus

$$E' - E = E - E_s(E, \theta_0) \quad (A-24)$$

and the equation for  $I_2^1$  (Equation (A-18)) becomes

$$I_2^1 = \int_0^{2\pi} \int_{-1}^{+1} \left\{ \left[ \frac{\partial}{\partial E} \sigma_s \psi \right] (E - E_s) + \frac{1}{2} \left[ \frac{\partial^2}{\partial E^2} \sigma_s \psi \right] (E - E_s)^2 \right\} d\mu_0 d\phi_0. \quad (A-25)$$

The next step in simplifying  $I_2$  is to perform a variable change from  $\mu_0$  to  $\tau$  where  $\tau$  is the energy loss ( $E - E_S$ ). Such a transformation yields

$$I_2 = 2\pi \int_0^{\tau_{\max}(E)} \left\{ \frac{\partial}{\partial E} [\sigma_S(E, \mu_0(\tau)) \psi(\mu, E)] \tau \right. \\ \left. + \frac{1}{2} \frac{\partial^2}{\partial E^2} [\sigma_S(E, \mu_0(\tau)) \psi(\mu, E)] \tau^2 \right\} \frac{d\mu_0}{d\tau} d\tau. \quad (A-26)$$

Since

$$2\pi \sigma_S(E, \mu_0(\tau)) \frac{d\mu_0}{d\tau} = \sigma_S(E, \tau) \quad (A-27)$$

then

$$I_2 = \int_0^{\tau_{\max}(E)} \frac{\partial}{\partial E} [\sigma_S(E, \tau) \psi(\mu, E) \tau] d\tau \\ + \frac{1}{2} \int_0^{\tau_{\max}(E)} \frac{\partial^2}{\partial E^2} [\sigma_S(E, \tau) \psi(\mu, E) \tau^2] d\tau. \quad (A-28)$$

We can bring the above indicated integrations inside of the partial derivatives and introduce only a very small amount of error. For example, using the Leibnitz rule on the first integral in Equation (A-28) gives

$$\int_0^{\tau_{\max}} \frac{\partial}{\partial E} [\sigma_s \psi \tau] d\tau = \frac{\partial}{\partial E} \int_0^{\tau_{\max}} \sigma_s \psi \tau d\tau$$

$$- \sigma_s(E, \tau_{\max}) \psi(\mu, E) \tau_{\max} \frac{d\tau_{\max}}{dE}. \quad (A-29)$$

The second term on the right-hand side of Equation (A-29) becomes negligible in comparison with the first term in the Fokker-Planck limit; i.e., as the cross section becomes more forward peaked. Thus,  $I_2'$  becomes

$$I_2' = \frac{\partial}{\partial E} \int_0^{\tau_{\max}(E)} \sigma_s(E, \tau) \psi(\mu, E) \tau d\tau$$

$$+ \frac{1}{2} \frac{\partial^2}{\partial E^2} \int_0^{\tau_{\max}(E)} \sigma_s(E, \tau) \psi(\mu, E) \tau^2 d\tau \quad (A-30)$$

or, in a different form,

$$I_2' = \frac{\partial}{\partial E} \left\{ \psi \int_0^{\infty} \sigma_s(E + E')(E - E') dE' \right\}$$

$$+ \frac{1}{2} \frac{\partial^2}{\partial E^2} \left\{ \psi \int_0^{\infty} \sigma_s(E + E')(E - E')^2 dE' \right\}. \quad (A-31)$$

The final result for  $\Gamma_{FP}\psi$ , upon substituting Equations (A-17a), (A-17b) and (A-31) into Equation (A-14) (and remembering the additional dependence of each variable on  $\bar{r}$ ), becomes

$$\nabla \cdot \bar{\Omega}\psi + \sigma_a \psi = \Gamma_{FP}\psi + Q, \quad (A-32a)$$

where

$$\Gamma_{FP} \psi = \frac{\alpha}{2} \frac{\partial}{\partial \mu} \left[ (1 - \mu^2) \frac{\partial}{\partial \mu} \psi(\bar{r}, \mu, E) \right] + \frac{\partial}{\partial E} \beta \psi(\bar{r}, \mu, E) + \frac{1}{2} \frac{\partial^2}{\partial E^2} \gamma \psi(\bar{r}, \mu, E) \quad (A-32b)$$

$$\alpha = 2\pi \int_{-1}^{+1} \sigma_s(\bar{r}, E, \mu_0) (1 - \mu_0) d\mu_0, \quad (A-32c)$$

$$\beta = \int_0^{\infty} \sigma_s(\bar{r}, E + E') (E - E') dE', \quad (A-32d)$$

and

$$\gamma = \int_0^{\infty} \sigma_s(\bar{r}, E + E') (E - E')^2 dE'. \quad (A-32e)$$

The terms ( $\alpha$ ,  $\beta$ , and  $\gamma$ ) found in the Fokker-Planck scattering operator are usually referred to as the momentum transfer, stopping power, and mean-square stopping power, respectively. Although stopping power ( $\beta$ ) is usually defined as being negative (if particles lose energy on the average), we have here defined it with the positive sign convention.

### Method Two

To begin the derivation, let us first examine Equation (A-32b) by dividing  $\Gamma_{FP} \psi$  into two segments:

$$\Gamma_{FP}^{\alpha} \psi = \frac{\alpha}{2} \frac{\partial}{\partial \mu} \left[ (1 - \mu^2) \frac{\partial}{\partial \mu} \psi(\bar{r}, \mu, E) \right] \quad (A-33a)$$

and

$$\Gamma_{FP}^{\beta} \psi = \frac{\partial}{\partial E} \beta \psi(\bar{r}, \mu, E) + \frac{1}{2} \frac{\partial^2}{\partial E^2} \gamma \psi(\bar{r}, \mu, E). \quad (A-33b)$$

The equation for  $\Gamma_{FP}^a \psi$  deals exclusively with angle dependence at some energy  $E$ , and the equation for  $\Gamma_{FP}^e \psi$  focuses on how certain quantities vary with respect to energy at some angle  $\mu$ . In other words, all coupling between energy and scattering angle are lost. Such decoupling would suggest that we might derive the Fokker-Planck equation by initially assuming that the scattering cross section itself is decoupled. The term  $\Gamma_{FP}^a \psi$  would be derived by using a cross section which redistributes in angle but not energy

$$\sigma_s(\vec{r}, E' \rightarrow E, \mu_0) = \sigma^a(\vec{r}, E, \mu_0) \delta(E' - E) \quad (A-34a)$$

and  $\Gamma_{FP}^e \psi$  would be derived by using a cross section which redistributes in energy but not angle

$$\sigma_s(\vec{r}, E' \rightarrow E, \mu_0) = \sigma^e(\vec{r}, E' \rightarrow E) \frac{1}{2\pi} \delta(\mu_0 - 1) . \quad (A-34b)$$

Inserting the new cross sections above into the Boltzmann equation gives

$$\begin{aligned} & \nabla \cdot \bar{\Omega} \psi + \sigma_t \psi \\ &= \int_0^\infty \int_0^{2\pi} \int_{-1}^{+1} \sigma^a(\vec{r}, E, \mu_0) \delta(E' - E) \psi(\vec{r}, \mu', E') d\mu' d\phi' dE' \\ &+ \int_0^\infty \int_0^{2\pi} \int_{-1}^{+1} \sigma^e(\vec{r}, E' \rightarrow E) \frac{1}{2\pi} \delta(\mu_0 - 1) \psi(\vec{r}, \mu', E') d\mu' d\phi' dE' \\ &+ Q . \end{aligned} \quad (A-35)$$

Recalling that we may change the variables of integration from  $(d\mu', d\phi')$  to  $(d\mu_0, d\phi_0)$ , where the Jacobian of the transformation equals 1, we integrate the first integrand with respect to  $E'$ , and the second with respect to  $\mu_0$  and  $\phi_0$ :

$$\nabla \cdot \bar{\nabla} \psi + \sigma_t \psi = \int_0^{2\pi} \int_{-1}^{+1} \sigma^\alpha(\bar{r}, E, \mu_0) \psi(\bar{r}, \mu', E) d\mu_0 d\phi_0 + \int_0^\infty \sigma^e(\bar{r}, E' + E) \psi(\bar{r}, \mu, E') dE' + Q . \quad (A-36)$$

If we separate the total cross section into its absorption and scattering components as before, i.e.,

$$\sigma_t \psi = (\sigma_a + \sigma_s) \psi \quad (A-37a)$$

$$= \sigma_a \psi + \int_0^{2\pi} \int_{-1}^{+1} \sigma^\alpha(\bar{r}, E, \mu_0) \psi(\bar{r}, \mu, E) d\mu_0 d\phi_0 + \int_0^\infty \sigma^e(\bar{r}, E + E') \psi(\bar{r}, \mu, E') dE' , \quad (A-37b)$$

and suppress the  $\bar{r}$  dependence for simplicity, then Equation (A-36) can be rearranged to give

$$\nabla \cdot \bar{\nabla} \psi + \sigma_a \psi = \Gamma_B^\alpha \psi + \Gamma_B^e \psi + Q , \quad (A-38a)$$

where

$$\Gamma_B^\alpha \psi = \int_0^{2\pi} \int_{-1}^{+1} \sigma^\alpha(E, \mu_0) [\psi(\mu', E) - \psi(\mu, E)] d\mu_0 d\phi_0 \quad (A-38b)$$

and

$$\Gamma_B^e \psi = \int_0^\infty [\sigma^e(E' + E) \psi(\mu, E') - \sigma^e(E + E') \psi(\mu, E)] dE' . \quad (A-38c)$$

As can be seen from Equations (A-38b) and (A-38c),  $\Gamma_B^a \psi$  represents the net gain of particles having a fixed direction  $\mu$ , and  $\Gamma_B^e \psi$  represents the net gain of particles having a fixed direction  $E$ . The next step in the derivation is to expand segments of each integrand in a Taylor series. Expanding the term  $\psi(\mu', E)$  in Equation (A-38b) about  $\theta_0 = 0$ , and retaining terms up to second-order gives

$$\begin{aligned} \psi(\mu', E) &= \psi(\mu, E) + \left[ \frac{\partial}{\partial \mu'} \psi(\mu', E) \frac{\partial \mu'}{\partial \theta_0} \right]_{\theta_0=0} (\theta_0) \\ &+ \left[ \frac{\partial^2}{\partial \mu'^2} \psi(\mu', E) \left( \frac{\partial \mu'}{\partial \theta_0} \right)^2 + \frac{\partial}{\partial \mu'} \psi(\mu', E) \frac{\partial^2 \mu'}{\partial \theta_0^2} \right]_{\theta_0=0} (\theta_0^2/2) . \end{aligned} \quad (A-39)$$

Evaluating the partial derivatives above using Equations (A-11a), (A-11b), and (A-11c), and rearranging slightly produces

$$\begin{aligned} \psi(\mu', E) - \psi(\mu, E) &= \left[ \frac{\partial}{\partial \mu} \psi \right] \left[ -\theta_0 (1 - \mu^2)^{1/2} \cos \phi_0 - \frac{\theta_0^2 \mu}{2} \right] \\ &+ \left[ \frac{\partial^2}{\partial \mu^2} \psi \right] \left[ \frac{\theta_0^2}{2} (1 - \mu^2) \cos^2 \phi_0 \right] . \end{aligned} \quad (A-40)$$

Upon substituting Equation (A-40) into the integrand of (A-38b), and integrating with respect to  $\phi_0$  and  $\mu_0$ , the final result becomes the same as in the first derivation

$$\Gamma_B^\alpha \psi \approx \Gamma_{FP}^\alpha \psi = \frac{\alpha}{2} \frac{\partial}{\partial \mu} \left[ (1 - \mu^2) \frac{\partial}{\partial \mu} \psi(\bar{r}, \mu, E) \right], \quad (A-41a)$$

where

$$\alpha = 2\pi \int_{-1}^{+1} \sigma^\alpha(E, \mu_0) (1 - \mu_0) d\mu_0. \quad (A-41b)$$

Now let us return to Equation (A-38c) and perform an expansion on the integrand of  $\Gamma_B^e \psi$ . The expansion is more easily understood, however, if we first express the integrand in terms of the variable  $\tau$ , where  $\tau$  represents the energy loss ( $E' - E$ ):

$$\Gamma_B^e \psi = \int_0^\infty [\sigma^e(E + \tau, \tau) \psi(\mu, E + \tau) - \sigma^e(E, \tau) \psi(\mu, E)] d\tau. \quad (A-42)$$

Expanding  $\sigma^e(E + \tau, \tau) \psi(\mu, E + \tau)$  in a Taylor series about  $\tau = 0$ , and retaining terms up to  $(\tau^2)$  gives

$$\begin{aligned} \sigma^e(E + \tau, \tau) \psi(\mu, E + \tau) &= \sigma^e(E, \tau) \psi(\mu, E) \\ &+ \left[ \frac{\partial}{\partial \tau} \sigma^e(E + \tau', \tau) \psi(\mu, E + \tau') \right]_{\tau'=0} (\tau) \\ &+ \left[ \frac{\partial^2}{\partial \tau'^2} \sigma^e(E + \tau', \tau) \psi(\mu, E + \tau') \right]_{\tau'=0} (\tau^2/2). \end{aligned} \quad (A-43)$$

Since

$$\left[ \frac{\partial}{\partial \tau} \sigma^e \psi \right]_{\tau'=0} = \left[ \frac{\partial}{\partial E'} \sigma^e(E', \tau) \psi(\mu, E') \frac{\partial E'}{\partial \tau} \right]_{E'=E} \quad (A-44a)$$

$$= \frac{\partial}{\partial E} [\sigma^e(E, \tau) \psi(\mu, E)], \quad (A-44b)$$

then Equation (A-43) becomes

$$\begin{aligned} \sigma^e(E + \tau, \tau) \psi(\mu, E + \tau) - \sigma^e(E, \tau) \psi(\mu, E) &= \left[ \frac{\partial}{\partial E} \sigma^e(E, \tau) \psi(\mu, E) \right] \tau \\ &+ \left[ \frac{\partial^2}{\partial E^2} \sigma^e(E, \tau) \psi(\mu, E) \right] \frac{\tau^2}{2} . \end{aligned} \quad (A-45)$$

Replacing the integrand in Equation (A-42) with (A-45), and then simplifying the integral in a manner analogous to that in Method 1, we obtain

$$\Gamma_B^e \psi \approx \Gamma_{FP}^e \psi = \frac{\partial}{\partial E} \beta \psi + \frac{1}{2} \frac{\partial^2}{\partial E^2} \gamma \psi , \quad (A-46a)$$

where

$$\beta = \int_0^\infty \sigma^e(E + E') (E - E') dE' \quad (A-46b)$$

and

$$\gamma = \int_0^\infty \sigma^e(E + E') (E - E') dE' . \quad (A-46c)$$

## APPENDIX B

### GENERALIZED GAUSS AND RADAU QUADRATURE

The Gauss and Radau quadrature methods will be developed in parallel in this appendix. Each discussion of a subtopic under Gauss quadrature will be followed with a corresponding discussion of Radau quadrature. The Radau quadrature, therefore, will be considered as an extension of the Gauss quadrature.

Since the MORSE code system uses the generalized Gauss quadrature technique to analyze its input cross sections, the theory and use of Gauss quadrature is explained in depth in the MORSE documentation, particularly in that by Emmett (1975). Much of the material given here on Gauss quadrature is taken directly from that reference. For the derivation of Radau quadrature, a closely followed reference is that by Hildebrand (1974). Other good references are that of Stroud and Secrest (1966), Stroud (1974), and Davis and Rabinowitz (1967).

#### Generation of the Generalized Gauss Quadrature

Statement of the Problem. Given a weight function  $\omega(x)$ ,  $a \leq x \leq b$ , such that  $\omega(x) \geq 0$  (Restriction I), find  $\{x_i, \omega_i\}$  for  $i = 1, n$  so that

$$\int_a^b \omega(x) g(x) dx = \sum_{i=1}^n \omega_i g(x_i) \quad (\text{Restriction II}) \quad (B-1)$$

holds for all  $g(x)$  where  $g(x)$  is a polynomial of degree  $2n-1$  or less.

Solution. Determine a set of polynomials  $Q_i(x)$  ( $i = 1, n$ ) orthogonal with respect to  $\omega(x)$ . That is

$$\int_a^b Q_i(x) Q_j(x) \omega(x) dx = \delta_{ij} N_i, \quad (B-2)$$

where  $\delta_{ij}$  is the Kronecker delta and  $N_i$  is a normalization constant. Then  $\{x_i\}_{i=1}^n$  are given by the roots of  $Q_n(x)$ ,  $Q_n(x_i) = 0$ , and

$$\omega_i = \left[ \sum_{k=0}^{n-1} Q_k^2(x_i) / N_k \right]^{-1}. \quad (B-3)$$

Derivation. Let  $g(x)$  be a polynomial of degree  $\leq n + r - 1$ . By simple division of polynomials, we can write the function  $g(x)$  as the sum

$$g(x) = p(x) \pi(x) + q(x), \quad (B-4)$$

where  $\pi(x)$  is chosen as a polynomial of degree  $n$  with roots  $x_1, \dots, x_n$ :

$$\pi(x) = (x - x_1)(x - x_2) \cdots (x - x_n). \quad (B-5)$$

The polynomial  $p(x)$  will be of degree  $\leq r-1$  and  $q(x)$  will be of degree  $\leq n-1$  (the exact form of  $p$  and  $q$  is of no interest to us).

Now, if we take the expression for  $g(x)$ , multiply it by a weight function  $\omega(x)$  and integrate, we obtain

$$\begin{aligned} \int_a^b \omega(x) g_{n+r-1}(x) dx &= \int_a^b \omega(x) p_{r-1}(x) \pi_n(x) dx \\ &+ \int_a^b \omega(x) q_{n-1}(x) dx. \end{aligned} \quad (B-6)$$

If we define the notation

$$E[I(x)] = \int_a^b \omega(x) I(x) dx , \quad (B-7)$$

then Equation (B-6) becomes

$$E[g_{n+r-1}(x)] = E[p_{r-1}(x) \pi_n(x)] + E[q_{n-1}(x)] . \quad (B-8)$$

If we choose  $\pi_n(x) = Q_n(x)$ , so that  $\pi_n(x)$  is orthogonal with respect to  $\omega(x)$  over the interval  $[a,b]$ , then

$$E[p_{r-1}(x) \pi_n(x)] = \int_a^b \omega(x) p_{r-1}(x) Q_n(x) dx = 0 , \quad (B-9)$$

where  $r - 1 < n$ . Now we desire a quadrature form such that

$$E[g_{n+r-1}(x)] = \sum_{i=1}^n g_{n+r-1}(x_i) \cdot \omega_i \quad (B-10a)$$

$$= \sum_{i=1}^n p_{r-1}(x_i) Q_n(x_i) \cdot \omega_i + \sum_{i=1}^n q_{n-1}(x_i) \cdot \omega_i \quad (B-10b)$$

$$= \sum_{i=1}^n p_{r-1}(x_i) Q_n(x_i) \cdot \omega_i + E[q_{n-1}(x)] . \quad (B-10c)$$

By subtracting Equation (B-8) from (B-10c), we find that we must require, for all polynomials,  $p_{r-1}(x)$ , that

$$\sum_{i=1}^n p_{r-1}(x_i) Q_n(x_i) \cdot \omega_i = 0 . \quad (B-11)$$

This condition can only be met if  $Q_n(x_i) = 0$ ; that is, the desired points  $x_i$  are the roots of  $Q_n(x)$ . The largest value of  $r$

for which the quadrature is exact is for  $r = n$ . Therefore, Gauss quadrature will integrate polynomials of degree  $2n-1$  or less.

Now we must pick the weights,  $\omega_i$ , so that

$$E[q_{n-1}(x)] = \sum_{i=1}^n q_{n-1}(x_i) \cdot \omega_i , \quad (B-12)$$

where  $q_{n-1}(x)$  is an arbitrary polynomial of order  $n-1$  or less.

Since  $q_{n-1}$  may be expanded as a linear sum of the orthogonal polynomials,  $Q_0, Q_1, \dots, Q_{n-1}$ , it is sufficient to require

$$E[Q_k(x)] = \sum_{i=1}^n Q_k(x_i) \cdot \omega_i \quad \text{for } k = 0, 1, \dots, n-1 . \quad (B-13)$$

However,

$$E[Q_k(x)] = E[Q_k(x) Q_0(x)] = N_0 \delta_{k0} . \quad (B-14)$$

Thus, we must have

$$\sum_{i=1}^n Q_k(x_i) \cdot \omega_i = N_0 \delta_{k0} \quad \text{for } k = 0, 1, \dots, n-1 . \quad (B-15)$$

Multiplying Equation (B-15) by  $[Q_k(x_j)/N_k]$  and summing over  $k$ , we find

$$\begin{aligned} \sum_{k=0}^{n-1} \frac{Q_k(x_j)}{N_k} \sum_{i=1}^n Q_k(x_i) \cdot \omega_i &= \sum_{i=1}^n \omega_i \sum_{k=0}^{n-1} \frac{Q_k(x_j) Q_k(x_i)}{N_k} \\ &= \sum_{k=0}^{n-1} \frac{Q_k(x_j)}{N_k} N_0 \delta_{k0} = \frac{Q_0(x_j)}{N_0} N_0 = 1 . \end{aligned} \quad (B-16)$$

Introducing the function

$$D_{n-1}(x, y) = \sum_{k=0}^{n-1} \frac{Q_k(x) Q_k(y)}{N_k} , \quad (B-17)$$

we can write Equation (B-16) as

$$\sum_{i=1}^n \omega_i D_{n-1}(x_j, x_i) = 1 . \quad (B-18)$$

To proceed further we must establish the Christoffel-Darboux identity. Using the standard three-term recurrence relation for orthogonal polynomials

$$Q_n(x) = (x - \mu_n) Q_{n-1}(x) - \sigma_{n-1}^2 Q_{n-2}(x) , \quad (B-19a)$$

where

$$\sigma_{n-1}^2 = N_{n-1}/N_{n-2} . \quad (B-19b)$$

(Note: the above recurrence relation will be derived in a later section of this appendix), then

$$\begin{aligned} & \frac{Q_n(x) Q_{n-1}(y) - Q_{n-1}(x) Q_n(y)}{N_{n-1}(x - y)} \\ &= \frac{1}{N_{n-1}(x - y)} \{ [(x - \mu_n) Q_{n-1}(x) - \sigma_{n-1}^2 Q_{n-2}(x)] Q_{n-1}(y) \\ & \quad - Q_{n-1}(x) [(y - \mu_n) Q_{n-1}(y) - \sigma_{n-1}^2 Q_{n-2}(y)] \} \quad (B-20a) \end{aligned}$$

$$= \frac{(x - y) Q_{n-1}(x) Q_{n-1}(y) + \sigma_{n-1}^2 [Q_{n-1}(x) Q_{n-2}(y) - Q_{n-2}(x) Q_{n-1}(y)]}{N_{n-1}(x - y)} \quad (B-20b)$$

$$= \frac{Q_{n-1}(x) Q_{n-1}(y)}{N_{n-1}} + \frac{Q_{n-1}(x) Q_{n-2}(y) - Q_{n-2}(x) Q_{n-1}(y)}{N_{n-1}(x - y)} \cdot \frac{N_{n-1}}{N_{n-2}} \quad (B-20c)$$

$$= \frac{Q_{n-1}(x) Q_{n-1}(y)}{N_{n-1}} + \frac{Q_{n-1}(x) Q_{n-2}(y) - Q_{n-2}(x) Q_{n-1}(y)}{N_{n-2}(x - y)} \quad (B-20d)$$

$$= \frac{Q_{n-1}(x) Q_{n-1}(y)}{N_{n-1}} + \frac{Q_{n-2}(x) Q_{n-2}(y)}{N_{n-2}} + \frac{Q_{n-2}(x) Q_{n-3}(y) - Q_{n-3}(x) Q_{n-2}(y)}{N_{n-3}(x - y)} \quad (B-20e)$$

$$= \sum_{k=1}^{n-1} \frac{Q_k(x) Q_k(y)}{N_k} + \frac{Q_1(x) Q_0(y) - Q_0(x) Q_1(y)}{N_0(x - y)} \quad (B-20f)$$

$$= \sum_{k=1}^{n-1} \frac{Q_k(x) Q_k(y)}{N_k} + \frac{(x - \mu_1) - (y - \mu_1)}{N_0(x - y)} \quad (B-20g)$$

$$= \sum_{k=1}^{n-1} \frac{Q_k(x) Q_k(y)}{N_k} + \frac{1}{N_0} = \sum_{k=1}^{n-1} \frac{Q_k(x) Q_k(y)}{N_k} + \frac{Q_0(x) Q_0(y)}{N_0} \quad (B-20h)$$

$$= \sum_{k=0}^{n-1} \frac{Q_k(x) Q_k(y)}{N_k} = D_{n-1}(x, y) . \quad (B-20i)$$

Therefore

$$D_{n-1}(x_j, x_i) = \frac{Q_n(x_j) Q_{n-1}(x_i) - Q_{n-1}(x_j) Q_n(x_i)}{N_{n-1}(x_j - x_i)} . \quad (B-21)$$

For  $i \neq j$  and  $Q_n(x_j) = Q_n(x_i) = 0$ ,

$$D_{n-1}(x_j, x_i) = 0 . \quad (B-22)$$

Therefore, returning to Equation (B-18),

$$\sum_{i=1}^n \omega_i D_{n-1}(x_j, x_i) = \omega_j D_{n-1}(x_j, x_j) = 1 \quad (B-23)$$

or

$$\omega_j = [D_{n-1}(x_j, x_j)]^{-1} = \left[ \sum_{k=0}^{n-1} \frac{Q_k^2(x_j)}{N_k} \right]^{-1}. \quad (B-24)$$

### Generation of the Generalized Radau Quadrature

Statement of the Problem. Given a weight function  $\omega(x)$ ,  $a \leq x \leq b$ , such that  $\omega(x) \geq 0$  (Restriction I), find  $x_0, \dots, x_{n-1}$  and  $\omega_0, \dots, \omega_n$  so that

$$\int_a^b \omega(x) g(x) dx = \sum_{i=1}^{n-1} \omega_i g(x_i) + \omega_n g(b) \quad (\text{Restriction II}) \quad (B-25)$$

holds for all  $g(x)$  where  $g(x)$  is a polynomial of degree  $2n-2$  or less.

Solution. Determine a set of polynomials  $Q_i(x)$  ( $i=1, n-1$ ) orthogonal with respect to  $\omega^*(x) = (b - x) \omega(x)$ . That is,

$$\int_a^b Q_i(x) Q_j(x) \omega^*(x) dx = \delta_{ij} N_i. \quad (B-26)$$

Then the  $\{x_i\}_{i=1}^{n-1}$  are given by the roots of  $Q_{n-1}(x)$ ,  $Q_{n-1}(x_i) = 0$ , and

$$\omega_i = \left[ (b - x_i) \sum_{k=0}^{n-2} Q_k^2(x_i) / N_k \right]^{-1} \quad \text{for } i=1, n-1. \quad (B-27)$$

The last weight ( $\omega_n$ ) which corresponds to the fixed abscissa ( $x_n = b$ ) is given by

$$\omega_n = 1 - \sum_{i=1}^{n-1} \omega_i. \quad (B-28)$$

Derivation. Let us define  $(n)$  as the total number of abscissas  $(x_i)$ ,  $(r)$  as the number of "free" abscissas which need to be calculated, and  $(n-r)$  as the number of preassigned abscissas.

In the Gauss quadrature case, we had

$$E[p_{r-1}(x) \pi_n(x)] = 0 . \quad (B-29)$$

If we predetermine some of the roots of  $\pi_n(x)$ , then we cannot guarantee that  $\pi_n(x)$  is still orthogonal to  $\omega(x)$  over  $[a,b]$ . In particular, let us preassign  $(n-r)$  roots so that

$$\pi(x) = \pi^*(x) v(x) , \quad (B-29a)$$

where

$$\pi^*(x) = (x - x_1)(x - x_2) \cdots (x - x_r) \quad (B-29b)$$

contains the "free" roots, and where

$$v(x) = (x - x_{r+1}) \cdots (x - x_n) \quad (B-29c)$$

contains the preassigned roots.

As in the Gauss case, we let  $g(x)$  be a polynomial of degree  $\leq n + r - 1$ , and write it as

$$g(x) = p(x) \pi(x) + q(x) . \quad (B-4)$$

Multiplying both sides by  $\omega(x)$  and integrating over the limits, we obtain

$$E[g_{n+r-1}(x)] = E[p_{r-1}(x) \pi_n(x)] + E[q_{n-1}(x)] . \quad (B-8)$$

Substituting in for  $\pi_n(x)$  using Equation (B-29a) gives

$$E[g_{n+r-1}(x)] = E[p_{r-1}(x) v_{n-r}(x) \pi^*(x)] + E[q_{n-1}(x)] . \quad (B-30)$$

If we choose  $\pi_r^*(x) = Q_r(x)$ , so that  $\pi_r^*(x)$  is orthogonal with respect to  $\omega^*(x) = \omega(x) v_{n-r}(x)$  over the interval  $[a,b]$ , then

$$E[p_{r-1}(x) v_{n-r}(x) \pi_r^*(x)] = \int_a^b \omega^*(x) p_{r-1}(x) Q_r(x) dx = 0. \quad (B-31)$$

Now, we desire a quadrature form such that

$$E[g_{n+r-1}(x)] = \sum_{i=1}^n \omega_i g(x_i) \quad (B-32)$$

is exact for a polynomial with degree  $\leq (n + r-1)$ . This is equivalent to specifying that

$$E[p_{r-1}(x) \pi_n(x)] = \sum_{i=1}^n \omega_i p_{r-1}(x_i) \pi(x_i). \quad (B-33)$$

Since we have already chosen the left-hand side to equal zero (Equation (B-31)), then the  $x_i$  on the right-hand side are still the zeros of  $\pi_n(x) = v_{n-r}(x) Q_r(x)$ . If only one abscissa is specified, then  $r = n-1$ , and the quadrature is exact for polynomials of degree  $\leq 2n-2$ .

The weights ( $\omega_i$ ) for Radau quadrature will be derived in a slightly different fashion from the Gauss weights. If we evaluate both sides of Equation (B-4) at the zeros of  $\pi(x)$ , we find that  $g(x_i) = q(x_i)$  for  $i = 1, n$ . Thus,  $q(x)$  is a polynomial of degree  $\leq n-1$  which interpolates  $g(x)$  at  $x = x_i$ ,  $i = 1, n$ . We can write  $q(x)$  as

$$q(x) = \sum_{i=1}^n g(x_i) \ell_i(x), \quad (B-34a)$$

Noting the similarity between this last expression and Equation (B-38),  $\omega_i$  becomes

$$\omega_i = \frac{N_{r-1}}{v(x_i) Q_r'(x_i) Q_{r-1}(x_i)} . \quad (B-43)$$

To simplify the expression for  $\omega_i$  further, we need to again refer to the Christoffel-Darboux identity. If we insert the equation

$$0 = -Q_r(y) Q_{r-1}(y) + Q_r(y) Q_{r-1}(y) \quad (B-44)$$

into the numerator on the right-hand side of the identity (Equation (B-39)) and factor, we get

$$\begin{aligned} & \sum_{j=0}^{r-1} \frac{Q_j(x) Q_j(y)}{N_j} \\ &= \frac{[Q_r(x) - Q_r(y)] Q_{r-1}(y) - [Q_{r-1}(x) - Q_{r-1}(y)] Q_r(y)}{N_{r-1}(x - y)} . \quad (B-45) \end{aligned}$$

By considering the limiting form of the above relation as  $y \rightarrow x$ , or as  $(x - y) \rightarrow dx$ , the identity becomes

$$\sum_{j=0}^{r-1} \frac{[Q_j(x)]^2}{N_j} = \frac{1}{N_{r-1}} [Q_r'(x) Q_{r-1}(x) - Q_{r-1}'(x) Q_r(x)] . \quad (B-46)$$

If we let  $x = x_i$ , it reduces to

$$\sum_{j=0}^{r-1} \frac{[Q_j(x_i)]^2}{N_j} = \frac{1}{N_{r-1}} [Q_r'(x_i) Q_{r-1}(x_i)] \quad (B-47)$$

since  $Q_r(x_i) = 0$ . And finally, inserting the above equation into Equation (B-43) gives

$$\omega_i = \left[ v(x_i) \cdot \sum_{j=0}^{r-1} \frac{[Q_j(x_i)]^2}{N_j} \right]^{-1}, \quad i = 1, r. \quad (B-48)$$

This last equation determines all the weights except those corresponding to the preassigned abscissas.

In the case when only the abscissa  $x = b$  is preassigned, so that  $v(x) = x - b$ , the corresponding weight is expressed by

$$\omega_n = \frac{1}{\pi'(b)} \int_a^b \omega(x) \frac{\pi(x)}{x - b} dx. \quad (B-49)$$

Noting that  $\pi(x) = v(x) Q_{n-1}(x) = (x - b) Q_{n-1}(x)$ , and that  $\pi'(b) = Q_{n-1}(b)$ , then  $\omega_n$  becomes

$$\omega_n = \frac{1}{Q_{n-1}(b)} \int_a^b \omega(x) Q_{n-1}(x) dx. \quad (B-50)$$

We recall that the  $Q_{n-1}(x)$  above is orthogonal with respect to  $\omega^*(x)$ , not  $\omega(x)$ . To determine an explicit expression for  $\omega_n$ , we refer to the Christoffel-Darboux identity where we have set  $y = b$  and  $r = n-1$ :

$$\sum_{i=0}^{n-2} \frac{Q_i(x) Q_i(b)}{N_i} = \frac{Q_{n-2}(b) Q_{n-1}(x) - Q_{n-1}(b) Q_{n-2}(x)}{N_{n-2}(x - b)}. \quad (B-51)$$

We then multiply the equal members by  $\omega^*(x) Q_0(x)$ , integrate from  $a$  to  $b$ , and take advantage of the orthogonality of the polynomials to obtain

$$1 = \frac{Q_{n-2}(b)}{N_{n-2}} \int_a^b \frac{\omega^*(x) Q_{n-1}(x)}{(x - b)} dx - \frac{Q_{n-1}(b)}{N_{n-2}} \int_a^b \frac{\omega^*(x) Q_{n-2}(x)}{(x - b)} dx. \quad (B-52)$$

Rearranging slightly and then substituting in Equation (B-50) gives

$$\omega_n = \frac{1}{Q_{n-2}(b)} \int_a^b \omega(x) Q_{n-2}(x) dx - \frac{N_{n-2}}{Q_{n-2}(b) Q_{n-1}(b)} . \quad (B-53)$$

In comparing the expressions for  $\omega_n$  in Equations (B-50) and (B-53), we find the identity:

$$\frac{1}{Q_j(b)} \int_a^b \omega(x) Q_j(x) dx = \frac{1}{Q_{j-1}(b)} \int_a^b \omega(x) Q_{j-1}(x) dx - \frac{N_{j-1}}{Q_{j-1}(b) Q_j(b)} . \quad (B-54)$$

If we substitute Equation (B-54) successively into (B-53), we obtain

$$\begin{aligned} \omega_n &= \frac{1}{Q_{n-3}(b)} \int_a^b \omega(x) Q_{n-3}(x) dx - \frac{N_{n-3}}{Q_{n-3}(b) Q_{n-2}(b)} - \frac{N_{n-2}}{Q_{n-2}(b) Q_{n-1}(b)} \\ &\vdots \end{aligned} \quad (B-55a)$$

$$\omega_n = \int_a^b \omega(x) dx - \sum_{i=0}^{n-2} \frac{N_i}{Q_i(b) Q_{i+1}(b)} . \quad (B-55b)$$

Since the actual weight function being used is a Legendre expansion,  $f(\mu)$ , the integral of that expansion is

$$\int_a^b \omega(x) dx = \int_{-1}^{+1} f(\mu) d\mu \quad (B-56a)$$

$$= \sum_{\ell=0}^{\infty} \frac{2\ell+1}{2} f_{\ell} \int_{-1}^{+1} P_{\ell}(\mu) P_0(\mu) d\mu \quad (B-56b)$$

$$= f_0 = 1 . \quad (B-56c)$$

Therefore, Equation (B-55b) becomes

$$\omega_n = 1 - \sum_{i=0}^{n-2} \frac{N_i}{Q_i(1) Q_{i+1}(1)} , \quad (B-57)$$

where we have set  $b = 1$ .

Another way to determine the weights corresponding to a prescribed end ordinate or ordinates is to use one or both of the relations:

$$\sum_{i=1}^n \omega_i = \int_a^b \omega(x) dx \quad (B-58)$$

or

$$\sum_{i=1}^n x_i \omega_i = \int_a^b x \omega(x) dx , \quad (B-59)$$

which require that the error vanish in the expression

$$\int_a^b \omega(x) f(x) = \sum_{i=1}^n \omega_i f(x_i) + \text{error} , \quad (B-60)$$

when  $f(x) = 1$  and when  $f(x) = x$ , respectively. Substituting Equation (B-56c) into (B-58), we have

$$\omega_n = 1 - \sum_{i=1}^{n-1} \omega_i . \quad (B-61)$$

Now all of the above analysis is based on the assumption that  $\omega^*(x)$  does not change sign on the interval  $(a,b)$ ; otherwise, the roots of  $Q_n$  may be complex or may not lie in the interval  $(a,b)$ . In order for  $\omega^*(x)$  not to change sign, the roots of  $v(x)$  must be either a or

b, multiple roots of a or b, or perhaps outside of the interval.

Note: The MORSE code system will reject any  $N_i$  which is negative.

Since  $\omega^*(x) = (x - b)$   $\omega(x)$  is a negative function, MORSE would theoretically generate  $N_i$  which are unacceptable. Hence, we use the weight function  $-\omega^*(x) = (b - x)$   $\omega(x)$  where we have factored out a -1.

### Equivalence of Moments and Legendre Coefficients

Gauss Quadrature. We shall use the following form for the normalized Legendre expansion of an angular distribution:

$$f(\mu) = \sum_{\ell=0}^{\infty} \frac{2\ell+1}{2} f_{\ell} P_{\ell}(\mu) . \quad (B-62)$$

From this it follows that

$$f_{\ell} = \int_{-1}^1 f(\mu) P_{\ell}(\mu) d\mu \quad \text{and} \quad f_0 \equiv 1 . \quad (B-63)$$

The moments of the distribution are defined by

$$M_n = \int_{-1}^1 \mu^n f(\mu) d\mu . \quad (B-64)$$

If the Legendre polynomials are written

$$P_{\ell}(\mu) = \sum_{n=0}^{\ell} p_{\ell n} \mu^n , \quad (B-65)$$

then it follows simply from Equation (B-63) that

$$f_\ell = \sum_{n=0}^{\ell} p_{\ell n} \int_{-1}^{+1} f(\mu) \mu^n d\mu = \sum_{n=0}^{\ell} p_{\ell n} M_n . \quad (B-66)$$

Equation (B-66) shows how the first  $n$  Legendre coefficients of an angular distribution may be derived from the first  $n$  moments. The  $p_{\ell n}$ 's may be derived from the recurrence relation for  $P_\ell(\mu)$ . Since

$$\ell P_\ell(\mu) = (2\ell - 1) \mu P_{\ell-1}(\mu) - (\ell - 1) P_{\ell-2}(\mu) , \quad (B-67)$$

then Equation (B-65) becomes

$$\sum_{n=0}^{\ell} p_{\ell n} \mu^n = \frac{2\ell - 1}{\ell} \sum_{n=0}^{\ell-1} p_{\ell-1, n} \mu^{n+1} - \frac{\ell - 1}{\ell} \sum_{n=0}^{\ell-2} p_{\ell-2, n} \mu^n . \quad (B-68)$$

As this is an identity, we may separately equate the coefficients of each power of  $\mu$  giving the relation

$$p_{\ell n} = \frac{2\ell - 1}{\ell} p_{\ell-1, n-1} - \frac{\ell - 1}{\ell} p_{\ell-2, n} . \quad (B-69)$$

Since  $P_0(\mu) = 1$  and  $P_1(\mu) = \mu$ , then we have as initial values for Equation (B-69),  $p_{0,n} = \delta_{0n}$  and  $p_{1,n} = \delta_{1n}$ .

We may also derive relations for calculating moments given the first  $n$  Legendre coefficients of an expansion. Substituting Equation (B-62) into (B-64), we have

$$M_n = \sum_{\ell=0}^{\infty} \frac{2\ell + 1}{2} f_\ell \int_{-1}^{+1} \mu^n P_\ell(\mu) d\mu . \quad (B-70)$$

From the orthogonality property we know that  $P_\ell(\mu)$  is orthogonal to any polynomial of degree less than  $\ell$ . Hence

$$\int_{-1}^{+1} \mu^n P_\ell(\mu) d\mu = 0 \quad \text{for } \ell > n. \quad (B-71)$$

Then

$$M_n = \sum_{\ell=0}^n f_\ell p_{n\ell}^{-1}, \quad (B-72a)$$

where

$$p_{n\ell}^{-1} = \frac{2\ell+1}{2} \int_{-1}^{+1} \mu^n P_\ell(\mu) d\mu \quad (B-72b)$$

are the coefficients for a Legendre expansion of  $\mu^n$ , that is,

$$\mu^n = \sum_{\ell=0}^n p_{n\ell}^{-1} P_\ell(\mu). \quad (B-72c)$$

In order to derive the recurrence relation for the  $p_{n\ell}^{-1}$ 's, we first recall the fundamental recurrence relation for Legendre polynomials:

$$(2\ell+1) \mu P_\ell(\mu) = \ell P_{\ell-1}(\mu) + (\ell+1) P_{\ell+1}(\mu). \quad (B-73)$$

(Equation (B-73) is equivalent to (B-67)). Substituting Equation (B-73) into (B-72b) gives

$$p_{n\ell}^{-1} = \frac{1}{2} \int_{-1}^{+1} \mu^{n-1} [\ell P_{\ell-1}(\mu) + (\ell+1) P_{\ell+1}(\mu)] d\mu \quad (B-74)$$

or, after integrating,

$$p_{n\ell}^{-1} = \frac{\ell}{2\ell-1} p_{n-1, \ell-1}^{-1} + \frac{\ell+1}{2\ell+3} p_{n-1, \ell+1}^{-1}. \quad (B-75)$$

Initial values for the above recursion formula are  $p_{0, \ell}^{-1} = \delta_{0\ell}$  and  $p_{1, \ell}^{-1} = \delta_{1\ell}$ .

The MORSE code system actually uses the recursion formulas above to calculate the moments, given  $f_0, f_1, \dots, f_n$ . Some example formulas for  $M_n$  are given below for several values of  $n$ :

$$M_0 = f_0 = 1 \quad (B-76a)$$

$$M_1 = f_1 \quad (B-76b)$$

$$M_2 = f_0/3 + 2 f_2/3 \quad (B-76c)$$

$$M_3 = 3 f_1/5 + 2 f_3/5 . \quad (B-76d)$$

Radau Quadrature. We will designate the "Radau" moments as  $M_n^*$  (the moments used for Gauss quadrature will remain as  $(M_n)$ ). In order to calculate the Radau moments, we use an altered weight function,  $f^*(\mu)$ , given by

$$f^*(\mu) = (1 - \mu) f(\mu) , \quad (B-77)$$

where we have preassigned an abscissa or point at  $\mu_n = 1$ . The formula for the moments then becomes

$$M_n^* = \int_{-1}^{+1} \mu^n f^*(\mu) d\mu = \int_{-1}^{+1} \mu^n (1 - \mu) f(\mu) \quad (B-78)$$

or

$$M_n^* = M_n - M_{n+1} . \quad (B-79)$$

Therefore, the Radau moments are calculated simply from the differences between successive Gauss moments. For example,

$$M_0^* = 1 - f_1 \quad (B-80a)$$

$$M_1^* = -f_0/3 + f_1 - 2 f_2/3 \quad (B-80b)$$

$$M_2^* = f_0/3 - 3 f_1/5 + 2 f_2/3 - 2 f_3/5. \quad (B-80c)$$

Given any set of Legendre coefficients  $(f_0, f_1, \dots, f_{n-1}, f_n)$ , MORSE will first calculate the Gauss moments  $(M_0, M_1, \dots, M_{n-1}, M_n)$  and then use Equation (B-79) to calculate the Radau moments  $(M_0^*, M_1^*, \dots, M_{n-1}^*)$ . The number of Legendre coefficients and Gauss moments is always greater than the number of Radau moments by one.

To go in the opposite direction and calculate Legendre coefficients given Radau moments becomes slightly more complicated. We begin by multiplying  $f^*(\mu)$  by  $P_k(\mu)$  and then integrating between the limits -1 to +1:

$$\int_{-1}^{+1} f^*(\mu) P_k(\mu) d\mu = \int_{-1}^{+1} f(\mu) P_k(\mu) d\mu - \int_{-1}^{+1} \mu f(\mu) P_k(\mu) d\mu \quad (B-81a)$$

$$= f_k - \sum_{\ell=0}^n \frac{2\ell+1}{2} f_\ell \int_{-1}^{+1} \mu P_\ell(\mu) P_k(\mu) d\mu. \quad (B-81b)$$

Substituting Equation (B-73) into the integrand on the right-hand side of Equation (B-81b) and integrating again gives

$$\int_{-1}^{+1} f^*(\mu) P_k(\mu) d\mu = f_k - \frac{k}{2k+1} f_{k-1} - \frac{k+1}{2k+1} f_{k+1}. \quad (B-82)$$

Noting that

$$P_k(\mu) = \sum_{n=0}^k p_{kn} \mu^n ,$$

we obtain

$$\sum_{n=0}^k p_{kn} M_n^* = f_k - \frac{k}{2k+1} f_{k-1} - \frac{k+1}{2k+1} f_{k+1} . \quad (B-83)$$

Therefore, given any set of Radau moments  $(M_0^*, \dots, M_k^*)$  and the Legendre coefficients  $(f_{k-1}, f_k)$ , the  $(k+1)$  Legendre coefficient may be calculated.

#### Generation of Polynomials Orthogonal with Respect to $\omega(x)$

Let us now presume that we are given the first  $2n$  moments,  $M_0, M_1, \dots, M_{2n-1}$ , of an arbitrary function  $\omega(x)$  and are given no additional information about  $\omega(x)$ . We shall attempt to derive a set of polynomials which are orthogonal with respect to  $\omega(x)$ . (The following analysis on orthogonal polynomials applies to Radau quadrature as well as Gauss quadrature--simply replace  $\omega(x)$  with  $\omega^*(x)$  and  $M_n$  with  $M_n^*$ .) Recalling the notation

$$E[I(x)] = \int_a^b I(x) \omega(x) dx , \quad (B-84)$$

then what we wish is to determine  $Q_0, Q_1, \dots, Q_n$  such that

$$Q_i(x) = \sum_{k=0}^i a_{ik} x^k , \quad (B-85)$$

with the normalization condition  $a_{ii} = 1$ , and such that

$$E[Q_i(x) Q_j(x)] = \delta_{ij} N_i . \quad (B-86)$$

Note that

$$N_i = E[Q_i^2(x)] = \int_a^b Q_i^2(x) \omega(x) dx . \quad (B-87)$$

Since  $\omega(x) \geq 0$  (Restriction I), then it follows that

$$N_i > 0 . \quad (B-88)$$

Note: Since we wish to relax the non-negativity restriction slightly but not completely, we will retain Equation (B-88) as a reasonable requirement for a "well-behaved"  $\omega(x)$ . This requirement is essential to allow full use of the properties of orthogonal polynomials. It is also essential to the eventual use of this development as a Monte Carlo selection technique since it is needed to ensure that the "probabilities,"  $\omega_i$ , be positive.

From the properties of orthogonal polynomials we know that an arbitrary polynomial of order  $i$ ,  $S_i(x)$ , may be expanded in terms of the  $Q$  polynomials,

$$S_i(x) = \sum_{k=0}^i s_{ik} Q_k(x) . \quad (B-89)$$

It follows that

$$E[S_i(x) Q_j(x)] = 0 \quad \text{for } i < j . \quad (B-90)$$

Let us presume that we have obtained the first  $i$  polynomials and are attempting to derive  $Q_{i+1}(x)$ . Due to our normalization condition ( $a_{ii} = 1$ ) we have

$$Q_{i+1}(x) = x^{i+1} + R_i(x) , \quad (B-91a)$$

where

$$R_i(x) = \sum_{k=0}^i a_{i+1,k} x^k . \quad (B-91b)$$

Expanding Equation (B-91a) further gives

$$Q_{i+1}(x) = x \cdot x^i + R_i(x) \quad (B-92a)$$

$$= x \cdot [Q_i(x) - R_{i-1}(x)] + R_i(x) \quad (B-92b)$$

$$= x Q_i(x) + [R_i(x) - x R_{i-1}(x)] . \quad (B-92c)$$

The term  $R_i(x) - x R_{i-1}(x)$  is a polynomial of order  $i$  and may be expanded in terms of the  $Q$ 's. Thus,

$$Q_{i+1}(x) = x Q_i(x) + \sum_{k=0}^i d_{ik} Q_k(x) . \quad (B-93)$$

In order to obtain the familiar three-term recurrence relation for orthogonal polynomials (and to have the recurrence relation defined in terms of moments), we will multiply Equation (B-93) by  $\omega(x) Q_j(x)$  where  $j \leq i - 2$  (Case 1),  $j = i - 1$  (Case 2), and  $j = i$  (Case 3), and then integrate over the limits from  $a$  to  $b$ .

Case 1: For  $j \leq i - 2$ , we obtain the orthogonality relation

$$E[Q_{i+1}(x) Q_j(x)] = 0 = E[x Q_i(x) Q_j(x)] + \sum_{k=0}^i d_{ik} E[Q_k(x) Q_j(x)] \quad (B-94a)$$

$$= E[Q_i(x)(x Q_j(x))] + d_{ij} N_j \quad (B-94b)$$

$$= d_{ij} N_j , \quad (B-94c)$$

since  $x Q_j(x)$  is a polynomial of order  $\leq i-1$  and is orthogonal to  $Q_i(x)$ . Since  $N_j > 0$  we must have  $d_{ij} = 0$ .

If we write

$$\mu_{i+1} = -d_{i,i} \quad (B-95)$$

and

$$\sigma_i^2 = -d_{i,i-1}, \quad (B-96)$$

then Equation (B-93) reduces to

$$Q_{i+1}(x) = (x - \mu_{i+1}) Q_i(x) - \sigma_i^2 Q_{i-1}(x). \quad (B-97)$$

This equation is the basic recurrence relation for our polynomials.

Case 2: If we multiply Equation (B-93) by  $\omega(x) Q_{i-1}(x)$  and integrate, we have

$$E[Q_{i+1}(x) Q_{i-1}(x)] = 0$$

$$= E[x Q_i(x) Q_{i-1}(x)] - \mu_{i+1} E[Q_i(x) Q_{i-1}(x)] - \sigma_i^2 E[Q_{i-1}^2(x)] \quad (B-98a)$$

$$= E[Q_i(x)(x Q_{i-1}(x))] - \sigma_i^2 N_{i-1} \quad (B-98b)$$

$$= E[Q_i(x) \{Q_i(x) - \sum_{k=0}^{i-1} d_{i-1,k} Q_k(x)\}] - \sigma_i^2 N_{i-1} \quad (B-98c)$$

$$= E[Q_i^2(x)] - \sigma_i^2 N_{i-1} \quad (B-98d)$$

$$= N_i - \sigma_i^2 N_{i-1}. \quad (B-98e)$$

This is easily solved for

$$\sigma_i^2 = N_i/N_{i-1} . \quad (B-99)$$

In order to define  $N_i$  (and hence  $\sigma_i^2$ ) in terms of the moments, we use Equation (B-86) in conjunction with (B-92a) to obtain

$$N_i = E[Q_i(x) Q_i(x)] = E[Q_i(x) x] + E[Q_i(x) R_{i-1}(x)] \quad (B-100a)$$

$$= E[Q_i(x) x^i] = \sum_{k=0}^i a_{ik} \int_a^b \omega(x) x^k x^i dx = \sum_{k=0}^i a_{ik} M_{k+i} . \quad (B-100b)$$

Case 3: We will first define

$$L_{i+1} = E[Q_i(x) x^{i+1}] \quad (B-101a)$$

$$= \sum_{k=0}^i a_{ik} M_{k+i+1} . \quad (B-101b)$$

Then the final orthogonality relation used in defining  $Q_{i+1}(x)$  gives us

$$E[Q_{i+1}(x) Q_i(x)] = 0$$

$$= E[Q_{i+1}(x) x^i] + E[Q_{i+1}(x) R_{i-1}(x)] \quad (B-102a)$$

$$= E[x Q_i(x) x^i] - \mu_{i+1} E[Q_i(x) x^i] - \sigma_i^2 E[Q_{i-1}(x) x^i] \quad (B-102b)$$

$$= L_{i+1} - \mu_{i+1} N_i - \sigma_i^2 L_i \quad (B-102c)$$

or

$$\mu_{i+1} = \frac{L_{i+1}}{N_i} - \sigma_i^2 \frac{L_i}{N_i} \quad (B-103a)$$

$$= \frac{L_{i+1}}{N_i} - \frac{L_i}{N_{i-1}} \quad (B-103b)$$

Thus far we have formulas to calculate the orthogonal polynomials  $Q_{i+1}$  in terms of  $\mu_{i+1}$  and  $\sigma_i^2$ . However, we may also express  $Q_{i+1}$  as a summation

$$Q_{i+1}(x) = \sum_{k=0}^{i+1} a_{i+1,k} x^k. \quad (B-104)$$

In order to calculate the  $a_{i+1,k}$ , we will substitute the above equation into the orthogonal polynomial recurrence formula (Equation (B-97))

$$\sum_{k=0}^{i+1} a_{i+1,k} x^k = x \sum_{k=0}^i a_{i,k} x^k - \mu_{i+1} \sum_{k=0}^i a_{i,k} x^k - \sigma_i^2 \sum_{k=0}^{i-1} a_{i-1,k} x^k. \quad (B-105)$$

Equating the coefficients of  $x^k$  on both sides of the equation gives

$$a_{i+1,k} = a_{i,k-1} - \mu_{i+1} a_{i,k} - \sigma_i^2 a_{i-1,k}. \quad (B-106)$$

Let us now review the procedure for obtaining  $Q_{i+1}(x)$  given  $Q_i(x)$ . One first uses the moments  $M_0, \dots, M_{2i}$  and the values of  $a_{ik}$  from  $Q_i$  to calculate  $N_i$  (Equation (B-100b)). The term  $N_i$ , along with the previously determined  $N_{i-1}$ , allows one to calculate  $\sigma_i^2$  (Equation (B-99)). The moments  $M_0, \dots, M_{2i+1}$  and the values of  $a_{ik}$  from  $Q_i(x)$  determine  $L_{i+1}$  (Equation (B-101b)). This in turn allows the calculation of  $\mu_{i+1}$  (Equation (B-103a)). With  $\sigma_i^2$  and  $\mu_{i+1}$ , the recurrence relation (Equation (B-97)) determines  $Q_{i+1}(x)$ . In sum, the moments  $M_0, M_1, \dots, M_{2n-1}$  of  $\omega(x)$  allow the determination of the orthogonal polynomials  $Q_0(x), Q_1(x), \dots, Q_n(x)$ .

### Properties of the Roots of the Orthogonal Polynomials

The roots of the orthogonal polynomials have two useful properties which we shall prove.

Lemma I:  $Q_n(x)$  has  $n$  distinct, real roots which "interleave" with the roots of  $Q_{n-1}(x)$ ; that is, between any two adjacent roots of  $Q_{n-1}(x)$  there is one and only one root of  $Q_n(x)$ , and furthermore, there is one root of  $Q_n(x)$  greater than the largest root of  $Q_{n-1}(x)$  and one smaller than the least root of  $Q_{n-1}(x)$ . Likewise, there is one and only one root of  $Q_{n-1}(x)$  between any two adjacent roots of  $Q_n(x)$ .

Proof: We assume the Lemma to be true for  $Q_{n-1}$  and  $Q_{n-2}$ . Let  $x_1 > x_2 > \dots > x_{n-1}$  be the roots of  $Q_{n-1}$ . Then it follows that the sequence  $Q_{n-2}(x_1), Q_{n-2}(x_2), \dots, Q_{n-2}(x_{n-1})$  alternates in sign. Since

$$Q_n(x_i) = (x_i - \mu_n) Q_{n-1}(x_i) - \sigma_{n-1}^2 Q_{n-2}(x_i) \quad (B-107a)$$

$$= -\sigma_{n-1}^2 Q_{n-2}(x_i) . \quad (B-107b)$$

The sequence  $Q_n(x_1), Q_n(x_2), \dots, Q_n(x_{n-1})$  also alternates in sign. This establishes that there is at least one root of  $Q_n$  between any two roots of  $Q_{n-1}$ . Because the  $Q_i$ 's are normalized to  $a_{ii} = 1$ , they are all positive at  $+\infty$  and alternate in sign at  $-\infty$ .  $Q_{n-2}$  has no root between  $x_i$  and  $+\infty$ ; hence  $Q_{n-2}(x_1) > 0$ . But  $\sigma_{n-1}^2 > 0$  (because  $N_{n-1} > 0$  and  $N_{n-2} > 0$ ); therefore,  $Q_n(x_1) < 0$  and  $Q_n$  must have at least one root greater than  $x_i$ . Similar reasoning leads to the conclusion that  $Q_{n-2}(x_{n-1})$ ,  $Q_{n-2}(x \rightarrow -\infty)$ , and  $Q_n(x \rightarrow -\infty)$  have the same

sign while  $Q_n(x_{n-1})$  is of the opposite sign. Thus,  $Q_n$  must have at least one root between  $x_{n-1}$  and  $-\infty$ . Since this gives us  $n$  intervals where  $Q_n$  must have "at least one" root, it is clear that  $Q_n$  has  $n$  distinct roots which interleave with the roots of  $Q_{n-1}$ .

The proof by induction may be completed by using similar arguments to show that one of the two roots of  $Q_2(x)$  lies above the single root of  $Q_1(x)$  and one below it.

Lemma II: The  $n$  roots of  $Q_n(x)$  lie in the interval  $(a,b)$ .

Proof: Assume that  $Q_n(x)$  has only  $s$  changes of sign in the interval  $(a,b)$  at the points  $x_1, x_2, \dots, x_s$ . Let

$$\theta(x) = (x - x_1)(x - x_2)(x - x_3), \dots, (x - x_s) , \quad (B-108)$$

then  $\theta(x) Q_n(x)$  does not change sign in the interval  $(a,b)$ . It follows that\*

$$E[\theta(x) Q_n(x)] = \int_a^b \theta(x) Q_n(x) \omega(x) dx \neq 0 . \quad (B-109)$$

However,  $\theta(x)$  is a polynomial of order  $s \leq n$ . Since  $Q_n(x)$  is orthogonal to all polynomials of order less than  $n$ , we must have  $s = n$ , thus proving the assertion.

---

\*Note: This step relies on the requirement that  $\omega(x)$  be non-negative. We wish to relax this restriction somewhat but not completely. Since Lemma II expresses a property which will be essential to the use of this development as a Monte Carlo selection technique, we will use this property as one of the requirements for a "well-behaved"  $\omega(x)$  with which we shall replace the non-negativity restriction.

### The Replacement of the Non-Negativity Requirement, $\omega(x) \geq 0$

Gauss Quadrature. All of the preceding material in this Appendix was derived under the assumption that the weight function ( $\omega(x)$ ) is strictly positive. However, in the MORSE code system, we do not work with the original angular distribution (which is everywhere positive), but with a truncated Legendre expansion which approximates the angular distribution and may not be everywhere positive. In order to ensure that the truncated expansion originates from at least one function which is everywhere positive, the non-negativity requirement may be replaced by two restrictions:

- 1)  $N_i > 0$  ;  $i = 1, \dots, n-1$  and
- 2)  $Q_n(x)$  has  $n$  roots in the interval  $(-1, +1)$ .

We will first show how the restriction,  $N_i > 0$ , may be stated in a different form. The quantity  $N_i$  was previously defined as

$$N_i = \int_a^b Q_i^2(x) \omega(x) dx , \quad (B-110a)$$

where

$$Q_i(x) = \sum_{k=0}^i a_{ik} x^k . \quad (B-110b)$$

Substituting Equation (B-110b) into (B-110a) gives

$$\begin{aligned} N_i &= a_{i0} \int_a^b Q_i(x) \omega(x) dx + a_{i1} \int_a^b x Q_i(x) \omega(x) dx \\ &+ a_{i2} \int_a^b x^2 Q_i(x) \omega(x) dx + \dots + a_{ii} \int_a^b x^i Q_i(x) \omega(x) dx . \end{aligned} \quad (B-111)$$

Since  $Q_i(x)$  is orthogonal to all polynomials of degree less than  $i$ , then the first  $i$  integrals equal zero and the last integral (with coefficient  $a_{ii} = 1$ ) equals  $N_i$ . If we again use Equation (B-110b) and substitute it into (B-111), and noting that

$$M_k = \int_a^b x^k \omega(x) dx , \quad (B-112)$$

then we obtain

$$\begin{aligned} N_i = & a_{i0} \sum_{k=0}^i a_{ik} M_k + a_{i1} \sum_{k=0}^i a_{ik} M_{k+1} + a_{i2} \sum_{k=0}^i a_{ik} M_{k+2} \\ & + \dots + a_{ii} \sum_{k=0}^i a_{ik} M_{k+i} . \end{aligned} \quad (B-113)$$

Since the first  $i$  integrals in Equation (B-111) were equal to zero, then the first  $i$  sets of summations are also equal to zero:

$$\sum_{k=0}^i a_{ik} M_k = 0 \quad (B-114a)$$

$$\sum_{k=0}^i a_{ik} M_{k+1} = 0 \quad (B-114b)$$

•  
•  
•

$$\sum_{k=0}^i a_{ik} M_{k+i} = N_i \quad (B-114c)$$

or, in the matrix form  $[M_i][A_i] = [B]$ ,

$$\begin{bmatrix} M_0 & M_1 & M_2 & \dots & M_i \\ M_1 & M_2 & M_3 & \dots & M_{i+1} \\ \vdots & & & & \\ \vdots & & & & \\ M_i & M_{i+1} & \dots & M_{2i} \end{bmatrix} \begin{bmatrix} a_{i0} \\ a_{i1} \\ \vdots \\ \vdots \\ a_{ii} \end{bmatrix} = \begin{bmatrix} 0 \\ 0 \\ \vdots \\ \vdots \\ N_i \end{bmatrix} .$$

(Note that Equation (B-114c) is the same as (B-100b).) The determinant of the matrix  $[M_i]$  is the Gram determinant of the functions  $1, x, x^2, \dots, x^i$ . In view of the fact that these functions are linearly independent, then the determinant of  $[M_i]$  is greater than zero, and  $[M_i]$  is nonsingular. Since  $N_i$  is required to be greater than zero, then we can obtain a unique and non-trivial solution  $(Q_i)$  to the above system of equations.

Now, let us assume for the moment that  $N_i = 0$  such that  $[M_i] [A_i] = 0$ . Referring back to Equation (B-113), we note that for  $N_i = 0$ ,

$$\sum_{k=0}^i a_{ik} M_{k+i} = -a_{i0} \sum_{k=0}^i a_{ik} M_k - a_{i1} \sum_{k=0}^i a_{ik} M_{k+1} - \dots - a_{i,i-1} \sum_{k=0}^i a_{ik} M_{k+i-1} . \quad (B-115)$$

Since the summation on the left-hand side of Equation (B-115) is a linear combination of the first  $i$  sets of summations with coefficients  $-a_{i0}, -a_{i1}, \dots, -a_{i,i-1}$ , then the last row of the matrix

$[M_i]$  is linearly dependent on the other rows. It then follows that the determinant of  $[M_i]$  equals zero and the solution will either be non-existent or non-unique.

In summary, then, the sequence of polynomials  $(Q_i(x))$  which satisfies

$$E[Q_i(x) Q_j(x)] = \delta_{ij} N_i \quad (B-116)$$

with  $N_i > 0$ , is unique if and only if the determinates  $M_i$ ,  $i = 0, 1, 2, \dots$  are greater than zero.

The second requirement which replaces the non-negativity requirement is that the roots lie between the limits  $(-1, +1)$ . However, instead of actually checking the position of each root, the MORSE code system utilizes the principle stated below.

Lemma III (Irving, 1970): The roots of  $Q_n(x)$  will be contained in the interval  $(a, b)$  if and only if the sign of  $Q_i(b)$  equals  $+1$  and the sign of  $Q_i(a)$  equals  $(-1)^i$  for  $i = 1, n$ .

Proof: Assume that the roots of  $Q_{n-1}(x)$  lie in the interval  $(a, b)$ . From Lemma I, we know that only one root of  $Q_n$  lies above the largest root of  $Q_{n-1}$ . Since  $\text{sign } (Q_n(x + +\infty)) = +1$ , the largest root of  $Q_n$  will be less than  $b$  if and only if  $\text{sign } (Q_n(b)) = +1$ .

Likewise, there is only one root of  $Q_n$  below the lowest root of  $Q_{n-1}$ . This root will be greater than  $a$  if and only if  $\text{sign } (Q_n(a)) = \text{sign } (Q_n(x + -\infty)) = (-1)^n$ .

Since the lemma is fairly obvious for  $Q_1(x)$ , the proof by induction is complete.

Radau Quadrature. This type quadrature uses the same restriction to replace the non-negativity requirement as Gauss quadrature; i.e.,

- 1)  $N_i > 0$ ,  $i = 1, \dots, n-2$  and
- 2)  $Q_{n-1}(x)$  has  $n-1$  roots in the interval  $(-1, +1)$ .

These restrictions force the first  $n-1$  weights and abscissas to be positive. However, they put no limits on the value of the weight ( $\omega_n$ ) corresponding to the abscissa  $x_n = 1$ . Therefore, the third restriction for Radau quadrature is that

- 3)  $\omega_n > 0$ .

Limits of  $\mu_i$  and  $\sigma_i^2$

Gauss Quadrature. In the calculations leading to the generalized Gaussian quadrature, we obtained two restrictions which had to be satisfied in order to have a positive distribution located on the interval  $(-1, +1)$ . These restrictions were:

- 1)  $N_i > 0$ .
- 2) All the roots of  $Q_i(x)$  lie in the interval  $(-1, +1)$ .

Let us determine first what limitations these two restrictions place on the quantities  $\mu_i$ ,  $\sigma_i^2$ . Consider first the effect of adding an infinitesimal amount  $\Delta\mu$  to  $\mu_i$ . We have

$$Q_i(x) = (x - \mu_i) Q_{i-1}(x) - \sigma_{i-1}^2 Q_{i-2}(x) \quad (B-117)$$

and

$$Q_i^*(x) = (x - \mu_i - \Delta\mu) Q_{i-1}(x) - \sigma_{i-1}^2 Q_{i-2}(x) = Q_i(x) - \Delta\mu Q_{i-1}(x) . \quad (B-118)$$

If  $Q_i$  has a root at  $x_0$ , then  $Q_i^*$  will have a root at  $x_0 + \Delta x_0$

$$Q_i^*(x_0 + \Delta x_0) = 0 = Q_i(x_0 + \Delta x_0) - \Delta\mu Q_{i-1}(x_0 + \Delta x_0) . \quad (B-119)$$

If we expand the right-hand side and keep only first-order terms

$$0 = Q_i(x_0) + \Delta x_0 Q_i'(x_0) - \Delta\mu Q_{i-1}(x_0) = \Delta x_0 Q_i'(x_0) - \Delta\mu Q_{i-1}(x_0) \quad (B-120)$$

or

$$\Delta x_0 = \frac{Q_{i-1}(x_0)}{Q_i'(x_0)} \Delta\mu . \quad (B-121)$$

Since  $Q_i(x)$  is positive as  $x$  approaches  $+\infty$ , then  $Q_i'(x_0) > 0$  at  $x_0$  equal to the largest root of  $Q_i$ . At successively smaller roots of  $Q_i$ , the sign of  $Q_i'(x)$  alternates from positive to negative.  $Q_{i-1}(x)$  is similarly positive at  $+\infty$ . Also, it has no roots greater than the largest root of  $Q_i$ . Therefore,  $Q_{i-1}(x) > 0$  at the largest root of  $Q_i$ . Because the roots of  $Q_{i-1}$  "interleave" with the roots of  $Q_i$ , the sign of  $Q_{i-1}(x)$  must alternate at successive roots of  $Q_i(x)$ . Therefore, at all roots of  $Q_i(x)$  we must have:

$$\frac{Q_{i-1}(x)}{Q_i'(x)} > 0 \quad (B-122)$$

or, going back to Equation (B-121),

$$\frac{dx_i}{d\mu_i} > 0. \quad (B-123)$$

Therefore, as  $\mu_i$  is increased, the roots of  $Q_i(x)$  shift to the right, and, as  $\mu_i$  is decreased, the roots shift downward. If  $\mu_i$  is steadily increased, the largest root of  $Q_i$  will eventually equal 1. This point is determined by

$$Q_i(1) = 0 = (1 - \mu_i) Q_{i-1}(1) - \sigma_{i-1}^2 Q_{i-2}(1) \quad (B-124)$$

or

$$\mu_i = 1 - \sigma_{i-1}^2 \frac{Q_{i-2}(1)}{Q_{i-1}(1)}. \quad (B-125)$$

This is clearly the maximum value of  $\mu_i$ , which will generate positivity in the interval  $(-1, +1)$ . Likewise, there is a minimum value at which the lowest root of  $Q_i$  occurs at  $x = -1$ :

$$Q_i(-1) = 0 = (-1 - \mu_i) Q_{i-1}(-1) - \sigma_{i-1}^2 Q_{i-2}(-1) \quad (B-126)$$

or

$$\mu_i^{\min} = -1 - \sigma_{i-1}^2 \frac{Q_{i-2}(-1)}{Q_{i-1}(-1)}. \quad (B-127)$$

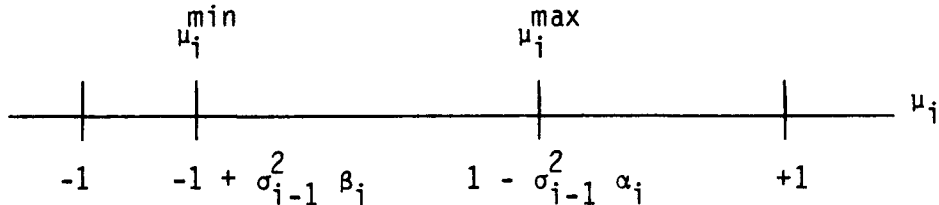
Note that

$$\alpha_i = \frac{Q_{i-2}(1)}{Q_{i-1}(1)} > 0, \quad (B-128)$$

due to the positivity of the functions as they approach  $+\infty$  and that

$$\beta_i = -\frac{Q_{i-2}(-1)}{Q_{i-1}(-1)} > 0, \quad (B-129)$$

due to their alternation in sign at  $-\infty$ . Since  $\sigma_{i-1}^2 > 0$ , we have the following picture on a  $\mu_i$ -axis



Now that we have upper and lower limits for  $\mu_i$ , what can we say about  $\sigma_i^2$ ? Since  $\sigma_i^2 = N_i/N_{i-1}$ , restriction I implies that  $\sigma_i^2 > 0$ . We can obtain an upper limit to  $\sigma_i^2$  by setting  $\mu_{i+1}^{\min} = \mu_{i+1}^{\max}$ . For larger values of  $\sigma_i^2$ ,  $\mu_{i+1}^{\min} > \mu_{i+1}^{\max}$ , which means that there is no value of  $\mu_{i+1}$  which will allow all the roots of  $Q_{i+1}(x)$  to lie inside  $(-1, +1)$ . Thus,

$$1 - (\sigma_i^2)_{\max} \frac{Q_{i-1}(+1)}{Q_i(+1)} = -1 - (\sigma_i^2)_{\max} \frac{Q_{i-1}(-1)}{Q_i(-1)} \quad (B-130a)$$

$$2 = (\sigma_i^2)_{\max} \left[ \frac{Q_{i-1}(+1)}{Q_i(+1)} - \frac{Q_{i-1}(-1)}{Q_i(-1)} \right] \quad (B-130b)$$

$$(\sigma_i^2)_{\max} = 2 / \left[ \frac{Q_{i-1}(+1)}{Q_i(+1)} - \frac{Q_{i-1}(-1)}{Q_i(-1)} \right] . \quad (B-130c)$$

We can work back from the limits on  $\mu_i$  and  $\sigma_i^2$  to obtain limits on the moments. Substituting the following two equations:

$$\sigma_i^2 = N_i/N_{i-1} \quad (B-131)$$

$$N_i = \sum_{k=0}^i a_{ik} M_{k+i} = M_{2i} + \sum_{k=0}^{i-1} a_{ik} M_{k+i} \quad \text{since } a_{ii} = 1 \quad (B-132)$$

into the equation for  $\sigma_i^2$  below

$$0 < \sigma_i^2 < 2 / \left[ \frac{Q_{i-1}(+1)}{Q_i(+1)} - \frac{Q_{i-1}(-1)}{Q_i(-1)} \right] \quad (B-133)$$

gives

$$- \sum_{k=0}^{i-1} a_{ik} M_{k+i} < M_{2i} < \frac{2N_{i-1}}{\frac{Q_{i-1}(+1)}{Q_i(+1)} - \frac{Q_{i-1}(-1)}{Q_i(-1)}} - \sum_{k=0}^{i-1} a_{ik} M_{k+i} \quad (B-134)$$

This last equation gives the upper and lower limits on the "even-numbered" moments. For the "odd-numbered" moments, we recall that

$$\mu_{i+1} = \frac{L_{i+1}}{N_i} - \frac{L_i}{N_{i-1}} \quad (B-135)$$

Rearranging, and setting  $L_{i+1}$  to its maximum, we obtain

$$L_{i+1}^{\max} = N_i (\mu_{i+1}^{\max}) + \frac{N_i L_i}{N_{i-1}} \quad (B-136a)$$

$$= N_i \left[ 1 - \sigma_i^2 \frac{Q_{i-1}(1)}{Q_i(1)} \right] + L_i \sigma_i^2 \quad (B-136b)$$

Since  $L_{i+1}$  is calculated by the expression

$$L_{i+1} = \sum_{k=0}^i a_{ik} M_{k+i+1} = M_{2i+1} + \sum_{k=0}^{i-1} a_{ik} M_{k+i+1} \quad (B-137)$$

then the upper limit for an "odd-numbered" moment is

$$M_{2i+1} < N_i \left[ 1 - \sigma_i^2 \frac{Q_{i-1}(1)}{Q_i(1)} \right] + L_i \sigma_i^2 - \sum_{k=0}^{i-1} a_{ik} M_{k+i+1}. \quad (B-138)$$

If we go through the same procedure again with  $L_{i+1}^{\min}$  and  $\mu_{i+1}^{\min}$ , we obtain the lower limit for the moments:

$$M_{2i+1} > N_i \left[ -1 - \sigma_i^2 \frac{Q_{i-1}(-1)}{Q_i(-1)} \right] + L_i \sigma_i^2 - \sum_{k=0}^{i-1} a_{ik} M_{k+i+1}. \quad (B-139)$$

To obtain the limits on the Legendre coefficients, take the set of moments already determined  $M_1, M_2, \dots, M_{2i-1}$  combined with  $M_{2i}^{\max}$  and convert from moments to Legendre coefficients. This gives  $f_{2i}^{\max}$ . When  $M_1, M_2, \dots, M_{2i-1}$  are combined with  $M_{2i}^{\min}$  and converted, one obtains  $f_{2i}^{\min}$ .

Radau Quadrature. In developing Radau quadrature, we obtained three restrictions which had to be satisfied in order to have a positive distribution:

- 1)  $N_i > 0$ ,
- 2) all the roots of  $Q_i(x)$  lie in the interval  $(-1, +1)$ , and
- 3)  $\omega_n \geq 0$ .

The first two restrictions are the same as those used for Gauss quadrature, and hence we could use them to obtain the same limits on  $\mu_i$  and  $\sigma_i^2$  as shown in the preceding section. However, we will find that the third restriction ( $\omega_n \geq 0$ ) is the most significant because it places even tighter limits on  $\mu_i$  and  $\sigma_i^2$ .

We recall that the formula for the Radau weight ( $\omega_n$ ) corresponding to the preset abscissa,  $x_n = 1$ , is

$$\omega_n = 1 - \sum_{i=1}^{n-1} \frac{N_{i-1}}{Q_{i-1}(1) Q_i(1)} . \quad (B-140)$$

Limiting  $\omega_n$  to positive values only, we have

$$0 \leq 1 - \sum_{i=1}^{n-2} \frac{N_{i-1}}{Q_{i-1}(1) Q_i(1)} - \frac{N_{n-2}}{Q_{n-2}(1) Q_{n-1}(1)} \quad (B-141)$$

or, after inserting the three-term recurrence formula for  $Q_{n-1}(1)$ ,

$$\frac{N_{n-2}}{Q_{n-2}(1)} \left[ 1 - \sum_{i=1}^{n-2} \frac{N_{i-1}}{Q_{i-1}(1) Q_i(1)} \right]^{-1} \leq (1 - \mu_{n-1}) Q_{n-2}(1) - \sigma_{n-2}^2 Q_{n-3}(1) . \quad (B-142)$$

Solving for  $\mu_{n-1}$ , and then setting the counter  $n-1$  to an arbitrary counter  $i$ , gives

$$\mu_i^{\max} \leq 1 - \sigma_{i-1}^2 \frac{Q_{i-2}(1)}{Q_{i-1}(1)} - G_{i-1}(1) , \quad (B-143a)$$

where

$$G_{i-1}(1) = \frac{N_{i-1}}{[Q_{i-1}(1)]^2} \left[ 1 - \sum_{k=1}^{i-1} \frac{N_{k-1}}{Q_{k-1}(1) Q_k(1)} \right]^{-1} . \quad (B-143b)$$

Comparing Equation (B-143a) with (B-125), we note that

$$\mu_i^{\max} = (\mu_i^{\max})_{\text{Gauss}} - G_{i-1}(1) . \quad (B-144)$$

The formula for  $\mu_i^{\min}$  remains the same as in the Gauss quadrature case

$$\mu_i^{\min} = -1 - \sigma_{i-1}^2 \frac{Q_{i-2}(-1)}{Q_{i-1}(-1)} . \quad (B-145)$$

We next calculate an average  $\mu_i$ :

$$\mu_i^{\text{avg}} = \frac{\mu_i^{\text{max}} + \mu_i^{\text{min}}}{2} \quad (\text{B-146a})$$

$$= - \left\{ \sigma_{i-1}^2 \left[ \frac{Q_{i-2}(1)}{Q_{i-1}(1)} + \frac{Q_{i-2}(-1)}{Q_{i-1}(-1)} \right] + G_{i-1}(1) \right\} / 2 \quad (\text{B-146b})$$

$$= (\mu_i^{\text{avg}})_{\text{Gauss}} - G_{i-1}(1)/2. \quad (\text{B-146c})$$

The lower limit for  $\sigma_i^2$  is zero (since  $N_i > 0$ ). To calculate the upper limit for  $\sigma_i^2$ , we set

$$\mu_{i+1}^{\text{max}} = \mu_{i+1}^{\text{min}} \quad (\text{B-147a})$$

$$1 - \sigma_i^2 \frac{Q_{i-1}(1)}{Q_i(1)} - G_i(1) = -1 - \sigma_i^2 \frac{Q_{i-1}(-1)}{Q_i(-1)}. \quad (\text{B-147b})$$

Therefore,

$$0 < \sigma_i^2 < 2 \cdot \left\{ \left[ \frac{Q_{i-1}(1)}{Q_i(1)} - \frac{Q_{i-1}(-1)}{Q_i(-1)} \right] + \frac{N_{i-1}}{N_i} G_i(1) \right\}^{-1}. \quad (\text{B-148})$$

Substituting Equation (B-131) and (B-132) into (B-148), we find the upper and lower limits to the even-numbered moments:

$$- \sum_{k=0}^{i-1} a_{ik} M_{k+i} < M_{2i} < (N_{i-1})(\sigma_i^2)_{\text{max}} - \sum_{k=0}^{i-1} a_{ik} M_{k+i}. \quad (\text{B-149})$$

The limits on the odd-numbered moments are obtained in the same way as in the Gauss quadrature case:

$$N_i(\mu_{i+1}^{\min}) + H_i < M_{2i+1} < N_i(\mu_{i+1}^{\max}) + H_i , \quad (B-150a)$$

where

$$H_i = L_i \sigma_i^2 - \sum_{k=0}^{i-1} a_{ik} M_{k+i+1} \quad (B-150b)$$

and  $\mu_{i+1}^{\min}$  and  $\mu_{i+1}^{\max}$  are given by Equations (B-145) and (B-143a), respectively.

## APPENDIX C

### IMPLEMENTATION OF RADAU QUADRATURE INTO THE MORSE CODE SYSTEM

The MORSE code system currently uses Gauss quadrature to calculate discrete directions and weights from Legendre polynomial expansions of group-to-group cross sections. The subroutines in the code which perform these calculations are XSEC5, ANGLES, GETMUS, FIND, Q, BADMOM, and MAMENT. The flowchart in Figure C-1 shows the calling sequence between these different subroutines in MORSE. A brief description of each subroutine follows:

XSEC5 retrieves the cross section data from mass-storage tapes, calls ANGLES to calculate the scattering angles and probabilities, and then stores the calculated results on a different mass-storage tape. It prints the angles and probabilities if requested by the user.

ANGLES is the executive routine for the generalized quadrature technique. It first computes the moments from the given Legendre coefficients. It then calls GETMUS to obtain the recurrence relations for the orthogonal polynomials, calls FIND to calculate the roots of the orthogonal polynomials, and then computes the weight factors associated with each root.

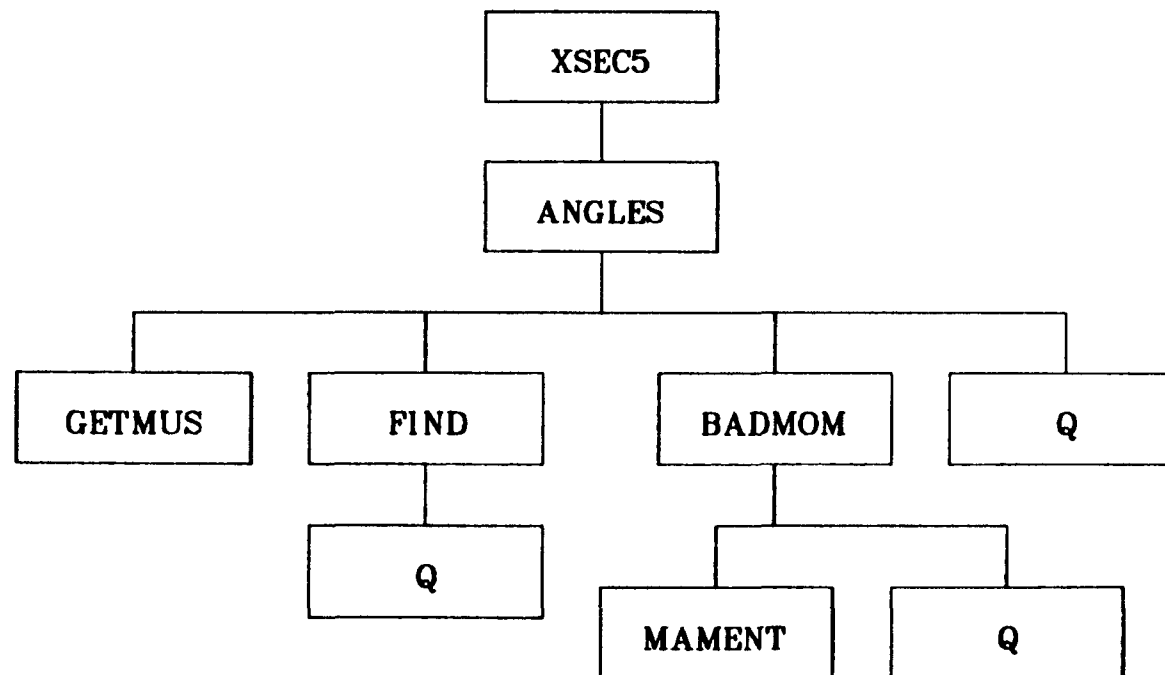


Figure C-1. Flowchart of quadrature subroutines in MORSE.

GETMUS calculates the quantities  $\mu_j$  and  $\sigma_j^2$  used in the recurrence relation for the orthogonal polynomials,  $Q_j(x)$ . It uses the moments,  $M_j$ , of the angular distribution as input. It also checks to determine if  $\sigma_j^2 > 0$ .

FIND first determines if the roots of  $Q_L(x)$  will lie within the range  $(-1, +1)$  by using the property of orthogonal polynomials that the roots of  $Q_L$  and  $Q_{L-1}$  "interleave". If the roots meet this criterion, then the subroutine proceeds to calculate them.

Q uses the recurrence relation for the orthogonal polynomials to calculate the value of  $Q_L(\mu)$  for some specified order L and specified angle  $\mu$ .

BADMOM calculates and prints any "bad" Legendre coefficients which have been rejected because of implied negativity in the cross sections (occurs when  $\sigma_j^2$  is negative or if the roots do not lie between  $(-1, +1)$ ). The allowed limits on the coefficients are also calculated and printed for the user.

MAMENT is called from BADMOM to convert cross-section moments to Legendre coefficients.

It is not within the bounds of our intent to provide thorough and detailed descriptions of the subroutines above. An adequate understanding of the subroutines may be easily obtained by referring to the documentation by Emmett (1975), Irving (1970), and Dupree and Lighthill (1982).

In Appendix B, the theory and use of Radau quadrature was developed as an extension of Gauss quadrature. Therefore, the implementation of Radau quadrature into MORSE was treated in the same way. Except for a few side comments, it is thought that the theory of Radau quadrature presented in Appendix B, along with the ample documentation available on Gauss quadrature and the various subroutines, should be sufficient for the user to understand the update coding for Radau quadrature. Note: this update coding does not include coding for the extended transport cross section correction.

Additional relevant comments on the code:

- (1) Only the subroutines XSEC5, ANGLES, GETMUS, MAMENT, and BADMOM were updated for Radau quadrature. Subroutines FIND and Q were not altered. The subroutines are provided in this appendix in alphabetical order.
- (2) All updates are identified in columns 73-78 of the code by the word RADAU. Coding left unaltered is identified by the word MORSE. All code lines are numbered for easy reference.
- (3) Recall that for  $n$  points or scattering angles, we require a  $P_N$  expansion with  $N=2n-1$  for Gauss quadrature, or with  $N=2n-2$  for Radau quadrature. However, if the expansion is one order less

than that required to obtain  $n$  points, then the code will effectively compute an average  $N^{\text{th}}$  Legendre coefficient ( $f_N$ ) from certain limiting equations to increase the expansion to  $P_N$ . Some examples of possible expansion orders for various ( $n$ ) are shown below:

<u>Scattering Angles</u>	<u>Expansion Orders</u>	
	<u>Gauss</u>	<u>Radau</u>
1	$P_1$	---
2	$P_2, P_3$	$P_1, P_2$
3	$P_4, P_5$	$P_3, P_4$
4	$P_6, P_7$	$P_5, P_6$

(4) The type of quadrature method is chosen locally in XSEC5 by setting a flag (IGOR) defined in line reference RADAU-195 and 213:

IGOR = +1 , code chooses Radau quadrature.

IGOR = -1 , code chooses Gauss quadrature.

IGOR = 0 , code chooses quadrature method based on the order  
of the Legendre expansion (N) and the number of  
scattering angles desired (n):

$N = \text{odd}$		Gauss
$N = \text{even}$	$N > 2n - 1$	Gauss
	$N < 2n - 1$	Radau

Gauss quadrature is used for  $N > 2n - 1$  (where  $n$  is even) in order to ensure that we use the maximum number of coefficients. For example, suppose we input  $P_6$  expansions into the code but we only wish to compute three scattering angles. Gauss quadrature would use  $f_0, \dots, f_5$  to compute the scattering angles while Radau quadrature would use only  $f_0, \dots, f_4$ .

- (5) Since the theory for Radau quadrature is not valid for any roots which coincide with preassigned abscissas, we perform a precheck on  $f_1$  to see if it originated from a delta function expansion near  $\mu_0 = 1$ . This precheck is performed in subroutine ANGLES starting at line reference RADAU-3. The characteristic of a delta function expansion is that its coefficients all equal 1.
- (6) In Gauss quadrature, "impossible" coefficients are checked for by seeing if  $\sigma_i^2 > 0$  and the roots are between  $(-1, +1)$ . In Radau quadrature, we have an additional restriction that the weight corresponding to  $\delta(\mu_0 - 1)$  is nonnegative. This check is performed in ANGLES at line reference RADAU-78.

```

SUBROUTINE ANGLES(IG1,MX) RADAU 1
COMMON/INPUT/IADJM,NSTRRT,NMOST,NITS,NQUIT,ISTAT,NSPLT,NKILL,IR8, MORSE 2858
1 IRR, NPAST, NOLEAK, IEBIAS, NKCALC, NORMF, MORSE 2859
2 MEDIA, NMIX, MEDALB, MXREG, MFISTP, NNGA, NGGA, NCOEF, NSCT, MAXGP, IRDSG, MORSE 2860
3 ISTR, IFMU, IMOM, IPRIN, IPUN, MORSE 2861
5 ISOUR, NGPFS, ISBIAS, NSOUR, MORSE 2862
6 ND, NNE, NE, NT, NA, NRESP, NEX, NEXND, IFLAG(16), MORSE 2863
7 TMAX, TCUT, WTSTRRT, AGSTRRT, XSTRRT, YSTRRT, ZSTRRT, UINP, VINP, WINP, ROMC, MORSE 2864
8 IXTAPE, NG, IFTG, IGG, NNUC, IDT, NRP, NIM, N2M, NSGPS, TITLE(20), DAT, JFTG, MORSE 2865
9 KFTG, LFTG MORSE 2866
COMMON/PERM/INN, IOUT MORSE 2867
COMMON/MEANS/NM, NV, XMU(14), VAR(13), XNORML(13) MORSE 2868
COMMON/RESULT/POINT(14), WEIGHT(14), ROOT(14,14) MORSE 2869
COMMON/MOMENT/NMOM, XMOMNT(25), F(25) MORSE 2870
COMMON/DRTACS/NR8, NR9, NR10 MORSE 2871
COMMON/RADAU/IGOR RADAU 2
DIMENSION P1(25), P2(25) MORSE 2872
C RADAU 3
C CHECK IF LEGENDRE COEFFICIENTS ORIGINATED FROM RADAU 4
C DELTA FUNCTION EXPANSION RADAU 5
C RADAU 6
IF(ABS(F(1)).LE.0.999) GO TO 205 RADAU 7
POINT(1) = SIGN(F(1),1.0) RADAU 8
WEIGHT(1) = 1.0 RADAU 9
NV = 0 RADAU 10
IF(IPUN.LE.0) GO TO 200 RADAU 11
WRITE(IOUT,1000)IG1,MX RADAU 12
1000 FORMAT(/* DELTA FUNCTION EXPANSION FOUND FOR TRANSFER NO. = *I3, RADAU 13
      1* MATERIAL = *I3) RADAU 14
200 RETURN RADAU 15
C RADAU 16
C CALCULATE GAUSS MOMENTS RADAU 17
C RADAU 18
205 NFM = NMOM-1 RADAU 19
P10 = 0.0 MORSE 2874
P1(1) = 1.0 MORSE 2875
XMOMNT(1) = F(1) MORSE 2876
IF(NMOM-2) 245,210,210 MORSE 2877
210 DO 215 L=2,NMOM MORSE 2878
215 P1(L) = 0.0 MORSE 2879
DO 240 N=2,NMOM MORSE 2880
P20 = P1(1)/3.0 MORSE 2881
P2(1) = P10 + 0.4*P1(2) MORSE 2882
IF(NMOM-2)245,230,220 MORSE 2883
220 DO 225 L=2,NFM MORSE 2884
FL = L MORSE 2885
225 P2(L) = FL*P1(L-1)/(2.0*FL-1.0) + (FL+1.0)*P1(L+1)/(2.0*FL+3.0) MORSE 2886
230 FNF = NMOM MORSE 2887
P2(NMOM) = FNF*P1(NFM)/(2.0*FNF-1.0) MORSE 2888
XMOMNT(N) = P20 MORSE 2889
DO 235 L=1,NMOM MORSE 2890
XMOMNT(N) = XMOMNT(N) + P2(L)*F(L) MORSE 2891
235 P1(L) = P2(L) MORSE 2892
240 P10 = P20 MORSE 2893
245 CONTINUE MORSE 2894
IF(IGOR.EQ.-1) 265,255 RADAU 20
C RADAU 21
C CALCULATE RADAU MOMENTS RADAU 22

```

```

C
255 NMOM = NMOM-1
      DO 260 N=1,NMOM
260 XMOMNT(N) = XMOMNT(N)-XMOMNT(N+1)
      XMOMNT(NMOM+1) = 0.0
      IF(NMOM) 125,125,265
265 CONTINUE
C
C      CALCULATE COEFFICIENTS USED IN ORTHOGONAL POLYNOMIAL
C      RECURRENCE RELATION.  DEFINITIONS =
C      NM= NUMBER OF MU VALUES ACCEPTED
C      NV= NUMBER OF VAR VALUES ACCEPTED
C      NM= NV OR NV+1
C      NP= NUMBER OF ANGLES IN DISCRETE DISTRIBUTION
C      NACC=NUMBER OF MOMENTS ACCEPTED
C
      DO 10 K=1,NSCT
      WEIGHT(K) = 0.0
10   POINT(K) = 0.0
      CALL GETMUS
      IF(IMOM)20,20,15
15   WRITE(IOUT,1010)(XMOMNT(I),I=1,NMOM)
1010 FORMAT(9H MOMENTS ,4X,1P10E12.5/(1X,11E12.5))
C
C      FIND ABSCISSAS OF ORTHOGONAL POLYNOMIALS
C
20   IF(IGOR.EQ.-1) 25,23
23   IF(XMU(1).LT.F(1)) 25,125
25   ROOT(1,1)=XMU(1)
      IF(NM-1)40,40,30
30   DO 35 L=2,NM
      CALL FIND(L,NCK)
      IF(NCK)35,35,120
35   CONTINUE
40   IF(NM-NV)45,45,55
45   XMU(NV+1)=-VAR(NV)*(Q(NV-1,1.)/Q(NV,1.)+Q(NV-1,-1.)/Q(NV,-1.))/2.
      IF(IGOR.EQ.-1) 50,46
46   QK = Q(1,1,0)
      SUM = 1.0-(1.0-F(1))/QK
      IF(NV-1) 49,49,47
47   DO 48 K = 2,NV
      QKM1 = QK
      QK = Q(K,1,0)
48   SUM = SUM-XNORML(K)/(QKM1*QK)
49   XMU(NV+1) = XMU(NV+1)-XNORML(NV)/(QK*QK*SUM*2.0)
50   CALL FIND(NV+1,NCK)
      IF(NCK) 55,55,53
53   NV = NV-1
55   NP=NV+1
      NACC=NM+NV
      DO 60 K=1,NP
60   POINT(K)=ROOT(K,NP)
      IF(IGOR.EQ.-1) 62,81
C
C      CALCULATE GAUSS WEIGHTS
C
62   IF(NV) 65,65,70
65   WEIGHT(1) = 1.0

```

```

GO TO 91
70  DO 80 K=1,NP
      SUM = 1.0
      DO 75 L=1,NV
      SUM = SUM + (Q(L,POINT(K)))**2/XNORML(L)
80  WEIGHT(K) = 1.0/SUM
      GO TO 91
C
C      CALCULATE RADAU WEIGHTS
C
81  IF(NV) 82,82,83
82  WEIGHT(1) = (1.0-F(1))/(1.0-POINT(1))
      GO TO 86
83  DO 85 K=1,NP
      SUM = 1.0/(1.0-F(1))
      DO 84 L=1,NV
      SUM = SUM+(Q(L,POINT(K)))**2/XNORML(L)
      WEIGHT(K) = 1.0/(SUM*(1.0-POINT(K)))
85  CONTINUE
86  POINT(NP+1) = 1.0
      SUM = 0.0
      DO 87 K=1,NP
      SUM = SUM+WEIGHT(K)
      WEIGHT(NP+1) = 1.0-SUM
      NP = NP+1
      IF(WEIGHT(NP)) 88,91,91
88  IF(IPUN) 90,90,89
89  WRITE(IOUT,1040) IG1,MX
1040 FORMAT(/* NEGATIVE WEIGHT FOUND FOR TRANSFER NO. = *I3,
      1*      MATERIAL = *I3)
90  NV = (NP+NM-3)/2
      NM = NP+NM-3-NV
      IF(NM) 125,125,40
C
C      ARRANGE POINTS AND WEIGHTS IN ORDER OF DECREASING PROBABILITY
C
91  DO 100 K=1,NP
      BIG = WEIGHT(K)
      J = K
      DO 95 L=K,NP
      IF(WEIGHT(L)-BIG) 95,95,92
92  BIG = WEIGHT(L)
      J = L
95  CONTINUE
      WEIGHT(J) = WEIGHT(K)
      WEIGHT(K) = BIG
      SPOINT = POINT(K)
      POINT(K) = POINT(J)
100  POINT(J) = SPOINT
      IF(NACC-NMOM)105,115,115
105  IF(IPUN)115,115,110
110  CALL BADMOM
      WRITE(IOUT,1020)NACC,IG1,MX
1020 FORMAT(* NUMBER OF MOMENTS ACCEPTED = *I3,
      1*      TRANSFER NO. = *I3,
      2*      MATERIAL = *I3,
      3//38H *      *      *      *      *      *      *//)
115  IF(IGOR.EQ.1) 116,118
      RADAU      55
      RADAU      56
      RADAU      57
      RADAU      58
      MORSE     2929
      MORSE     2930
      RADAU      59
      RADAU      60
      RADAU      61
      RADAU      62
      RADAU      63
      RADAU      64
      RADAU      65
      RADAU      66
      RADAU      67
      RADAU      68
      RADAU      69
      RADAU      70
      RADAU      71
      RADAU      72
      RADAU      73
      RADAU      74
      RADAU      75
      RADAU      76
      RADAU      77
      RADAU      78
      RADAU      79
      RADAU      80
      RADAU      81
      RADAU      82
      RADAU      83
      RADAU      84
      RADAU      85
      RADAU      86
      RADAU      87
      RADAU      88
      RADAU      89
      MORSE     2932
      MORSE     2933
      MORSE     2934
      RADAU      90
      RADAU      91
      MORSE     2937
      MORSE     2938
      MORSE     2939
      MORSE     2940
      MORSE     2941
      MORSE     2942
      MORSE     2943
      MORSE     2944
      MORSE     2945
      MORSE     2946
      MORSE     2947
      MORSE     2948
      MORSE     2949
      MORSE     2950
      MORSE     2951
      RADAU      92

```

116	NV = NV+1	RADAU	93
	NMOM = NMOM+1	RADAU	94
118	RETURN	RADAU	95
120	NM=L-1	MORSE	2953
	NV=L-1	MORSE	2954
	GO TO 45	MORSE	2955
125	CONTINUE	MORSE	2956
	NM = 0	RADAU	96
	NV = 0	RADAU	97
	NP = 1	RADAU	98
	NACC = 0	RADAU	99
	POINT(1) = (F(1)-1.0)/2.0	RADAU	100
	GO TO 82	RADAU	101
	END	MORSE	2967

```

SUBROUTINE BADMOM                                MORSE 2968
  REAL MU,MOMENT,NORM,MUT,MUB,MOM,MOMT,MOMB,L    MORSE 2969
  COMMON/PERM/INN, IOUT                           MORSE 2970
  COMMON/MOMENT/NMOM,MOMENT(25),F(25)             MORSE 2971
  COMMON/MEANS/NN,N,MU(14),VAR(13),NORM(13)       MORSE 2972
  COMMON/QAL/QR(14),A(13,14),L(14)                MORSE 2973
  COMMON/RADAU/IGOR                             RADAU 102
  NM = N + NN                                     MORSE 2974
  NBAD = NM + 1                                   MORSE 2975
  NM1 = N - 1                                     MORSE 2976
  NP1 = N + 1                                     MORSE 2977
  WRITE(IOUT,1010)NBAD                           MORSE 2978
1010 FORMAT(14H0-----MOMENT(,I2,28H) IS BAD, OUTPUT FROM BADMOM) MORSE 2979
  IF(IGOR.EQ.1) GO TO 100                         RADAU 103
  IF(N)25,10,25                                     MORSE 2980
10  IF(NN)20,15,20                                   MORSE 2981
15  MUT = 1.                                       MORSE 2982
  MUB = -1.                                       MORSE 2983
  MU(1) = MOMENT(1)                                MORSE 2984
  MOMT = 1.                                       MORSE 2985
  MOMB = -1.                                       MORSE 2986
  GO TO 40                                         MORSE 2987
20  VART = 2. / (1./Q(1,1.) - 1./Q(1,-1.))      MORSE 2988
  VARB = 0.                                         MORSE 2989
  MOMB = MOMENT(1)**2                            MORSE 2990
  MOMT = MOMB + VART                            MORSE 2991
  GO TO 55                                         MORSE 2992
25  IF(N-NN)45,30,45                            MORSE 2993
30  MUT = 1. - VAR(N)*Q(NM1,1.)/Q(N,1.)        MORSE 2994
C   THE 2N+1 MOMENT IS BAD                      MORSE 2995
  MUB = -1. - VAR(N)*Q(NM1,-1.)/Q(N,-1.)       MORSE 2996
  MU(NP1) = QR(NP1) - QR(N)                      MORSE 2997
  MOM = NORM(N) * QR(N)                          MORSE 2998
  DO 35 K=1,N                                     MORSE 2999
35  MOM = MOM - A(N,K) * MOMENT(N+K)            MORSE 3000
  MOMT = MOM + NORM(N) * MUT                     MORSE 3001
  MOMB = MOM + NORM(N) * MUB                     MORSE 3002
C   READY TO OUTPUT MOMB,MOMENT(NBAD),MOMT,MUB,MU(NP1),MUT      MORSE 3003
40  WRITE(IOUT,1020)MUB,NP1,MU(NP1),MUT          MORSE 3004
1020 FORMAT(9H MUBOT =,F15.9,5H MU(,I2, 4H) = ,F14.9,9H MUTOP =,F16.  MORSE 3005
19)
  GOTO 60                                         MORSE 3006
45  VART = 2. / (Q(N,1.)/Q(NP1,1.) - Q(N,-1.)/Q(NP1,-1.)) MORSE 3007
C   NBAD IS 2N+2, VAR(N+1) IS BAD                MORSE 3008
  MOMB = 0.                                         MORSE 3009
  VARB = 0.                                         MORSE 3010
  DO 50 K=1,NP1                                    MORSE 3011
50  MOMB = MOMB - A(NP1,K) * MOMENT(N+K)        MORSE 3012
  MOMT = MOMB + VART * NORM(N)                   MORSE 3013
C   READY TO OUTPUT MOMB,MOMENT(NBAD),MOMT,VAR(NP1),VART      MORSE 3014
55  WRITE(IOUT,1030)VARB,NP1,VAR(NP1),VART        MORSE 3015
1030 FORMAT( 9H VARBOT =,F15.9,5H VAR(,I2,3H) = ,F15.9,10H VARTOP = ,F15  MORSE 3016
1.9)
60  MOM = MOMENT(NBAD)                           MORSE 3017
  FA = F(NBAD)                                     MORSE 3018
  MOMENT (NBAD) = MOMT                           MORSE 3019
  CALL MAMENT (NBAD)                           MORSE 3020
  FT = F(NBAD)                                     MORSE 3021
                                         MORSE 3022
                                         MORSE 3023

```

```

MOMENT(NBAD) = MOMB          MORSE 3024
CALL MAMENT (NBAD)          MORSE 3025
FB = F(NBAD)                MORSE 3026
MOMENT(NBAD) = MOM          MORSE 3027
F(NBAD) = FA                RADAU 104
IF(IGOR.EQ.-1) 64,62        RADAU 105
62  FA = F(NBAD+1)          RADAU 106
C1 = NBAD                  RADAU 107
C2 = C1+1.0                RADAU 108
C3 = 2.0*C1+1.0            RADAU 109
FZERO = 1.0                 RADAU 110
IF(NBAD.NE.1) FZERO=F(NBAD-1) RADAU 111
FUN = F(NBAD)-C1*FZERO/C3  RADAU 112
C4 = C3*(FUN-FT)/C2        RADAU 113
C5 = C3*(FUN-FB)/C2        RADAU 114
FB = C4                    RADAU 115
FT = C5                    RADAU 116
64  IF(MOM-MOMT) 70,70,65    RADAU 117
65  DELM = MOM - MOMT      MORSE 3029
DELF = FA - FT            MORSE 3030
IF(IGOR.EQ.1) DELF = FA-FB RADAU
GO TO 75                  MORSE 3031
70  DELM = MOM - MOMB      MORSE 3032
DELF = FA - FB            MORSE 3033
IF(IGOR.EQ.1) DELF = FA-FT RADAU
75  RANGEM = MOMT - MOMB   MORSE 3034
RANGEF = FT - FB          MORSE 3035
C  NOW READY TO OUTPUT FB,FA,FT          MORSE 3036
      WRITE(IOUT,1040)MOMB,NBAD,MOMENT(NBAD),MOMT,RANGEM,DELM  MORSE 3037
1040 FORMAT( 9H MOMBOT =,F15.9,5H MOM(,I2,3H) =,F15.9,10H MOMTOP = ,F15 MORSE 3038
1.9,5X,8HRANGE = ,F9.6,11H  ERROR = ,F9.6)          MORSE 3039
IF(IGOR.EQ.1) NBAD=NBAD+1          RADAU 118
      WRITE(IOUT,1050)FB,NBAD,FA,FT,RANGEF,DELF  MORSE 3040
1050 FORMAT( 9H FBOT =,F15.9,5H F(,I2,3H) =,F15.9,9H  FTOP = ,F16. MORSE 3041
19,5X,8HRANGE = ,F9.6,11H  ERROR = ,F9.6)          MORSE 3042
      RETURN          MORSE 3043
C  CALCULATE UPPER AND LOWER BOUNDARIES FOR RADAU QUADRATURE RADAU 119
100  IF(N) 125,110,125          RADAU 120
110  IF(NN) 120,115,120          RADAU 121
C  THE FIRST MOMENT IS BAD          RADAU 122
115  MUT = F(1)                RADAU 123
MUB = -1.0                  RADAU 124
MU(1) = QR(1)                RADAU 125
MOMT = (1.0-F(1))*F(1)        RADAU 126
MOMB = F(1)-1.0              RADAU 127
GO TO 40                    RADAU 128
C  THE SECOND MOMENT IS BAD          RADAU 129
120  QI = Q(1,1.0)              RADAU 130
ADD = (1.0-F(1))/(QI*QI*(1.0-(1.0-F(1))/QI))          RADAU 131
VART = (2.0)/(ADD+1.0/QI-1.0/Q(1,-1.0))          RADAU 132
VARB = 0.0                  RADAU 133
MOMB = QR(1)*MOMENT(1)        RADAU 134
MOMT = MOMB+VART*(1.0-F(1))          RADAU 135
GO TO 55                    RADAU 136
125  IF(N-NN) 145,130,145          RADAU 137
C  THE 2N+1 MOMENT IS BAD          RADAU 138
130  MUB = -1.0-VAR(N)*Q(NM1,-1.0)/Q(N,-1.0)          RADAU 139
QIM1 = 1.0                  RADAU

```

132	QI = Q(1,1.0)	RADAU	140
	SUM = 1.0-(1.0-F(1))/QI	RADAU	141
	IF(N-1) 134,134,132	RADAU	142
	DO 133 I = 2,N	RADAU	143
	QIM1 = QI	RADAU	144
	QI = Q(I,1.0)	RADAU	145
133	SUM = SUM-NORM(I-1)/(QIM1*QI)	RADAU	146
134	MUT = 1.0-VAR(N)*QIM1/QI-NORM(N)/(QI*QI*SUM)	RADAU	147
	MU(NP1) = QR(NP1)-QR(N)	RADAU	148
	MOM = NORM(N)*QR(N)	RADAU	149
	DO 135 K = 1,N	RADAU	150
135	MOM = MOM-A(N,K)*MOMENT(N+K)	RADAU	151
	MOMT = MOM+NORM(N)*MUT	RADAU	152
	MOMB = MOM+NORM(N)*MUB	RADAU	153
	GO TO 40	RADAU	154
C	THE 2N+2 MOMENT IS BAD	RADAU	155
145	QI = Q(1,1.0)	RADAU	156
	SUM = 1.0-(1.0-F(1))/QI	RADAU	157
	DO 146 I = 2,NP1	RADAU	158
	QIM1 = QI	RADAU	159
	QI = Q(I,1.0)	RADAU	160
146	SUM = SUM-NORM(I-1)/(QIM1*QI)	RADAU	161
	SUM = NORM(N)/(QI*QI*SUM)	RADAU	162
	VART = (2.0)/(SUM+Q(N,1.0)/Q(NP1,1.0)-Q(N,-1.0)/Q(NP1,-1.0))	RADAU	163
	VARB = 0.0	RADAU	164
	MOMB = 0.0	RADAU	165
	DO 150 K = 1,NP1	RADAU	166
150	MOMB = MOMB-A(NP1,K)*MOMENT(N+K)	RADAU	167
	MOMT = MOMB+VART*NORM(N)	RADAU	168
	GO TO 55	RADAU	169
	END	MORSE	3044

```

SUBROUTINE FIND(L,NF)                                MORSE 3045
COMMON/INPUT/LADJM,NSTRT,NMOST,NITS,NQUIT,ISTAT,NSPLT,NKILL,IR8,  MORSE 3046
1 IRRA,NPAST,NOLEAK,IEBLAS,NKCALC,NORMF,             MORSE 3047
2 MEDIA,NMIX,MEDALB,MXREG,MFISTP,NNGA,NGGA,NCOEF,NSCT,MAXGP,IRDG, MORSE 3048
3 ISTR,IFMU,IMOM,IPRIN,IPUN,                      MORSE 3049
5 ISOUR,NGPFS,ISBIAS,NSOUR,                      MORSE 3050
6 ND,NNE,NE,NT,NA,NRESP,NEX,NEXND,IFLAG(16),        MORSE 3051
7 TMAX,TCUT,WSTRT,AGSRT,XSTR,YSTRT,ZSTR,UINP,VINP,WINP,ROMC,  MORSE 3052
8 IXTAPE,NG,IFTG,IGG,NNUC,IDL,NRP,N1M,N2M,NSGPS,TITLE(20),DAT,JFTG, MORSE 3053
9 KFTG,LFTG                                         MORSE 3054
COMMON/PERM/INN,IOUT                                MORSE 3055
COMMON/RESULT/POINT(14),WEIGHT(14),ROOT(14,14)      MORSE 3056
DIMENSION VALUE(13)                                MORSE 3057
LM1 = L - 1                                         MORSE 3058
DO 10 I=1,LM1                                         MORSE 3059
10 VALUE(I) = Q(L,ROOT(I,LM1))                      MORSE 3060
ROOT(L,LM1) = 1.0                                     MORSE 3061
QTOP = Q(L,1.0)                                      MORSE 3062
IF(QTOP)15,15,30                                     MORSE 3063
15 IF(IPUN)25,25,20                                   MORSE 3064
20 WRITE(IOUT,1010)L                                 MORSE 3065
1010 FORMAT(11H0-----FIND,/12H ROOTS OF Q(,I2,18H) EXTEND BEYOND +1) MORSE 3066
25 NF=1                                              MORSE 3067
RETURN                                              MORSE 3068
30 XLOW = -1.                                         MORSE 3069
QLOW = Q(L,-1.)                                     MORSE 3070
IF(QLOW*VALUE(1))50,50,35                           MORSE 3071
35 IF(IPUN)45,45,40                                   MORSE 3072
40 WRITE(IOUT,1020)L                                 MORSE 3073
1020 FORMAT(11H0-----FIND,/12H ROOTS OF Q(,I2,18H) EXTEND BEYOND -1) MORSE 3074
45 NF=1                                              MORSE 3075
RETURN                                              MORSE 3076
50 DO 85 K=1,L                                       MORSE 3077
XUP = ROOT(K,LM1)                                    MORSE 3078
NSP=0                                              MORSE 3079
55 NSP=NSP+1                                         MORSE 3080
XTRY = ( XLOW + XUP )*0.5                           MORSE 3081
QTRY = Q(L,XTRY)                                     MORSE 3082
IF(QTRY*QLOW)65,80,60                               MORSE 3083
60 XLOW = XTRY                                         MORSE 3084
QLOW = QTRY                                         MORSE 3085
GO TO 70                                           MORSE 3086
65 XUP = XTRY                                         MORSE 3087
70 IF(XUP-XLOW)75,80,75                           MORSE 3088
75 IF(NSP-48) 55,80,80                           MORSE 3089
80 ROOT(K,L) = XTRY                                 MORSE 3090
XLOW = ROOT(K,LM1)                                    MORSE 3091
85 QLOW = VALUE(K)                                    MORSE 3092
ROOT(L,LM1) = 0.0                                     MORSE 3093
NF = 0                                              MORSE 3094
RETURN                                              MORSE 3095
END                                                 MORSE 3096

```

```

SUBROUTINE GETMUS                                MORSE 3268
COMMON/INPUT/IADJM,NSTRRT,NMOST,NITS,NQUIT,ISTAT,NSPLT,NKILL,IR8,  MORSE 3269
1  IRRA,NPAST,NOLEAK,IEBIAS,NKCALC,NORMF,      MORSE 3270
2  MEDIA,NMIX,MEDALB,MXREG,MFISTP,NNGA,NGGA,NCOEF,NSCT,MAXGP,IRDSG, MORSE 3271
3  ISTR,IFMU,IMOM,IPRIN,IPUN,                  MORSE 3272
5  ISOUR,NGPFS,ISBIAS,NSOUR,                  MORSE 3273
6  ND,NNE,NE,NT,NA,NRESP,NEX,NEXND,IFLAG(16),  MORSE 3274
7  TMAX,TCUT,WTSTRT,AGSTRT,XSTRT,YSTRT,ZSTRT,UINP,VINP,WINP,ROMC, MORSE 3275
8  IXTAPE,NG,IFTG,IGG,NNUC,IDL,NRP,N1M,N2M,NSGPS,TITLE(20),DAT,JFTG, MORSE 3276
9  KFTG,LFTG,                                MORSE 3277
COMMON/PERM/INN,IOUT,                            MORSE 3278
COMMON/MOMENT/NMOM,MOMENT(25),F(25)            MORSE 3279
COMMON/MEANS/NM,NV,MU(14),SIG(13),NORM(13)    MORSE 3280
COMMON/QAL/Q(14),A(13,14),L(14)                MORSE 3281
COMMON/RADAU/IGOR,                            RADAU 170
REAL MOMENT,L,MU,NORM,                          MORSE 3282
NV=NMOM/2,                                      MORSE 3283
NM=NMOM-NV,                                      MORSE 3284
C   INITIALIZE VARIABLES TO ZERO,                RADAU 171
DO 10 I=1,NV,                                  MORSE 3285
MU(I) = 0.0,                                     MORSE 3286
SIG(I) = 0.0,                                     MORSE 3287
NORM(I) = 0.0,                                    MORSE 3288
L(I) = 0.0,                                      MORSE 3289
Q(I) = 0.0,                                      MORSE 3290
DO 10 K=1,NM,                                  MORSE 3291
A(I,K) = 0.0,                                     MORSE 3292
L(NM)=0.,                                         MORSE 3293
Q(NM)=0.,                                         MORSE 3294
MU(NM)=0.0,                                       MORSE 3295
IF(IGOR.EQ.-1) 12,21,                            RADAU 172
C   START CALCULATING COEFFICIENTS FOR GAUSS QUADRATURE, RADAU 173
12  MU(1) = MOMENT(1),                           RADAU 174
Q(1) = MOMENT(1),                               MORSE 3297
L(1) = MOMENT(1),                               MORSE 3298
A(1,1) = -MOMENT(1),                           MORSE 3299
A(1,2) = 1.0,                                    MORSE 3300
SIG(1) = MOMENT(2) - MOMENT(1)**2,             MORSE 3301
NORM(1) = SIG(1),                               MORSE 3302
IF(SIG(1))85,85,15,                            MORSE 3303
15  IF(NV-1)55,55,20,                            MORSE 3304
20  L(2) = MOMENT(3) - MOMENT(1)*MOMENT(2),    MORSE 3305
Q(2) = L(2)/NORM(1),                           MORSE 3306
MU(2) = Q(2) - Q(1),                           MORSE 3307
A(2,3) = 1.,                                    MORSE 3308
A(2,2) = -Q(2),                                MORSE 3309
A(2,1) = (MOMENT(1)*MOMENT(3)-MOMENT(2)**2)/SIG(1), MORSE 3310
GO TO 24,                                         RADAU 175
C   START CALCULATING COEFFICIENTS FOR RADAU QUADRATURE, RADAU 176
21  L(1) = MOMENT(1),                           RADAU 177
Q(1) = MOMENT(1)/(1.0-F(1)),                  RADAU 178
MU(1) = Q(1),                                    RADAU 179
A(1,1) = -Q(1),                                RADAU 180
A(1,2) = 1.0,                                    RADAU 181
NORM(1) = -Q(1)*MOMENT(1)+MOMENT(2),          RADAU 182
SIG(1) = NORM(1)/(1.0-F(1)),                  RADAU 183
IF(SIG(1)) 85,85,22,                           RADAU 184
22  IF(NV-1) 55,55,23,                           RADAU 185

```

```

23  L(2) = -Q(1)*MOMENT(2)+MOMENT(3)          RADAU 186
    Q(2) = L(2)/NORM(1)                      RADAU 187
    MU(2) = Q(2)-Q(1)                      RADAU 188
    A(2,1) = MU(2)*Q(1)-SIG(1)          RADAU 189
    A(2,2) = -Q(2)                      RADAU 190
    A(2,3) = 1.0                      RADAU 191
24  NORM(2) = MOMENT(4)+A(2,2)*MOMENT(3)+A(2,1)*MOMENT(2)  RADAU 192
    SIG(2) = NORM(2)/NORM(1)          MORSE 3312
    IF(SIG(2))90,90,25          MORSE 3313
25  IF(NV-2)55,55,30          MORSE 3314
30  DO 50 I=3,NV          MORSE 3315
    IM1 = I - 1          MORSE 3316
    IP1 = I + 1          MORSE 3317
    DO 35 K=1,I          MORSE 3318
35  L(I) = L(I) + A(IM1,K)*MOMENT(IM1+K)          MORSE 3319
    Q(I) = L(I)/NORM(IM1)          MORSE 3320
    MU(I) = Q(I) - Q(IM1)          MORSE 3321
    A(I,IP1) = 1.0          MORSE 3322
    A(I,I) = -Q(I)          MORSE 3323
    DO 40 K=2,IM1          MORSE 3324
40  A(I,K) = A(IM1,K-1) - MU(I)*A(IM1,K) - SIG(IM1)*A(I-2,K)  MORSE 3325
    A(I,1) = -MU(I)*A(IM1,1) - SIG(IM1)*A(I-2,1)  MORSE 3326
    DO 45 K=1,IP1          MORSE 3327
45  NORM(I) = NORM(I) + A(I,K)*MOMENT(IM1+K)          MORSE 3328
    SIG(I) = NORM(I)/NORM(IM1)          MORSE 3329
    IF(SIG(I))95,95,50          MORSE 3330
50  CONTINUE          MORSE 3331
55  IF(NM-NV)75,75,60          MORSE 3332
60  IF(NV)75,75,65          MORSE 3333
65  DO 70 K=1,NM          MORSE 3334
70  L(NM)=L(NM)+A(NV,K)*MOMENT(NV+K)          MORSE 3335
    Q(NM)=L(NM)/NORM(NV)          MORSE 3336
    MU(NM)=Q(NM)-Q(NV)          MORSE 3337
75  IF(IFMU)105,80,105          MORSE 3338
80  RETURN          MORSE 3339
85  I = 1          MORSE 3340
    GO TO 95          MORSE 3341
90  I = 2          MORSE 3342
95  NM=I          MORSE 3343
    NV=I-1          MORSE 3344
    IF(IPUN)120,120,100          MORSE 3345
100  WRITE(IOUT,1030)I          MORSE 3346
105  WRITE(IOUT,1010)(MU(I),SIG(I),NORM(I),L(I),Q(I),I=1,NV)  MORSE 3347
    WRITE(IOUT,1040)MU(NM),L(NM),Q(NM)          MORSE 3348
1040  FORMAT(1PE24.5,48X2E24.5)          MORSE 3349
    IF(NV)120,120,110          MORSE 3350
110  DO 115 I=1,NV          MORSE 3351
    IP1 = I + 1          MORSE 3352
115  WRITE(IOUT,1020)I,(A(I,K),K=1,IP1)          MORSE 3353
120  RETURN          MORSE 3354
1010  FORMAT(/* INTERMEDIATE RESULTS OF MEANS CALCULATION*/13X, 4HMEA MORSE 3355
    1N,19X,8HVARIANCE,16X,13HNORMALIZATION,12X,1HL,23X,1HQ/(1P5E24.5)) MORSE 3356
1020  FORMAT(* COEFFICIENTS OF ORTHOGONAL POLYNOMIALS, I, A(I,K)/I5,10X MORSE 3357
    11P7E15.5/(8E15.5))          MORSE 3358
1030  FORMAT(13H0-----GETMUS/10H VARIANCE(,I2, 22H) IS NEGATIVE OR ZERO MORSE 3359
    1.)          MORSE 3360
    END          MORSE 3361

```

```

SUBROUTINE MAMENT(NMO)                                MORSE 3592
COMMON/MOMENT/NMOM,XMOMNT(25),F(25)                MORSE 3593
COMMON/RADAU/IGOR                                 RADAU
DIMENSION P0(25), P1(25), P2(25)                  MORSE 3594
DO 10 I=1,NMO                                     MORSE 3595
P1(I)=0.                                         MORSE 3596
10  P0(I)=0.                                     MORSE 3597
P00=1.                                         MORSE 3598
P1(1)=1.                                         MORSE 3599
P10=0.                                         MORSE 3600
IF(NMO.EQ.1) F(1) = XMOMNT(1)                      RADAU
IF(NMO-2)40,15,15                                 MORSE 3602
15  DO 35 L=2,NMO                                MORSE 3603
FL=L
P20=-(FL-1.)/FL*P00                               MORSE 3604
P2(1)=(2*FL-1.)/FL*P10-(FL-1.)/FL*P0(1)          MORSE 3605
DO 20 N=2,L                                     MORSE 3606
20  P2(N)=(2*FL-1)/FL*P1(N-1)-(FL-1)/FL*P0(N)    MORSE 3607
DO 30 I=1,L                                     MORSE 3608
P0(I)=P1(I)                                     MORSE 3612
30  P1(I)=P2(I)                                MORSE 3613
P00=P10                                         MORSE 3614
35  P10=P20                                     MORSE 3615
F(NMO) = P10                                     MORSE 3616
IF(IGOR.EQ.1) F(NMO) = P10*(1.-F(1))            RADAU
DO 37 M=1,NMO                                RADAU
37  F(NMO) = F(NMO)+P2(M)*XMOMNT(M)            RADAU
40  RETURN                                     MORSE 3617
END                                         MORSE 3618

```

FUNCTION Q(ND,X)	MORSE	3619
COMMON/MEANS/NM,NV,XMU(14),VAR(13),XNORML(13)	MORSE	3620
A = 1	MORSE	3621
B = X-XMU(1)	MORSE	3622
IF(ND-1)25,20,10	MORSE	3623
10 DO 15 I=2,ND	MORSE	3624
C = ((X-XMU(I))*B ) - VAR(I-1)*A	MORSE	3625
A = B	MORSE	3626
15 B = C	MORSE	3627
20 Q = B	MORSE	3628
RETURN	MORSE	3629
25 Q = A	MORSE	3630
RETURN	MORSE	3631
END	MORSE	3632

```

SUBROUTINE XSEC5(NRD,NR,MWA,SIGN,L1,L2,L3,L4,L5,L8      MORSE 5120
* ,SIGNG,SI GG,NSGL,NSGN,NRE,NMTG,L10,KD1,KD2,KD3)      MORSE 5121
C TO CONVERT CROSS SECTIONS ON DISK 8 TO ANGLES AND PROBABILITIES MORSE 5122
C AND PUT THE RESULTS ON DISK 9      MORSE 5123
C L1=MAX OF N1M OR N2M      MORSE 5124
C L2=MAX OF NCOEF OR (2*NSCT+1)      MORSE 5125
C L3=MEDIA      MORSE 5126
C L4=NNGA+NGGA      MORSE 5127
C L5=NSGPS, NO OF SUPERGROUPS      MORSE 5128
C NRD IS TO CONTAIN POINTERS TO FINAL CROSS SECTIONS STORED ON DISK9 MORSE 5129
C L8=3+4*NSCT+2*NPL      MORSE 5130
C NSGN GIVES SUPERGROUP NUMBER OF EACH GROUP      MORSE 5131
C NSGL GIVES GROUP LIMITS OF EACH SUPERGROUP      MORSE 5132
COMMON/PERM/INN, IOUT      MORSE 5133
COMMON/MOMENT/NMOM, XMOMNT(25), F(25)      MORSE 5134
COMMON/RESULT/POINT(14), WEIGHT(14), ROOT(14,14)      MORSE 5135
COMMON/MEANS/ITEST, NANS, MEAN(14), VAR(13), NORMAL(13)      MORSE 5136
COMMON/INPUT/IADJM, NSTRT, NMOST, NITS, NQUIT, ISTAT, NSPLT, NKILL, IR8,      MORSE 5137
1 ITRA, NPAST, NOLEAK, IEBIAS, NKCALC, NORMF,      MORSE 5138
2 MEDIA, NMIX, MEDALB, MXREG, MFISTP, NNGA, NGGA, NCOEF, NSCT, MAXGP, IRDSG,      MORSE 5139
3 ISTR, IFMU, IMOM, IPRIN, IPUN,      MORSE 5140
5 ISOUR, NGPFS, IEBIAS, NSOUR,      MORSE 5141
6 ND, NNE, NE, NT, NA, NRESP, NEX, NEXND, IFLAG(16),      MORSE 5142
7 TMAX, TCUT, WTSTR, AGSTR, XSTR, YSTR, ZSTR, UINP, VINP, WINP, ROMC,      MORSE 5143
8 IXTAPE, NG, IFTG, IGG, NNUC, IDT, NRP, N1M, N2M, NSGPS, TITLE(20), DAT, JFTG,      MORSE 5144
9 KFTG, LFTG      MORSE 5145
COMMON/DRTACS/NR8, NR9, NR10      MORSE 5146
COMMON/RADAU/IGOR      RADAU 193
DIMENSION NR(1), MWA(L4,L3), SIGN(L1,L2), NRD(L8,L3,L5)      MORSE 5147
DIMENSION SIGNG(KD1,KD2), SI GG(L1,L2), NSGL(L5,2), NSGN(NMTG),      MORSE 5148
* NRE(L10, KD3, L5)      MORSE 5149
LEVEL 2, NRD, NR, MWA, SIGN, SIGNG, SI GG, NSGL, NSGN, NRE      MORSE 5150
C KD1=NNGA      MORSE 5151
C KD2=NGGA      MORSE 5152
C KD3=MEDIA      MORSE 5153
DO 90 I=1,25      MORSE 5155
XMOMNT(I)=0.0      MORSE 5156
90 F(I)=0.0      MORSE 5157
NR9=1      MORSE 5158
NPL=NCOEF-1      MORSE 5159
DO 110 J=1, MEDIA      MORSE 5160
IF(NNGA.LE.0)GO TO 109      MORSE 5161
IF(NGGA.LE.0)GO TO 601      MORSE 5162
IRP=2+NPL+(J-1)*(3+2*NPL)      MORSE 5163
NR8=NR(IRP)      MORSE 5164
N=NNGA*NGGA      MORSE 5165
CALL REED(SIGNG, N, 8)      MORSE 5166
M2=NSGN(NNGA)      MORSE 5167
M1=NSGN(1)      MORSE 5168
DO 116 L6=M1, M2      MORSE 5169
N2=NSGL(L6, 2)      MORSE 5170
IF(N2.GT.NNGA)N2=NNGA      MORSE 5171
N1=NSGL(L6, 1)      MORSE 5172
LZ=(N2-N1+1)*NGGA      MORSE 5173
NRD(2+2*NSCT+NPL, J, L6)=NR9      MORSE 5174
116 CALL RITE(SIGNG(1, N1), LZ, 9)      MORSE 5175
IF(ISTR.LE.0)GO TO 601      MORSE 5176
WRITE(IOUT, 26)J      MORSE 5177

```

```

26  FORMAT(1H1,* NEUTRON TO GAMMA PROBABILITIES FOR MATERIAL NUMBER*I5 MORSE 5178
1/
DO 600 I=1,NNGA MORSE 5179
WRITE(IOUT,30)I MORSE 5180
30  FORMAT(6H GROUP,I5,3X9HSIGMA N-G) MORSE 5181
600 WRITE(IOUT,21)(SIGNG(K,I),K=1,NGGA) MORSE 5182
601 CONTINUE MORSE 5183
      M2=NSGN(NNGA) MORSE 5184
      M1=NSGN(1) MORSE 5185
      DO 500 L6=M1,M2 MORSE 5186
      N2=NSGL(L6,2) MORSE 5187
      IF(N2.GT.NNGA)N2=NNGA MORSE 5188
      N1=NSGL(L6,1) MORSE 5189
      N3=MWA(N1-1,J)+1 MORSE 5190
      IF(N1.EQ.1)N3=1 MORSE 5191
      N4=MWA(N2,J) MORSE 5192
      LZ=N4-N3+1 MORSE 5193
      NSKIP=N3-1 MORSE 5194
      DO 100 K=1,NCOEF MORSE 5195
      NR10=NRE(K,J,L6) MORSE 5196
100  CALL REED(SIGN(1,K),LZ,10) MORSE 5197
      IF(NCOEF.LE.1)GO TO 131 MORSE 5198
      DO 512 I=1,LZ MORSE 5199
      DO 511 K=2,NCOEF MORSE 5200
      IF(SIGN(I,1).NE.0.0)GO TO 521 MORSE 5201
      SIGN(I,K)=0.0 MORSE 5202
      GO TO 522 MORSE 5203
      SIGN(I,K)=SIGN(I,K)/SIGN(I,1) MORSE 5204
522  L=K-1 MORSE 5205
511  CONTINUE MORSE 5206
512  CONTINUE MORSE 5207
      IF(NPL.LE.0)GO TO 131 MORSE 5208
      IF(ISTAT.LE.0)GO TO 131 MORSE 5209
      DO 403 K=1,NPL MORSE 5210
      NRD(1+2*NSCT+K,J,L6)=NR9 MORSE 5211
403  CALL RITE(SIGN(1,K+1),LZ,9) MORSE 5212
      IF(ISTR.LE.0)GO TO 131 MORSE 5213
      WRITE(IOUT,25)J MORSE 5214
      MORSE 5215
25  FORMAT(1H1,* LEGENDRE COEFFICIENTS FOR MATERIAL NUMBER*I5/) MORSE 5216
      DO 502 K=1,NPL MORSE 5217
      DO 503 I=N1,N2 MORSE 5218
      WRITE(IOUT,22)K,I MORSE 5219
      LZ1=MWA(I-1,J)+1 MORSE 5220
      IF(I.EQ.1)LZ1=1 MORSE 5221
      LZ2=MWA(I,J) MORSE 5222
      LZ1=LZ1-NSKIP MORSE 5223
      LZ2=LZ2-NSKIP MORSE 5224
503  WRITE(IOUT,21)(SIGN(L,K+1),L=LZ1,LZ2) MORSE 5225
502  CONTINUE MORSE 5226
22  FORMAT(4H PL=,I5,3X6HGROUP=,I5,9H    PCOEFN) MORSE 5227
131  CONTINUE MORSE 5228
C   SET FLAGS FOR GAUSS OR RADAU QUADRATURE
IGOR = 1 RADAU 194
IF(NSCT.EQ.1) GO TO 320 RADAU 195
IF(IGOR) 320,300,330 RADAU 196
300  K = MOD(NPL,2) RADAU 197
      IF(K) 320,310,320 RADAU 198
310  IF(2*NSCT-1-NPL) 320,320,330 RADAU 199
                                RADAU 200

```

320	IGOR = -1	RADAU	201
	NMOM = 2*NSCT-1	RADAU	202
	WRITE(IOUT,1000)	RADAU	203
1000	FORMAT(/* POINTS AND WEIGHTS OBTAINED BY GAUSS QUADRATURE */)	RADAU	204
	GO TO 340	RADAU	205
330	IGOR = 1	RADAU	206
	NMOM = 2*NSCT-2	RADAU	207
	WRITE(IOUT,1010)	RADAU	208
1010	FORMAT(/* POINTS AND WEIGHTS OBTAINED BY RADAU QUADRATURE */)	RADAU	209
340	IF(NPL.LT.NMOM) NMOM=NPL	RADAU	210
	NC=2*NSCT+1	MORSE	5231
	IF(NCOEF.GT.NC)NC=NCOEF	MORSE	5232
	DO 102 I=1,LZ	MORSE	5233
	IF(NSCT.LE.0)GO TO 102	MORSE	5234
	IF(NCOEF.LE.1)GO TO 104	MORSE	5235
	DO 101 K=2,NCOEF	MORSE	5236
	L=K-1	MORSE	5237
101	F(L)=SIGN(I,K)/(2*K-1)	MORSE	5238
	DO 117 K=2,NC	MORSE	5239
117	SIGN(I,K)=0.0	MORSE	5240
	DO 115 L=1,NMOM	MORSE	5241
	IF(F(L).NE.0)GO TO 114	MORSE	5242
115	CONTINUE	MORSE	5243
104	SIGN(I,2+NSCT)=-1.	MORSE	5244
	GO TO 102	MORSE	5245
114	CALL ANGLES(I,J)	RADAU	211
	SIGN(I,2)=POINT(1)	MORSE	5247
	SIGN(I,2+NSCT)=WEIGHT(1)	MORSE	5248
	IF(NANS.EQ.0)GO TO 108	MORSE	5249
	DO 105 K=1,NANS	MORSE	5250
	SIGN(I,2+K)=POINT(1+K)	MORSE	5251
105	SIGN(I,2+NSCT+K)=SIGN(I,1+NSCT+K)+WEIGHT(1+K)	MORSE	5252
108	C=SIGN(I,2+NSCT+NANS)	MORSE	5253
	NP1=NANS+1	MORSE	5254
	DO 106 K=1,NP1	MORSE	5255
	INDX=1+NSCT+K	MORSE	5256
106	SIGN(I,INDX)=SIGN(I,INDX)/C	MORSE	5257
102	CONTINUE	MORSE	5258
C	TO NORMALIZE THE NEUTRON P-ZERO MATRIX	MORSE	5259
	DO 120 K=N1,N2	MORSE	5260
	IND1=MWA(K-1,J)+2-N3+1	MORSE	5261
	IF(K.EQ.1)IND1=2	MORSE	5262
	IND2=MWA(K,J)-N3+1	MORSE	5263
	SUM=SIGN(IND1-1,1)	MORSE	5264
	IF(IND2.LT.IND1)GO TO 122	MORSE	5265
	DO 121 I=IND1,IND2	MORSE	5266
	SUM=SUM+SIGN(I,1)	MORSE	5267
121	CONTINUE	MORSE	5268
122	IND1=IND1-1	MORSE	5269
	DO 123 I=IND1,IND2	MORSE	5270
123	SIGN(I,1)=SIGN(I,1)/SUM	MORSE	5271
120	CONTINUE	MORSE	5272
	NRD(1,J,L6)=NR9	MORSE	5273
	CALL RITE(SIGN(1,1),LZ,9)	MORSE	5274
	IF(NSCT.LE.0)GO TO 404	MORSE	5275
	DO 401 K=1,NSCT	MORSE	5276
	NRD(1+K,J,L6)=NR9	MORSE	5277
401	CALL RITE(SIGN( 1,K+1),LZ,9)	MORSE	5278

DO 402 K=1,NSCT	MORSE	5279
NRD(1+NSCT+K,J,L6)=NR9	MORSE	5280
402 CALL RITE(SIGN( 1,K+1+NSCT),LZ,9)	MORSE	5281
404 IF((IPRIN.LE.0).AND.(ISTR.LE.0))GO TO 500	MORSE	5282
IF(ISTR.LE.0)GO TO 550	MORSE	5283
PRINT 46	MORSE	5284
46 FORMAT(1H1)	MORSE	5285
WRITE(IOUT,15)J	MORSE	5286
15 FORMAT(1H0,* 2-D CROSS SECTIONS FOR MATERIAL NUMBER*I5/)	MORSE	5287
DO 501 I=N1,N2	MORSE	5288
WRITE(IOUT,20)I	MORSE	5289
LZ1=MWA(I-1,J)+1	MORSE	5290
IF(I.EQ.1)LZ1=1	MORSE	5291
LZ2=MWA(I,J)	MORSE	5292
LZ1=LZ1-NSKIP	MORSE	5293
LZ2=LZ2-NSKIP	MORSE	5294
501 WRITE(IOUT,21)(SIGN(K,1),K=LZ1,LZ2)	MORSE	5295
20 FORMAT(1X, 5HGROUP,I5,3X, 9HSIGMA N-N)	MORSE	5296
21 FORMAT(1X1P8E14.4)	MORSE	5297
550 IF(IPRIN.LE.0)GO TO 500	MORSE	5298
IF(NSCT.LE.0)GO TO 500	MORSE	5299
WRITE(IOUT,24)J	MORSE	5300
24 FORMAT(* ANGLES AND PROBABILITIES FOR MATERIAL NUMBER*I5/)	MORSE	5301
WRITE(IOUT,23)(K,K=1,NSCT)	MORSE	5302
23 FORMAT(3X9HGP TO GP ,4(6X5HANGLE,I3,6X4HPROB4X)//)	MORSE	5303
DO 504 I=N1,N2	MORSE	5304
LZ1=MWA(I-1,J)+1	MORSE	5305
IF(I.EQ.1)LZ1=1	MORSE	5306
LZ2=MWA(I,J)	MORSE	5307
LZ1=LZ1-NSKIP	MORSE	5308
LZ2=LZ2-NSKIP	MORSE	5309
DO 505 L=LZ1,LZ2	MORSE	5310
LL=I+L-LZ1	MORSE	5311
IF((I.GT.IFTG).AND.(I.LE.JFTG))LL=IFTG+L-LZ1	MORSE	5312
WRITE(IOUT,27)I,LL	MORSE	5313
27 FORMAT(15,1X15)	MORSE	5314
505 WRITE(IOUT,506)(SIGN(L,K+1),SIGN(L,K+1+NSCT),K=1,NSCT)	MORSE	5315
506 FORMAT(1H+,12X8E14.4/(12X8E14.4))	MORSE	5316
504 CONTINUE	MORSE	5317
500 CONTINUE	MORSE	5318
109 IF(NGGA.LE.0)GO TO 110	MORSE	5319
M2=NSGN(NMTG)	MORSE	5320
M1=NSGN(NNGA+1)	MORSE	5321
DO 207 L6=M1,M2	MORSE	5322
N2=NSGL(L6,2)	MORSE	5323
N1=NSGL(L6,1)	MORSE	5324
IF(N1.LE.NNGA)N1=NNGA+1	MORSE	5325
N3=MWA(N1-1,J)+1	MORSE	5326
IF(N1.EQ.NNGA+1)N3=1	MORSE	5327
N4=MWA(N2,J)	MORSE	5328
LZ=N4-N3+1	MORSE	5329
NSKIP=N3-1	MORSE	5330
DO 200 K=1,NCOEF	MORSE	5331
NR10=NRE(K+NCOEF,J,L6)	MORSE	5332
200 CALL REED(SIGG(1,K),LZ,10)	MORSE	5333
IF(NCOEF.LE.1)GO TO 231	MORSE	5334
DO 812 I=1,LZ	MORSE	5335
DO 811 K=2,NCOEF	MORSE	5336

```

IF(SIGG(I,1).NE.0.0)GO TO 821      MORSE 5337
SIGG(I,K)=0.0                      MORSE 5338
GO TO 822                          MORSE 5339
821 SIGG(I,K)=SIGG(I,K)/SIGG(I,1)  MORSE 5340
822 L=K-1                          MORSE 5341
811 CONTINUE                        MORSE 5342
812 CONTINUE                        MORSE 5343
IF(ISTAT.LE.0)GO TO 231            MORSE 5344
IF(NPL.LE.0)GO TO 231            MORSE 5345
DO 703 K=1,NPL                    MORSE 5346
NRD(3+4*NSCT+NPL+K,J,L6)=NR9    MORSE 5347
703 CALL RITE(SIGG(1,K+1),LZ,9)   MORSE 5348
IF(ISTR.LE.0)GO TO 231            MORSE 5349
WRITE(IOUT,25)J                   MORSE 5350
DO 802 K=1,NPL                    MORSE 5351
DO 803 I=N1,N2                   MORSE 5352
WRITE(IOUT,82)K,I                 MORSE 5353
LZ1=MWA(I-1,J)+1                MORSE 5354
IF(I.EQ.NNGA+1)LZ1=1            MORSE 5355
LZ2=MWA(I,J)                     MORSE 5356
LZ1=LZ1-NSKIP                    MORSE 5357
LZ2=LZ2-NSKIP                    MORSE 5358
803 WRITE(IOUT,21)(SIGG(L,K+1),L=LZ1,LZ2)  MORSE 5359
802 CONTINUE                        MORSE 5360
82 FORMAT(4H PL=I5,3X6HGROUP=I5,9H    PCOEGF)  MORSE 5361
231 CONTINUE                        MORSE 5362
C   SET FLAGS FOR GAUSS OR RADAU QUADRATURE
IGOR = 1                           RADAU 212
IF(NSCT.EQ.1) GO TO 370            RADAU 213
IF(IGOR) 370,350,380              RADAU 214
350 K = MOD(NPL,2)                 RADAU 215
IF(K) 370,360,370                 RADAU 216
360 IF(2*NSCT-1-NPL) 370,370,380  RADAU 217
370 IGOR = -1                      RADAU 218
NMOM = 2*NSCT-1                   RADAU 219
WRITE(IOUT,1000)                   RADAU 220
GO TO 390                          RADAU 221
380 IGOR = 1                        RADAU 222
NMOM = 2*NSCT-2                   RADAU 223
WRITE(IOUT,1010)                   RADAU 224
390 IF(NPL.LT.NMOM) NMOM=NPL      RADAU 225
NC=2*NSCT+1                        MORSE 5365
IF(NCOEF.GT.NC)NC=NCOEF           MORSE 5366
DO 202 I=1,LZ                      MORSE 5367
DO 201 K=2,NCOEF                  MORSE 5368
IF(NSCT.LE.0)GO TO 202            MORSE 5369
IF(NCOEF.LE.1)GO TO 204            MORSE 5370
L=K-1                            MORSE 5371
201 F(L)=SIGG(I,K)/(2*K-1)        MORSE 5372
DO 217 K=2,NC                      MORSE 5373
217 SIGG(I,K)=0.0                  MORSE 5374
DO 215 L=1,NMOM                   MORSE 5375
IF(F(L).NE.0)GO TO 214            MORSE 5376
215 CONTINUE                        MORSE 5377
204 SIGG(I,2+NSCT)=-1.            MORSE 5378
GO TO 202                          MORSE 5379
214 CALL ANGLES(I,J)              RADAU 227
SIGG(I,2)=POINT(1)                MORSE 5381

```

```

SIGG(I,2+NSCT)=WEIGHT(1)                                MORSE 5382
IF(NANS.EQ.0)GO TO 208                                  MORSE 5383
DO 205 K=1,NANS                                         MORSE 5384
SIGG(I,2+K)=POINT(1+K)                                  MORSE 5385
205 SIGG(I,2+NSCT+K)=SIGG(I,1+NSCT+K)+WEIGHT(1+K)    MORSE 5386
208 C=SIGG(I,2+NSCT+NANS)                               MORSE 5387
NP1=NANS+1                                              MORSE 5388
DO 206 K=1,NP1                                         MORSE 5389
INDX=1+NSCT+K                                         MORSE 5390
206 SIGG(I,INDX)=SIGN(I,INDX)/C                         MORSE 5391
202 CONTINUE                                           MORSE 5392
C      TO NORMALIZE THE GAMMA P-ZERO MATRIX             MORSE 5393
DO 220 K=N1,N2                                         MORSE 5394
IND1=MWA(K-1,J)+2-N3+1                                MORSE 5395
IF(K.EQ.NNGA+1)IND1=2                                  MORSE 5396
IND2=MWA(K,J)-N3+1                                  MORSE 5397
SUM=SIGG(IND1-1,1)                                    MORSE 5398
IF(IND2.LT.IND1)GO TO 222                            MORSE 5399
DO 221 I=IND1,IND2                                    MORSE 5400
SUM=SUM+SIGG(I,1)                                    MORSE 5401
221 CONTINUE                                           MORSE 5402
222 IND1=IND1-1                                     MORSE 5403
DO 223 I=IND1,IND2                                    MORSE 5404
223 SIGG(I,1)=SIGG(I,1)/SUM                           MORSE 5405
220 CONTINUE                                           MORSE 5406
NRD(3+2*NSCT+NPL,J,L6)=NR9                           MORSE 5407
CALL RITE(SIGG( 1,1),LZ,9)                           MORSE 5408
IF(NSCT.LE.0)GO TO 704                               MORSE 5409
DO 701 K=1,NSCT                                     MORSE 5410
NRD(3+2*NSCT+NPL+K,J,L6)=NR9                           MORSE 5411
701 CALL RITE(SIGG( 1,K+1),LZ,9)                      MORSE 5412
DO 702 K=1,NSCT                                     MORSE 5413
NRD(3+3*NSCT+NPL+K,J,L6)=NR9                           MORSE 5414
702 CALL RITE(SIGG( 1,K+1+NSCT),LZ,9)                 MORSE 5415
704 IF((IPRIN.LE.0).AND.(ISTR.LE.0))GO TO 207        MORSE 5416
IF(ISTR.LE.0)GO TO 850                               MORSE 5417
WRITE(IOUT,15)J                                      MORSE 5418
DO 801 I=N1,N2                                     MORSE 5419
WRITE(IOUT,80)I                                      MORSE 5420
LZ1=MWA(I-1,J)+1                                  MORSE 5421
IF(I.EQ.NNGA+1)LZ1=1                               MORSE 5422
LZ2=MWA(I,J)                                      MORSE 5423
LZ1=LZ1-NSKIP                                     MORSE 5424
LZ2=LZ2-NSKIP                                     MORSE 5425
801 WRITE(IOUT,21)(SIGG(K,1),K=LZ1,LZ2)             MORSE 5426
80 FORMAT(1X, 5HGROUP,I5,3X, 9HSIGMA G-G)          MORSE 5427
850 IF(IPRIN.LE.0)GO TO 207                           MORSE 5428
IF(NSCT.LE.0)GO TO 207                           MORSE 5429
WRITE(IOUT,24)J                                      MORSE 5430
WRITE(IOUT,23)(K,K=1,NSCT)                           MORSE 5431
DO 804 I=N1,N2                                     MORSE 5432
LZ1=MWA(I-1,J)+1                                  MORSE 5433
IF(I.EQ.NNGA+1)LZ1=1                               MORSE 5434
LZ2=MWA(I,J)                                      MORSE 5435
LZ1=LZ1-NSKIP                                     MORSE 5436
LZ2=LZ2-NSKIP                                     MORSE 5437
DO 805 L=LZ1,LZ2                                    MORSE 5438
LL=I+L-LZ1                                         MORSE 5439

```

```
IF((I.GT.KFTG).AND.(I.LE.LFTG))LL=KFTG+L-LZ1          MORSE  5440
WRITE(IOUT,27)I,LL          MORSE  5441
805  WRITE(IOUT,506)(SIGG(L,K+1),SIGG(L,K+1+NSCT),K=1,NSCT)  MORSE  5442
804  CONTINUE          MORSE  5443
207  CONTINUE          MORSE  5444
110  CONTINUE          MORSE  5445
      RETURN          MORSE  5446
      END            MORSE  5447
```

## SELECTED BIBLIOGRAPHY

Antal, M. J. and Lee, C. E., 1976, "Charged Particle Mass and Energy Transport in a Thermonuclear Plasma," Journal of Computational Physics, p. 298-312, vol. 20.

Abramowitz, M. and Stegun, I. A., Editors, 1972, Handbook of Mathematical Functions, National Bureau of Standards, Applied Mathematics Series (55).

Bell, G. I. et al., 1967, "Multitable Treatments of Anisotropic Scattering in  $S_N$  Multigroup Transport Calculations," Nuclear Science and Engineering, p. 376-383, vol. 28.

Bell, G. I. and Glasstone, S., 1979, Nuclear Reactor Theory, New York: Robert E. Krieger Publishing Company.

Berger, M. J., 1963, "Monte Carlo Calculation of the Penetration and Diffusion of Fast Charged Particles," Methods in Computational Physics, p. 135-215, vol. 1, New York: Academic Press, Inc.

Bucholz, J. A., 1980, "An Analytical Angular Integration Technique for Generating Multigroup Transfer Matrices," Nuclear Science and Engineering, p. 163-167, vol. 74.

Carter, L. L. and Cashwell, E. D., 1975, "Particle-Transport Simulation with the Monte Carlo Method," ERDA Critical Review Series, TID-26607.

Carter, L. L. and Forest, C. A., 1976, "Transfer Matrix Treatments for Multigroup Monte Carlo Calculations--The Elimination of Ray Effects," Nuclear Science and Engineering, p. 27-45, vol. 59.

Christophorou, L. G., 1971, Atomic and Molecular Radiation Physics, London: Wiley-Interscience.

Cordaro, M. C. and Zucker, M. S., 1971, "A Method for Solving Time-Dependent Electron Transport Problems," Nuclear Science and Engineering, p. 107-116, vol. 45.

Corman, E. G. et al., 1975, "Multi-group Diffusion of Energetic Charged Particles," Nuclear Fusion, p. 337-386, vol. 15.

Coveyou, R. R. et al., 1967, "Adjoint and Importance in Monte Carlo Application," Nuclear Science and Engineering, p. 219-234, vol. 27.

Davis, P. J., 1963, Interpolation and Approximation, New York: Blaisdell Publishing Company.

Davis, P. J. and Rabinowitz, P., 1967, Numerical Integration, Waltham, Massachusetts: Blaisdell Publishing Company.

Davis, S. K., 1966, "Compilation, Evaluation and Reduction of Neutron Differential Scattering Data," Conference on Neutron Cross Section Technology, CONF-660303, U.S. Atomic Energy Commission, p. 335-353.

Duderstadt, J. J. and Martin, W. R., 1979, Transport Theory, New York: John Wiley and Sons, Inc.

Dupree, S. A. and Lighthill, R. E., 1982, Sandia National Laboratories CDC 7600 Version of MORSE-SGC, SAND80-1337.

Emmett, M. B., 1975, The MORSE Monte Carlo Radiation Transport Code System, ORNL-4972.

Evans, R. D., 1955, The Atomic Nucleus, New York: McGraw-Hill Book Company.

Golub, G. H., 1973, "Some Modified Matrix Eigenvalue Problems," SIAM Review, p. 318-334, vol. 13, no. 2.

Golub, G. H. and Welsch, J. H., 1969, "Calculation of Gauss Quadrature Rules," Mathematics of Computation, p. 221-230, vol. 23.

Gradshteyn, I. S. and Ryzhik, I. M., 1965, Table of Integrals, Series, and Products, New York: Academic Press, Inc.

Greene, N. M. et al., 1976, AMPX: A Modular Code System for Generating Coupled Multigroup Neutron-Gamma Libraries from ENDF/B, ORNL/TM-3706.

Halbleib, J. A. and Vandevender, W. H., 1974, TIGER: A One-Dimensional Multilayer Electron/Photon Monte Carlo Transport Code, SLA-73-1026.

Halbleib, J. A. and Morel, J. E., 1980, "Adjoint Monte Carlo Electron Transport in the Continuous-Slowing-Down Approximation," Journal of Computational Physics, p. 211-230, vol. 34.

Haldy, P. A. and Ligou, J., 1977, "A Moment Method for Calculating the Transport of Energetic Charged Particles in Hot Plasmas," Nuclear Fusion, p. 1225-1235, vol. 17.

Hanson, G. E. and Sandmeier, H. A., 1965, "Neutron Penetration Factors Obtained by Using Adjoint Transport Calculations," Nuclear Science and Engineering, p. 315-320, vol. 22.

Hildebrand, F. B., 1974, Introduction to Numerical Analysis, New York: McGraw-Hill, Inc.

Hill, T. R., 1975, ONETRAN: A Discrete Ordinates Finite Element Code for the Solution of the One-Dimensional Multigroup Transport Equation, LA-5990-MS.

Hoffman, T. J. et al., 1972, "The Adjoint Difference Method and Its Application to Deep-Penetration Radiation Transport," Nuclear Science and Engineering, p. 179-188, vol. 48.

Horsley, A., 1966, "Computer Evaluation of Neutron Scattering Angular Distribution Data," Conference on Neutron Cross Section Technology, CONF-660303, U.S. Atomic Energy Commission, p. 293-303.

Irving, D. C., 1970, LEGCK, A Subroutine to Analyze Legendre Coefficients for Negativity in the Angular Distribution, ORNL-TM-2903.

Irving, D. C. et al., 1966, "Impossible Legendre Coefficients," Conference on Neutron Cross Section Technology, CONF-660303, U.S. Atomic Energy Commission, p. 328-334.

Kidman, R. B. et al., 1972, "The Shielding Factor Method of Generating Multigroup Cross Sections for Fast Reactor Analysis," Nuclear Science and Engineering, p. 189-201, vol. 48.

Kopal, Z., 1955, Numerical Analysis, New York: John Wiley and Sons, Inc.

LASL Group X-6, 1981, MCNP-A General Monte Carlo Code for Neutron and Photon Transport, LA-7396M.

Lathrop, K. D., 1965, "Anisotropic Scattering Approximations in the Monoenergetic Boltzman Equation," Nuclear Science and Engineering, p. 498-508, vol. 21.

Mehlhorn, T. A. and Duderstadt, J. J., 1980, "A Discrete Ordinates Solution of the Fokker-Planck Equation Characterizing Charged Particle Transport," Journal of Computational Physics, p. 86-106, vol. 38.

Morel, J. E., 1979, "On the Validity of the Extended Transport Cross-Section Correction for Low-Energy Electron Transport," Nuclear Science and Engineering, p. 64-71, vol. 71.

Morel, J. E., 1979, "Discrete Ordinates Electron Transport Calculations Using Standard Neutron Transport Codes," Transactions of the American Nuclear Society, p. 676-677, vol. 33.

Morel, J. E., 1981, "Fokker-Planck Calculations Using Standard Discrete Ordinates Transport Codes," Nuclear Science and Engineering, p. 340-356, vol. 79.

Morel, J. E., 1983, Personnal Communication.

Moses, G. A., 1977, "Laser Fusion Hydrodynamics Calculations," Nuclear Science and Engineering, p. 49-63, vol. 64.

Odom, J. P. and Shultz, J. K., 1976, Anisotropic Neutron Transport Without Legendre Expansions," Technical Notes, Nuclear Science and Engineering, p. 278-281, vol. 59.

Peek, J. M., 1979, Cross Sections for Electron and Photon Processes Required by Electron-Transport Calculations, SAND79-0772.

Renken, J. H., 1970, Use of Solutions to the Adjoint Transport Equation for the Evaluation of Radiation Shield Designs, SC-RR-70-98.

Renken, J. H., 1980, Application of Transport Calculations to Radiation Attenuation Studies, unpublished.

Segre, E., 1965, Nuclei and Particles, New York: W. A. Benjamin, Inc.

Selph, W. E. and Garrett, C. W., 1973, "Monte Carlo Methods for Radiation Transport," Reactor Shielding for Nuclear Engineers, ch. 5, TID-25951.

Spanier, J. and Gelbard, E. M., 1969, Monte Carlo Principles and Neutron Transport Problems, Reading, Massachusetts: Addison-Wesley Publishing Company.

Straker, E. A. et al., 1970, MORSE Code: A Multigroup Neutron and Gamma-Ray Monte Carlo Transport Code, ORNL-4585.

Straker, E. A. et al., 1971, MORSEC: A Revised Cross-Section Module for the MORSE Multigroup Monte Carlo Code, ORNL-4716.

Stroud, A. H., 1974, Numerical Quadrature and Solution of Ordinary Differential Equations, New York: Springer-Verlag, Inc.

Stroud, A. H. and Secrest, D., 1966, Gaussian Quadrature Formulas, Englewood Cliffs, New Jersey: Prentice-Hall, Inc.

Szegö, G., 1959, Orthogonal Polynomials, New York: American Mathematical Society.

Tanenbaum, B. S., 1967, Plasma Physics, New York: McGraw-Hill Book Company.

Wang, M. C. and Guth, E., 1951, "On the Theory of Multiple Scattering, Particularly of Charged Particles," Physical Review, p. 1092-1111, vol. 84, no. 6.

Weisbin, C. R. et al., 1974, "A New Procedure for the Determination of Neutron Multigroup Transfer Matrices," Nuclear Science and Engineering, p. 329-341, vol. 55.

Distribution:  
Unlimited Release

Department of Chemical and Nuclear Engineering  
Attn: Dr. David Woodall  
University of New Mexico  
Albuquerque, New Mexico 87131 (1)

0314 S. A. Dupree (1)  
1231 T. P. Wright (1)  
1231 J. E. Morel (10)  
1231 J. A. Halbleib (1)  
3141 (5)  
3151 (3)  
3154-3 (25)  
8214 (1)  
9336 Attn: J. H. Renken  
R. E. Lighthill  
P. J. McDaniel (1)